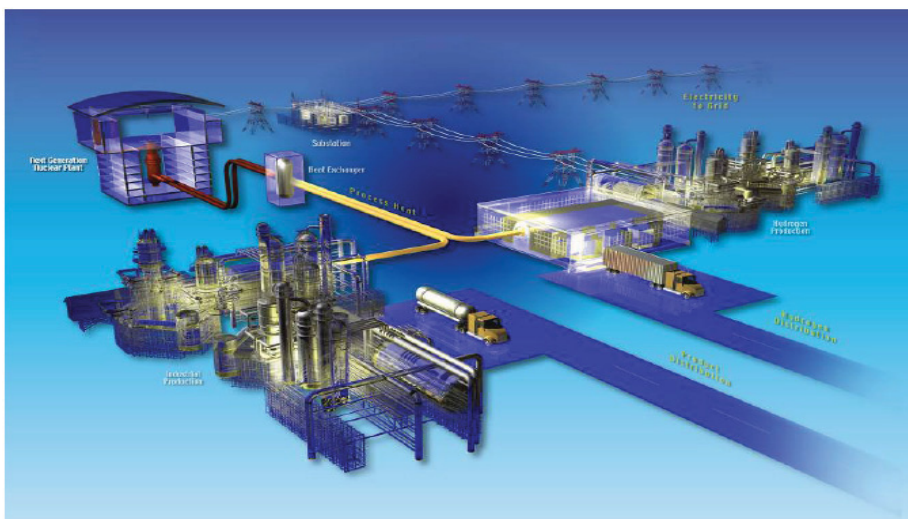


COMBINE7.1 – A Portable ENDF/B-VII.0 Based Neutron Spectrum and Cross-Section Generation Program

W. Y. Yoon
R. A. Grimesey
D. W. Nigg
R. L. Curtis

August 2009



The INL is a U.S. Department of Energy National Laboratory
operated by Battelle Energy Alliance



COMBINE7.1 – A Portable ENDF/B-VII.0 Based Neutron Spectrum and Cross-Section Generation Program

**W. Y. Yoon
R. A. Grimesey
D. W. Nigg
R. L. Curtis**

August 2009

**Idaho National Laboratory
Idaho Falls, Idaho 83415**

<http://www.inl.gov>

**Prepared for the
U.S. Department of Energy
Office of Nuclear Energy
Under DOE Idaho Operations Office
Contract DE-AC07-05ID14517**

DISCLAIMER

This information was prepared as an account of work sponsored by an agency of the U.S. Government. Neither the U.S. Government nor any agency thereof, nor any of their employees, makes any warranty, expressed or implied, or assumes any legal liability or responsibility for the accuracy, completeness, or usefulness, of any information, apparatus, product, or process disclosed, or represents that its use would not infringe privately owned rights. References herein to any specific commercial product, process, or service by trade name, trade mark, manufacturer, or otherwise, does not necessarily constitute or imply its endorsement, recommendation, or favoring by the U.S. Government or any agency thereof. The views and opinions of authors expressed herein do not necessarily state or reflect those of the U.S. Government or any agency thereof.

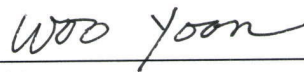
Nuclear Energy

**COMBINE7.1—A Portable ENDF/B-VII.0 Based
Neutron Spectrum and Cross-Section Generation
Program**

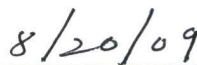
INL/EXT-08-14729
Rev 1

August 2009

Approved by:



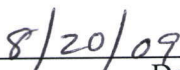
Woo Yoon
Author



Date



Diane V. Croson
VHTR TDO Project Manager



Date



Hans D. Gougar
VHTR TDO Deputy Technical Director



Date

ABSTRACT

COMBINE7.1 is a FORTRAN 90 computer code that generates multigroup neutron constants for use in the deterministic diffusion and transport theory neutronics analysis. The cross-section database used by COMBINE7.1 is derived from the Evaluated Nuclear Data Files (ENDF/B-VII.0). The neutron energy range covered is from 20 MeV to $1.0E-5$ eV. The Los Alamos National Laboratory NJOY code is used as the processing code to generate a 167 fine-group cross-section library in MATXS format for Bondarenko self-shielding treatment. Resolved resonance parameters are extracted from ENDF/B-VII.0 File 2 for a separate library to be used in an alternate Nordheim self-shielding treatment in the resolved resonance energy range. The equations solved for energy dependent neutron spectrum in the 167 fine-group structure are the B-3 or B-1 approximations to the transport equation. The fine group cross sections needed for the spectrum calculation are first prepared by Bondarenko self-shielding interpolation in terms of background cross section and temperature. The geometric lump effect, when present, is accounted for by augmenting the background cross section. Nordheim self-shielded fine group cross sections for a material having resolved resonance parameters overwrite correspondingly the existing self-shielded fine group cross sections when this option is used. The fine group cross sections in the thermal energy range are replaced by those self-shielded with the Amouyal/Benoist/Horowitz method in the three region geometry when this option is requested. COMBINE7.1 coalesces fine group cross sections into broad group macroscopic and microscopic constants. The coalescing is performed by utilizing fine-group fluxes and/or currents obtained by spectrum calculation as the weighting functions. The multigroup constant may be output in any of several standard formats including ANISN 14** free format, CCCC ISOTXS format, and AMPX working library format. ANISN-PC, a one-dimensional, discrete-ordinate transport code, is incorporated into COMBINE7.1. As an option, the 167 fine-group constants generated by COMBINE portion in the program can be used to calculate regionwise spectra in the ANISN portion, all internally to reflect the one-dimensional transport correction. Results for the criticality validation calculations are included as a part of verification and validation.

ACKNOWLEDGMENTS

A number of individuals contributed to the successful development of the COMBINE7.1 code, which was derived from COMBINE5 and 6 codes . Gilbert Singer provided an initial standard FORTRAN version of the CVI free-format input processing routines used in COMBINE/PC. Jerry Judd, J. Russell Johnson, Blair Briggs, and Bruce Schnitzler contributed to the programming of several routines. Dr. D. Parsons, formerly with Idaho National Laboratory Laboratory (INL), is greatly appreciated for the use of ANISN/PC. Several members of the INL/University/Industry PC software review committee provided useful comments and tested the software prior to its release. Dr. Hans Gougar extensively tested the COMBINE7.1 beta versions and his inputs were invaluable. The Next Generation Nuclear Program at INL deserves a special mention for helping realize the current code version.

CONTENTS

Nuclear Energy	3
1. INTRODUCTION	1
1.1 COMBINE7.1 Code Abstract	3
2. THEORETICAL FOUNDATIONS	5
2.1 Derivation of BN Equations.....	5
2.1.1 B-3 Approximation	7
2.1.2 B-1 Approximation	11
2.1.3 Convergence on Gauss-Seidel Iterative Scheme.....	12
2.2 Bondarenko Method.....	12
2.2.1 Fine-Group Cross Section Generation in Bondarenko Format	15
2.2.2 Bondarenko Self-Shielding Interpolation	15
2.3 Resonance Region.....	16
2.3.1 Resolved Resonances—Nordheim Numerical Method.....	16
2.3.2 Doppler Broadening of Resolved Resonance Parameters.....	19
2.3.3 Determination of E_1/E_2 and the Number of Meshes for a Resonance.....	20
2.3.4 Absorber Narrow Resonance- Moderator Asymptotic Flux Approximation	21
2.3.5 Self-Shielding Elastic Scattering Transfer Matrix	21
2.3.6 Numerical Integration with Simpson’s Rule.....	21
2.3.7 Group Averaging.....	22
2.3.8 Dancoff-Ginsburg Correction Factor Calculation.....	22
2.4 Computation of Thermal Disadvantage Factors.....	25
2.4.1 Slab Geometry Disadvantage Weights.....	27
2.5 Age Equations	28
2.6 Transport Approximations	29
3. ONE-DIMENSIONAL TRANSPORT CALCULATION	31
4. USER’S GUIDE	32
4.1 Derivation of Diffusion Coefficient and Transport Cross Section.....	32
4.2 Summary Edits for Broad Group Constants.....	33
4.2.1 Average Macroscopic Cross Sections	34
4.2.2 Monoenergetic Transport Cross Section.....	38
4.2.3 Average Microscopic Cross Sections.....	38
4.2.4 Effective Diffusion Theory Constants (Blackness Theory)	39
4.2.5 Mixed Number Density (MIND) Constants.....	40
4.2.6 Multiplication Factors	41
4.2.7 The Spatial Coalescing Formulas	42
5. COMBINE7.1 FILES DESCRIPTION	45
6. COMBINE7.1 INPUT DATA FILE ORGANIZATION	46
6.1 Problem/1-D Data Records	47
6.2 Title Record and Integer Data Records.....	48

6.2.1	Title Record	48
6.2.2	Problem Basic Control Information Record 1010101	48
6.2.3	Energy Group Structure Record 10102YY	49
6.2.4	Resonance Calculation Option Record 102010Y.	49
6.2.5	Macroscopic Interface File Option Record 1030101	50
6.2.6	Microscopic Interface File Option Record 10302XX	51
6.3	Floating Point Data Records	52
6.3.1	General Floating Point Data Record 1041001	52
6.3.2	Material Specification Record 10420XX.....	52
6.3.3	Material Resonance Specification Record 1043XXY.....	53
6.3.4	Material Dancoff Specification Record 1044XXY.....	54
6.3.5	Material General Resonance Data Record 10450XX	54
6.3.6	Material Self-Shielding Factor Records (146XXYY).....	55
6.3.7	Broad Group Buckling Factor Records (14700YY)	55
6.3.8	Broad Group Buckling Sign Records (14710YY)	55
6.3.9	Blackness calculation option Record (1480001).....	56
6.3.10	MND calculation option Record (1490001)	56
6.4	Mixed Integer and Floating Point Data Records.....	57
6.4.1	ABH REGION DESCRIPTION RECORDS 2010401.....	57
6.4.2	ABH Material Description for Each Region Record 2015XYY	57
6.5	Fine Energy Group Structure	58
6.6	Materials in the “MATXS” Fine Group Cross Section Library and the “RERES” Resolved Resonance Library.....	59
6.7	MATXS.LIB File Description	64
6.8	Description of Resolved Resonance Library (reres.lib) Format.....	68
6.9	Cross section and constants internal record	69
6.9.1	First Data Record for Material k.....	69
6.9.2	Second Data Record for Material k.....	70
6.10	Thermal $S(\alpha,\beta)$ and Free Scattering Cross Section Internal Record	71
7.	PROGRAMMER’S GUIDE.....	72
7.1	Flow Diagram	72
7.2	Summary of Contents of Subroutines	75
7.2.1	Program COMBINE7.1 and Supporting Subroutines	75
8.	REFERENCES	82
	B. REFERENCE.....	91
	ISOTXS—Nuclide (Isotope) Ordered, Multigroup Neutron Cross-Sections	95
	D. REFERENCE	122

FIGURES

Figure 1.	COMBINE7.1 implementation scheme.....	3
-----------	---------------------------------------	---

Figure 2. An example of Doppler broadened resonance cross sections.....	20
Figure 3. Parameters of the rectangular cell.....	24
Figure 4. Spectrum group structure.....	34

TABLES

Table A-1. The library material title record summary.	87
Table A-2. The library material floating point data summary.	88
Table B-1. Cross-section arrangement.....	91
Table D.1: Criticality Validation Suite	105
Table D.2: Calculated keff eigenvalues against the measured keff =1.000 B1 and No Sn Transport Correction	112
Table D.3: Calculated keff eigenvalues against the measured keff =1.000 B1 and Sn Transport Correction	113
Table D.4: Calculated keff eigenvalues against the measured keff =1.000 B3 and No Sn Transport Correction.....	114
Table D.5: Calculated keff eigenvalues against the measured keff =1.000 B3 and Sn Transport Correction	115

ACRONYMS

ABH	Amouyal/Benoist/Horowitz
ENDF	Evaluated Nuclear Data Files
HTR	High Temperature Reactor
INL	Idaho National Laboratory
MLBW	Multilevel Breit-Wigner
NGNP	Next Generation Nuclear Plant
PBMR	Pebble Bed Modular Reactor
R-M	Reich-Moore
SLBW	single level Breit-Wigner
MND	mixed number density

COMBINE7.1—A Portable ENDF/B-VII.0 Based Neutron Spectrum and Cross-Section Generation Program

1. INTRODUCTION

COMBINE7.1 is a FORTRAN 90 computer code for generation of spectrum-averaged, multigroup, neutron, cross-section data suitable for use in the deterministic diffusion and transport theory reactor design analysis. The cross-section database used by COMBINE7.1 is derived from Evaluated Nuclear Data Files (ENDF/B-VII.0¹). The neutron energy ranging from 20 MeV to 1.0E-5 eV is treated by a total of 167 discrete energy groups. The equations solved for the energy-dependent neutron spectrum are the B_3 or B_1 approximations to the transport equation.

COMBINE7.1 has evolved from its predecessor Versions 5 and 6. The earlier version, COMBINE/PC—a Portable ENDF/B Version 5 Neutron Spectrum and Cross-Section Generation Program² (COMBINE5)—combined the preexisting neutron spectrum codes, PHROG³ (fast) and INCITE⁴ (thermal spectrum), previously developed at Idaho National Laboratory (INL), by suitably integrating them into a single package, thus, the name COMBINE. The cross-section database used by COMBINE5 is derived from the ENDF/B-V⁵. In the fast spectrum calculation, the B_3 spherical harmonics equations are solved by Gauss elimination and the B_1 spherical harmonics equations are solved simultaneously, beginning with the highest energy group. In INCITE, the B_1 thermal equations have been cast in the form of a normalized Gauss-Seidel iterative scheme where extrapolation and iteration in both directions have been included as options. The fast and thermal energy ranges are coupled by using slowing down theory and energy-dependent scattering and spectra data to generate average transfer cross sections from the PHROG broad groups into INCITE broad groups. The results are then normalized to the total scatter below the fast range cutoff as produced by PHROG.

The 1990 release of ENDF/B-VI nuclear data⁶ of ENDF-6 format created problems for the INL's Version 5 processing codes used to generate cross-section libraries for COMBINE5, requiring major revisions of these codes. An alternative to the modifications of the INL's processing codes was to utilize the NJOY code system⁷ developed at the Los Alamos National Laboratory. NJOY optionally processes all resonance self-shielding through the Bondarenko approximation. In the Bondarenko model,⁸ the narrow resonance (NR) approximation and the B_N approximation for large systems are invoked.⁹ Two cross section libraries were generated by NJOY for the fast (72 group) and thermal (101 energy points) spectrum calculations, maintaining the same energy structures as in COMBINE5. The fast cross section library was based on sets of background cross sections and temperatures for Bondarenko self-shielding interpolation. The geometric effects of fuel lump and lattice are accounted for by the combination of Rational Approximation and Dancoff-Ginsburg correction, including a double heterogeneity due to fuel grains present within the macroscopic fuel lump by augmenting the background cross section. The weakness of the Bondarenko model occurs for thermal reactor analysis in the "epithermal" energy region from about 4 eV to around 200 to 300 eV.¹⁰ In this region, the resonances are no longer "narrow" and the flux shape given by Bondarenko method is no longer sufficiently accurate. An alternate approach is the Nordheim resonance integral treatment method.¹¹ A separate resolved resonance library was also created, including formats in single level Breit-Wigner (SLBW), Multilevel Breit-Wigner (MLBW), Reich-Moore (R-M), and no resonance, extracted directly from ENDF/B-VI nuclear data files to be used in the Nordheim self-shielding treatment in the resolved resonance energy range. The Version 5 code was modified to handle the new cross section and resolved resonance libraries. The new code was designated as COMBINE6.¹² The ENDF/B-VI derived thermal cross-section library is based on the infinite dilution and temperature dependence is only present if thermal scattering data is available for an isotope. This format of the thermal cross-section library is same as that of COMBINE5's. The INCITE portion of COMBINE5 is therefore fully retained, including the Amouyal/Benoist/Horowitz (ABH) option for self-shielding in the thermal energy range. The energy range treated is from 0.001 eV to 16.905 MeV spanned

by a total of 166 discrete energy points/groups. A routine was also retained to calculate a Dancoff-Ginsburg correction factor in conjunction with the resonance calculation for either a rectangular or hexagonal arrangement of cylindrical absorber pins. Several routines to process MLBW and R-M resonance formats were adopted from the NJOY code. Nordheim self-shielded cross sections, when requested for a material having resolved resonance parameters, overwrite the corresponding multigroup Bondarenko self-shielded cross sections. An iterative scheme was also introduced for better fission-rate weighted χ values. In both COMBINE5 and COMBINE6, the energy boundary between the fast spectrum module and thermal spectrum module can be chosen by the user at one of the eight overlapping mutual energy group boundaries, the highest being 2.3824 eV and the lowest 0.414 eV. No resonance treatment is considered below the chosen energy boundary. No thermal upscattering is allowed into the energy above the highest boundary. Thermal upscattering does not take place between the highest (2.3824 eV) and chosen boundary of less energy, even though it is possible from below to above the boundary when the boundary is below the highest. The adequate self-shielding treatment of resonances in the thermal energy range is critical where thermal upscattering is also significant because of high operating temperature. Overlap and interference effect of resonances among admixed absorbing isotopes was not accounted.

COMBINE7.1 has been modified to resolve the above issues. The B_1 and B_3 transport algorithms for the full range multigroup treatment, including thermal upscattering, were identified and implemented to unify fast and thermal spectrum calculations. The neutron energy ranging from 20 MeV to 1.0E-5 eV is treated by a total of 167 discrete energy groups, adding one more group (20–16.905 MeV) to the previous versions' group structure. The thermal upscattering takes place between 1.0E-5 eV and 5.0435 eV (high enough for most reactor applications) with no energy boundary restriction. Up to g-wave resonances are now treated to obtain the elastic scattering cross section, although the isotropic scattering is still used for energy transfer. In the Nordheim resonance treatment, up to three admixed resonance absorbers can be present to account for the resonance overlap and interference effect. Thermal upscattering was also added in the resonance treatment solution. The interpolation algorithm in the Bondarenko scheme to self-shield cross sections has been modified for improvement and revamped to afford additional temperature-only-dependent thermal scatterings, free and/or $S(\alpha, \beta)$. The interpolation is now performed first for the background cross sections at each temperature and the generated cross sections for the set of preselected temperatures are then interpolated for the problem-dependent temperature. Negative buckling algorithms have been implemented in addition to a real B : one with the positive imaginary B and the other with the negative imaginary B . Previously, only the positive and real B of cosine spatial shape was allowed. The mixed use of three different modes of buckling in the broad group wise input is implemented. All resonances are Doppler broadened by the method called "kernel broadening" as practiced in NJOY, thus eliminating the need to evaluate Doppler line functions (ψ and χ) previously calculated in the SLBW treatment. The GAM-1 resolved-resonance calculation routine,¹³ a fast alternative to the much more accurate but time consuming Nordheim numerical method, was scrapped since speed is no longer a factor. Many of the INCITE routines were removed or combined with PHROG due to the unified energy scheme.

The necessity of better treat spatial self-shielding and reflector effects when dealing with neutron-optically thin reactors like the annular core design of gas-cooled, graphite-moderated high temperatures (HTRs) such as proposed for the Next Generation Nuclear plant (NGNP) requires the transport correction in generating the cross sections for use in reactor physics. For this, 1-D discrete-ordinate transport code, ANISN-PC,¹⁴ is incorporated into COMBINE7.1 to reflect one-dimensional (1-D) transport correction. With this incorporation, a fuel such as TRISO/PEBBLE can be also better modeled to generate cross sections for the pebble bed reactor (PBR) analyses. The 167 fine-group constants generated by COMBINE for multiregions via stack cases are fed into ANISN to calculate regionwise spectra, which are used in the COMBINE to generate the regionwise spatial self-shielded broad group constants. The detail of ANISN code will be deferred to its manual. Figure 1 shows the COMBINE7.1 implementation scheme.

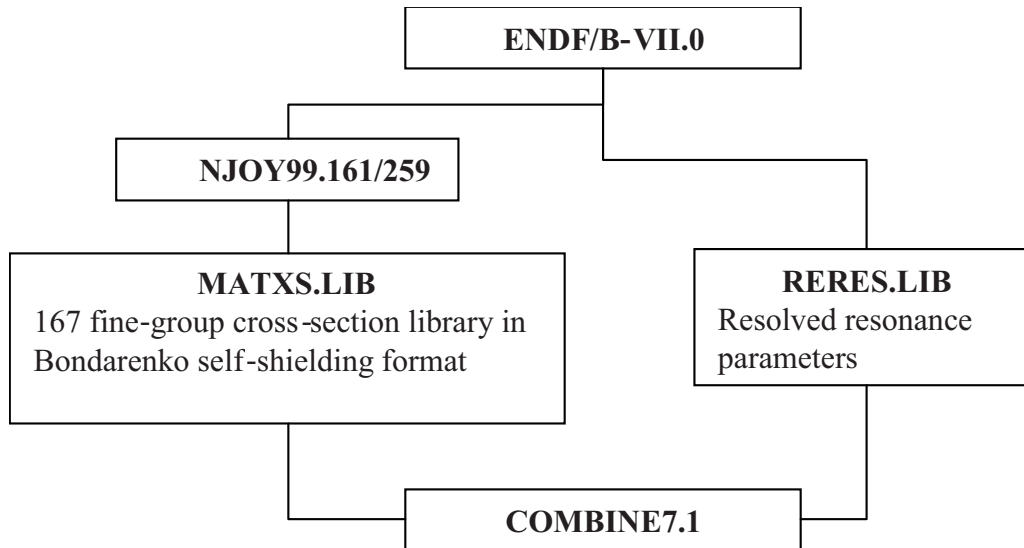


Figure 1. COMBINE7.1 implementation scheme.

ENDF/B-VII.0 nuclear data was released in December 2006 using the same ENDF-6 format.¹ The cross-section database is now derived entirely from ENDF/B-VII.0 nuclear data with the exception of Zr element cross-section data, which is based on ENF/B-VI.8 nuclear data. The NJOY99.259 version¹⁵ was used to generate a 167 fine-group cross-section library, MATXS.LIB, in MATXS format (Bondarenko format) on sets of background cross sections and temperatures including thermal scattering cross sections. This cross-section library includes damage, heating, kerma, and gas production cross sections in addition to those vector and matrix cross sections required for transport calculations. Only those materials designated by ENDF/B File 7 formats as moderators and included in NJOY99.259 contain thermal $S(\alpha,\beta)$ scattering matrices. The nonmoderating materials in the library possess free thermal scattering matrices. A separate resolved resonance library, RERES.LIB, was also created that includes formats in SLBW, MLBW, R-M, and no resonance, extracting all resolved resonance parameters directly from ENDF/B-VII.0 nuclear data files. Along with the cross section library in Bondarenko format and the resolved resonance data library, the upgraded COMBINE version is now called COMBINE7.1.

As the code has evolved, further improvements are expected in the future. It is also anticipated that the next revision would include calculation experiences involving PBR.

1.1 COMBINE7.1 Code Abstract

1. **Program Identification:** COMBINE7.1
2. **Description of Problem:** COMBINE7.1 is a FORTRAN 90 computer code that generates multigroup neutron constants for use in the deterministic diffusion and transport theory neutronics analysis. The cross-section database used by COMBINE7.1 is derived from ENDF/B-VII.0. The neutron energy range covered is from 20 MeV to 1.0E-5 eV. The equations solved for energy dependent neutron spectrum are the B-3 or B-1 approximations to the transport equation. It is also capable of performing a 1D discrete-coordinates transport calculation for multiregions to generate regionwise broad group constants.
3. **Method of Solution:** The energy range is broken into 167 fine groups for the spectrum calculation. The resulting matrix of flux equations is then solved using standard numerical techniques to obtain the spectral weight function for generation of group-averaged constants. An alternate resolved resonance shielding of the fine-mesh cross section data is performed using the Nordheim method. An option to treat thermal self shielding using the ABH method is provided. User-defined self-shielding

factors (from an auxiliary transport code such as ANISN/PC) may be entered. Calculated cross sections may be issued in any of several standard formats.

4. **Related Material:** A MATXS library file and a resolved resonance parameter library file are provided with the code package in ASCII format. Processors to convert the MATXS file to the required binary format or to convert the binary file to the ASCII file are provided.

cv700.f90: COMBINE-7 Cycle 0 Fortran 90 source program.
It requires matxs.lib and reres.lib to run a problem.
matxs.asc: 167 fine-group cross section library in ascii format
matxs.lib: 167 fine-group cross section library in binary format
reres.lib: resolved resonance library in ascii format
matxscv.f: Fortran program to convert matxs.asc (ascii file) to matxs.lib (binary file)
matxsca.f: Fortran program to convert matxs.lib to matxs.asc
anisn.pdf: ANISN/PC Manual (pdf file).

5. **Restrictions:** COMBINE7.1 is written to function properly on 32-bit word length machine. Accuracy to four or five decimal places in the computed spectrum and cross sections may be expected.
6. **Computers:** COMBINE7.1 is written in standard FORTRAN with the objective of total machine independence. The program has been successfully compiled by the Intel Visual Fortran Compiler (Version 10) and by the Lahey/Fujitsu Fortran compiler (LF95) on the Windows 32-bit platform.
7. **Run Time:** Variable from a few seconds to several minutes on PC-class hardware, depending primarily on the number and type of resonance self-shielding calculations required for a particular case.
8. **Programming Language:** Standard FORTRAN 90.
9. **Operating System:** COMBINE7.1 has successfully functioned under Windows and Linux operating systems.
10. **Machine Requirements:** As stated in item 6, Computers.
11. **Authors:** W. Y. Yoon
R. A. Grimesey
D. W. Nigg
R. L. Curtis
Idaho National Laboratory
Battelle Energy Alliance
P.O. Box 1625
Idaho Falls, ID 83415

2. THEORETICAL FOUNDATIONS

2.1 Derivation of BN Equations

The equations solved by COMBINE are the energy-dependent B_1 or B_3 spherical harmonic approximations to the transport equation originally developed by D. S. Selengut.¹⁶ A derivation of the B_N spherical harmonics equations is straightforward, but rather tedious because of the complicated expansion integrals. The physical model is a homogeneous, critical, 1-D bare slab core. As such, the time-independent, energy dependent, Boltzmann neutron transport equation in plane geometry may be written

$$\mu \frac{\partial \Phi(x, \mu, E)}{\partial x} + \Sigma_t(x, E)\Phi(x, \mu, E) = \iint \Sigma_s(x; \Omega', E' \rightarrow \Omega, E)\Phi(x, \mu', E')d\Omega' dE' + Q(x, \mu, E) \quad (1)$$

where: $\Phi(x, E, \mu)$ is the neutron flux in the direction $\mu = \cos \theta$ relative to the 1-D x axis of the slab at energy E and position x and Ω and Ω' are the azimuthal angles associated with μ and μ' , respectively; Σ_t is the total cross section; and $\Sigma_s(x; \Omega', E' \rightarrow \Omega, E)$ is the neutron transfer cross section, including the multiplicity of neutrons emitted in each reaction event. Q represents the independent (or extraneous) neutron sources that are not dependent on the neutron density of the system. All cross sections are macroscopic here. It will be assumed that the angular variation of the transfer cross section, Σ_s , depends only on the scattering angle, $\mu_0 = \Omega \cdot \Omega'$. Then Σ_s may be expanded in a set of Legendre polynomials of μ_0 ; thus,

$$\Sigma_s(x; \Omega', E' \rightarrow \Omega, E) = \sum_{l=0}^{\infty} \frac{2l+1}{4\pi} \Sigma_{sl}(x; E' \rightarrow E) P_l(\mu_0), \quad (2)$$

where the expansion coefficients $\Sigma_{sl}(x; E' \rightarrow E)$ are given by

$$\Sigma_{sl}(x; E' \rightarrow E) = 2\pi \int_{-1}^1 \Sigma_s(x; E' \rightarrow E, \mu) P_l(\mu) d\mu \quad (3)$$

If the expansion of Equation (3) is inserted into Equation (1), use of the addition theorem for Legendre polynomials and integration over azimuthal angles gives

$$\mu \frac{\partial \Phi(x, \mu, E)}{\partial x} + \Sigma_t(x, E)\Phi(x, \mu, E) = \sum_{l=0}^{\infty} \frac{2l+1}{2} P_l(\mu) \int_{E'}^{\infty} \Sigma_s(x, E' \rightarrow E) \int_{-1}^1 \Phi(x; \mu', E') P_l(\mu') d\mu' dE' + Q(x, \mu, E). \quad (4)$$

The basis of the B_N method, as a means of estimating within-group neutron fluxes, is to assume the spatial distribution to be independent of neutron energy in plane geometry,

$$\Phi(x, \mu, E) = e^{-iBx} \psi(B, \mu, E), \quad (5)$$

where only the real part of e^{-iBx} satisfies the spatial boundary conditions for the scalar flux. The complex form of the spatial dependence is necessary for the equations to remain homogeneous. In Equation (5) the spatial dependence of the flux is eliminated by assuming that the solution is separable in (E, μ) and x and characterizing the spatial dependence of each of the variables by a simple buckling mode. If Equation (5) is inserted into the neutron transport Equation (4) with $Q(x, \mu, E)$ replaced by an isotropic fission

source, $\frac{1}{2} \chi(E) e^{-iBx}$, and the transfer cross section is now designated as Σ_{sl} signifying the absence of fission contribution, the result is

$$\begin{aligned} & \Sigma_t(E) \left(1 - \frac{iB\mu}{\Sigma_t}\right) \psi(B, \mu, E) \\ &= \sum_{l=0}^{\infty} \frac{2l+1}{2} P_l(\mu) \int_{\Sigma_{sl}(E' \rightarrow E)} \int_{-1}^1 \psi(B, \mu', E') P_l(\mu') d\mu' dE' + \frac{1}{2} \chi(E). \end{aligned} \quad (6)$$

The neutron source is assumed to have the same spatial dependence as the flux. This assumption is also necessary in order for the equations to remain homogeneous. The source term, $\frac{1}{2}\chi(E)$, in

Equation (6) is the result of Legendre polynomial expansion and truncation to the first term, assuming the fission source to be isotropic in lab coordinates. It is also noted that independent (or extraneous) neutron sources, which are not dependent on the neutron density of the system, are not included in this equation.

Equation (6) could be multiplied by $P_n(\mu)$ and integrated over μ from -1 to 1 to obtain equations satisfied by the Legendre components of $\psi(B, \mu, E)$. More rapid convergence of the expansion is achieved, however, when equation (6) is divided by $\Sigma_t(1 - iB\mu/\Sigma_t)$, multiplied by $P_n(\mu)$, and then integrated to obtain, for $n = 0, 1, 2, \dots$,

$$\begin{aligned} & \phi_n(B, E) \\ &= \sum_{l=0}^{\infty} (2l+1) \frac{A_{nl}(B, E)}{\Sigma_t(E)} \int_{\Sigma_{sl}(E' \rightarrow E)} \phi_l(B, E') dE' + \frac{A_{n0}(B, E)}{\Sigma_t(E)} \chi(E), \end{aligned} \quad (7)$$

using the following definitions:

$$(i)^n \phi_n(B, E) \equiv \int_{-1}^1 \psi(B, \mu, E) P_n(\mu) d\mu. \quad \text{when } B \text{ is real,} \quad (8)$$

$$\phi_n(B, E) \equiv \int_{-1}^1 \psi(B, \mu, E) P_n(\mu) d\mu. \quad \text{when } B \text{ is imaginary (} B = \pm iC, \text{ where } C \text{ is real),} \quad (9)$$

$$A_{nl}(B, E) \equiv \frac{(i)^{l-n}}{2} \int_{-1}^1 \frac{P_n(\mu) P_l(\mu)}{1 - \frac{iB\mu}{\Sigma_t(E)}} d\mu \quad \text{when } B \text{ is real,} \quad (10)$$

$$A_{nl}(B, E) \equiv \frac{1}{2} \int_{-1}^1 \frac{P_n(\mu) P_l(\mu)}{1 - \frac{iB\mu}{\Sigma_t(E)}} d\mu \quad \text{when } B \text{ is imaginary.} \quad (11)$$

When $n = 0$, for example, the value $P_0(\mu)$ is 1; hence, it follows from Equation (8) that $\Phi_0(B, E)$ is simply the total flux at E .

From Equations (10) and (11), the following symmetry and recursion relations can be derived

$$(i)^{n-l} A_{nl} = (i)^{l-n} A_{ln} \quad \text{when } B \text{ is real,} \quad (12)$$

$$A_{nl} = A_{ln} \quad \text{when } B \text{ is imaginary,} \quad (13)$$

$$\frac{1}{B/\Sigma_t} (2l+1) A_{nl} - (l+1) A_{n,l+1} + l \cdot A_{n,l-1} = \frac{\delta_{nl}}{B/\Sigma_t} \quad \text{when } B \text{ is real,} \quad (14)$$

$$\frac{1}{C/\Sigma_t} (2l+1)A_{nl} + (l+1)A_{n,l+1} + l \cdot A_{n,l-1} = \frac{\delta_{nl}}{C/\Sigma_t} \text{ when } B = iC \text{ and } C \text{ is real,} \quad (15)$$

$$\frac{1}{C/\Sigma_t} (2l+1)A_{nl} - (l+1)A_{n,l+1} - l \cdot A_{n,l-1} = \frac{\delta_{nl}}{C/\Sigma_t} \text{ when } B = -iC \text{ and } C \text{ is real.} \quad (16)$$

where δ_{nl} is the Kronecker delta.

Now, all of the Φ_n in Equation (7) is real quantity. l is the limit for the Legendre expansion of the differential scattering cross section; the expansion is truncated at $l + 1$. However, l does not determine the order of the B_N equations. The integral in Equation (7) may be solved to any order n independent of the value of l . As n is increased beyond l , no particular advantage is gained in a spectrum code like COMBINE because the ultimate purpose of the solution fluxes is to collapse the cross sections to a few group libraries for spatial transport codes. For $n > l$ there are no cross sections in the library because the elastic scattering matrix was truncated at $l + 1$. Therefore, there is no reason to include higher order fluxes than $n = 3$ in the B_3 solution. The same argument pertains to the B_1 approximation; in this case n is truncated at 1.

The coefficients, A_{nl} , will become a function of $\alpha = B/\Sigma_t$ and $A_{00} = \beta = \frac{\tan^{-1} \alpha}{\alpha}$ when B is real or

$$\alpha = C/\Sigma_t \text{ and } A_{00} = \beta = \frac{\tanh^{-1} \alpha}{\alpha} \text{ when } B = \pm iC \text{ with a real } C.$$

2.1.1 B-3 Approximation

Evaluation of Equation (10) for the B_3 approximation, limiting l and n to 3, is straightforward but rather tedious for the higher order coefficients.

$$A_{00} = \beta = \frac{\tan^{-1} \alpha}{\alpha}$$

$$A_{01} = -\frac{1-\beta}{\alpha}$$

$$A_{02} = -\frac{3}{2} \frac{(1-\beta)}{\alpha^2} + \frac{\beta}{2}$$

$$A_{11} = -\frac{1-\beta}{\alpha^2}$$

$$A_{12} = -\frac{3}{2} \frac{(1-\beta)}{\alpha^3} - \frac{\beta}{2\alpha}$$

$$A_{22} = \frac{1}{4\alpha} \left[\left(\frac{9}{\alpha^3} + \frac{6}{\alpha} + \alpha \right) \beta - \frac{3}{\alpha} - \frac{9}{\alpha^3} \right]$$

$$A_{03} = \frac{1}{2\alpha} \left[\left(\frac{5}{\alpha^2} + 3 \right) \beta - \frac{4}{3} - \frac{5}{\alpha^2} \right]$$

$$A_{13} = \frac{1}{2\alpha^2} \left[\left(\frac{5}{\alpha^2} + 3 \right) \beta - \frac{4}{3} - \frac{5}{\alpha^2} \right]$$

$$\begin{aligned}
A_{23} &= -\frac{1}{4\alpha} \left[\frac{15}{\alpha^4} + \frac{9}{\alpha^2} + \frac{4}{3} - \left(\frac{15}{\alpha^4} + \frac{14}{\alpha^2} + 3 \right) \beta \right] \\
A_{33} &= -\frac{1}{4\alpha^2} \left[\frac{25}{\alpha^4} + \frac{65}{3\alpha^2} + 4 - \left(\frac{25}{\alpha^4} + \frac{30}{\alpha^2} + 9 \right) \beta \right]
\end{aligned} \tag{17}$$

Evaluation of Equation (11) with $B = iC$ results in

$$\begin{aligned}
A_{00} &= \beta = \frac{\tanh^{-1} \alpha}{\alpha} \\
A_{01} &= \frac{1 - \beta}{\alpha} \\
A_{02} &= -\frac{3(1 - \beta)}{2} \frac{\beta}{\alpha^2} - \frac{\beta}{2} \\
A_{11} &= -\frac{1 - \beta}{\alpha^2} \\
A_{12} &= \frac{3(1 - \beta)}{2} \frac{\beta}{\alpha^3} + \frac{\beta}{2\alpha} \\
A_{22} &= \frac{1}{4\alpha} \left[\left(\frac{9}{\alpha^3} - \frac{6}{\alpha} + \alpha \right) \beta + \frac{3}{\alpha} - \frac{9}{\alpha^3} \right] \\
A_{03} &= -\frac{1}{2\alpha} \left[\left(\frac{5}{\alpha^2} - 3 \right) \beta + \frac{4}{3} - \frac{5}{\alpha^2} \right] \\
A_{13} &= \frac{1}{2\alpha^2} \left[\left(\frac{5}{\alpha^2} - 3 \right) \beta + \frac{4}{3} - \frac{5}{\alpha^2} \right] \\
A_{23} &= \frac{1}{4\alpha} \left[\frac{15}{\alpha^4} - \frac{9}{\alpha^2} + \frac{4}{3} - \left(\frac{15}{\alpha^4} - \frac{14}{\alpha^2} + 3 \right) \beta \right] \\
A_{33} &= -\frac{1}{4\alpha^2} \left[\frac{25}{\alpha^4} - \frac{65}{3\alpha^2} + 4 - \left(\frac{25}{\alpha^4} - \frac{30}{\alpha^2} + 9 \right) \beta \right]
\end{aligned} \tag{18}$$

Evaluation of Equation (11) with $B = -iC$ results in

$$\begin{aligned}
A_{00} &= \beta = \frac{\tanh^{-1} \alpha}{\alpha} \\
A_{01} &= \frac{\beta - 1}{\alpha} \\
A_{02} &= -\frac{3(1 - \beta)}{2\alpha^2} - \frac{\beta}{2} \\
A_{11} &= \frac{\beta - 1}{\alpha^2} \\
A_{12} &= \frac{3(\beta - 1)}{2\alpha^3} - \frac{\beta}{2\alpha} \\
A_{22} &= \frac{1}{4\alpha} \left[\left(\frac{9}{\alpha^3} - \frac{6}{\alpha} + \alpha \right) \beta + \frac{3}{\alpha} - \frac{9}{\alpha^3} \right] \\
A_{03} &= -\frac{1}{2\alpha} \left[\left(\frac{5}{\alpha^2} - 3 \right) \beta - \frac{4}{3} + \frac{5}{\alpha^2} \right] \\
A_{13} &= \frac{1}{2\alpha^2} \left[\left(\frac{5}{\alpha^2} - 3 \right) \beta + \frac{4}{3} - \frac{5}{\alpha^2} \right] \\
A_{23} &= \frac{1}{4\alpha} \left[-\frac{15}{\alpha^4} + \frac{9}{\alpha^2} - \frac{4}{3} + \left(\frac{15}{\alpha^4} - \frac{14}{\alpha^2} + 3 \right) \beta \right] \\
A_{33} &= -\frac{1}{4\alpha^2} \left[\frac{25}{\alpha^4} - \frac{65}{3\alpha^2} + 4 - \left(\frac{25}{\alpha^4} - \frac{30}{\alpha^2} + 9 \right) \beta \right]
\end{aligned} \tag{19}$$

Thus, using the coefficients defined by Equation (17), (18), and (19), Equation (7) defines the B_3 fluxes, which are all real. When B is real, the spatial distribution is of cosine(Bx), where B^2 is the geometric buckling of the fundamental mode of the critical homogeneous geometry. When $B = iC$ with a real constant C , the spatial distribution is of positive exponential form with the negative buckling. In this case, there is a neutron leakage into the region, i.e., a negative leakage, which might be useful under certain circumstances. When $B = -iC$ with a real constant C , the spatial distribution is of negative exponential form with the negative buckling and the solution would behave like the case with the positive buckling. In the COMBINE7.1 coding, the series expansions of $\tan^{-1} \alpha$ and $\tanh^{-1} \alpha$ are utilized to calculate these coefficients. The fundamental limitation of the cases with the negative buckling is in the fact that solutions involve a hyperbolic tangent, $\tanh^{-1}(B/\Sigma_t)$. As can be seen in

$$\tanh^{-1}(B/\Sigma_t) = \frac{1}{2} \log \left[\frac{(1 + B/\Sigma_t)}{(1 - B/\Sigma_t)} \right],$$

B/Σ_t should be less than 1. Normally, B/Σ_t is much less than 1; however, it can be reset to a value less than 1 (0.8, e.g.) to avoid divergence when it is large.

The energy dependence of Equation (7) is approximated by a 167 fine group representation, spanning the energy range from 20 MeV to 1.0E-5 eV, for solution of the neutron spectrum. Integrating Equation (7) over the group energy interval, i.e., $E_g \leq E \leq E_{g-1}$ and truncating to L+1 terms generates

$$\begin{aligned} \phi_n^g &= \sum_{l=0}^L (2l+1) \frac{A_{nl}^g}{\Sigma_t^g} \sum_{g'=1}^G \sum_{sl}^{g' \rightarrow g} \phi_l^{g'} \frac{\Delta g'}{\Delta g} + \frac{A_{n0}^g}{\Sigma_t^g} \frac{\chi^g}{\Delta g} \end{aligned} \quad (20)$$

where

$$\begin{aligned} \phi_n^g &= \int_{E_g}^{E_g^{g-1}} \phi_n(E) \frac{dE}{E} / \Delta g \\ \Delta g &= \int_{E_g}^{E_g^{g-1}} \frac{dE}{E} \end{aligned}$$

The maximum group number is designated as G in Equation (20). It is noted that the fluxes are now expressed as per-unit energy in lethargy coordinates. Equation (20) includes neutrons scattered down from all higher energy groups. It also includes neutrons scattered up from all lower energy groups if thermal upscattering occurs.

The B_3 solution to Equation (20) is given by the following matrix equation for each energy group g.

$$\left[I - C_g \right] \Phi_g = R_g \quad (21)$$

$$\Phi_g = \left[\Phi_0^g, \Phi_1^g, \Phi_2^g, \Phi_3^g \right]. \quad (22)$$

$$C_{nl}^g = (2l+1) \frac{A_{nl}^g}{\Sigma_t^g} \sum_{sl}^{g \rightarrow g} \quad (23)$$

where I is the four-rowed unit matrix, C_g is the matrix with 4 rows and 4 columns, and n, l are the row and column index, respectively, for C_g in Equation (21).

$$R_n^g = \frac{A_{n0}^g}{\Sigma_t^g} \frac{\chi^g}{\Delta g} + \sum_{l=0}^3 (2l+1) \frac{A_{nl}^g}{\Sigma_t^g} \sum_{g'=1, g' \neq g}^G \sum_{sl}^{g' \rightarrow g} \Phi_l^{g'} \frac{\Delta g'}{\Delta g} \quad (24)$$

$$R_g = \left[R_0^g, R_1^g, R_2^g, R_3^g \right]. \quad (25)$$

When there is no thermal upscattering, Equation (21) is solved by Gauss elimination, sweeping from the highest energy to the lowest energy. When the thermal upscattering is present, it is solved by the combination of Gauss elimination and Gauss-Seidel iterative scheme. In this case, the thermal upscattering terms will be included, initially using assumed flux guess.

The fission source, χ , can be chosen from a fissile/fissionable isotope or calculated from the steady-state and fission rate weighted source spectrum. The steady-state fission spectrum for an isotope, i , is defined by

$$\chi_{i,g}^{SS} = \frac{\sum_{g'} \sigma_{f,g' \rightarrow g} \Phi_{g'} + \chi_g^D \sum_{g'} \nu_{g'}^D \sigma_{f,g'} \Phi_{g'}}{\sum_g \sum_{g'} \sigma_{f,g' \rightarrow g} \Phi_{g'} + \sum_g \chi_g^D \sum_{g'} \nu_{g'}^D \sigma_{f,g'} \Phi_{g'}}. \quad (26)$$

The fission rate weighted spectrum is then

$$\chi_g = \frac{\sum_i \chi_{i,g}^{SS} \sum_{g'} v_{tot,g'}^i N_i \sigma_{f,g'}^i \Phi_{g'}}{\sum_i \sum_{g'} v_{tot,g'}^i N_i \sigma_{f,g'}^i \Phi_{g'}}. \quad (27)$$

The flux as defined in Equation (41) and included in the cross section library is initially used in Equation (27) and then the B_N spectrum calculated flux when once more spectrum calculation is performed.

2.1.2 B-1 Approximation

The B_1 equations can be the degenerate forms of B_3 . Instead, B_1 equations with real B for instance are derived from Equation (7), emphasizing the physical approximations

$$\begin{aligned} & \phi_0(B, E) \\ &= \frac{\beta}{\Sigma_t(E)} \int T_{S0}(E' \rightarrow E) \phi_0(B, E) dE' + 3 \frac{(\beta-1)}{\alpha \Sigma_t} \int T_{S1}(E' \rightarrow E) \phi_1(B, E) dE' + \frac{\beta}{\Sigma_t} \chi(E) \end{aligned} \quad (28)$$

$$\begin{aligned} & \phi_1(B, E) \\ &= -\frac{(\beta-1)}{\alpha \Sigma_t(E)} \int \Sigma_{S0}(E' \rightarrow E) \phi_0(B, E) dE' + 3 \frac{(1-\beta)}{\alpha^2 \Sigma_t(E)} \int \Sigma_{S1}(E' \rightarrow E) \phi_1(B, E) dE' - \frac{(\beta-1)}{\alpha \Sigma_t(E)} \chi(E) \end{aligned} \quad (29)$$

Solve Equations (28) and (29) for ϕ_0 and ϕ_1 to obtain

$$B\Phi_1 + \Sigma_t\Phi_0 = \int_{E'} \Sigma_{S0}(E' \rightarrow E)\Phi_0(E')dE' + \chi(E), \quad (30)$$

$$\gamma(E)\Sigma_t(E)\Phi_1(E) - \frac{B}{3}\Phi_0(E) = \int_{E'} \Sigma_{S1}(E' \rightarrow E)\Phi_1(E')dE' \quad (31)$$

where

$$\gamma(E) = \frac{1}{3} \frac{\beta\alpha^2}{(1-\beta)}.$$

$\Phi_0(E)$ and $\Phi_1(E)$ are interpreted as the energy-dependent flux and current, respectively. By examining Equations (30) and (31), it is seen that the B_1 approximation differs from the P_1 approximation by the factor $\gamma(E)$ in Equation (31). If $\gamma(E)$ is set to equal to 1.0, Equations (30) and (31) become the continuity equations for the P_1 approximation. The factor $\gamma(E)$ tends to improve the B_1 estimation of the energy-dependent transport current, $\Phi_1(E)$, for small homogeneous system.¹⁶

Similarly, for $B = -iC$

$$-C\Phi_1 + \Sigma_t\Phi_0 = \int_{E'} \Sigma_{S0}(E' \rightarrow E)\Phi_0(E')dE' + \chi(E), \quad (32)$$

$$-\gamma(E)\Sigma_t(E)\Phi_1(E) - \frac{C}{3}\Phi_0(E) = \int_{E'} \Sigma_{S1}(E' \rightarrow E)\Phi_1(E')dE' \quad (33)$$

For $B = iC$

$$C\Phi_1 + \Sigma_t\Phi_0 = \int_{E'} \Sigma_{S0}(E' \rightarrow E)\Phi_0(E')dE' + \chi(E), \quad (34)$$

$$-\gamma(E)\Sigma_t(E)\Phi_1(E) + \frac{C}{3}\Phi_0(E) = \int_{E'}\Sigma_{s1}(E' \rightarrow E)\Phi_1(E')dE' \quad (35)$$

Equations (30) and (31) in multigroup form reduce to

$$B\Phi_1^g + \sum_t^g \Phi_0^g = \sum_{s_0=1}^G \sum_{s_1=0}^{g \rightarrow s_0} \Phi_0^{s_1} \frac{\Delta g'}{\Delta g} + \frac{\chi^g}{\Delta g} \quad (36)$$

and

$$\gamma^g \sum_t^g \Phi_1^g - \frac{B}{3}\Phi_0^g = \sum_{s_1=1}^G \sum_{s_0=1}^{g \rightarrow s_1} \Phi_1^{s_0} \frac{\Delta g'}{\Delta g} . \quad (37)$$

Equations similar to (36) and (37) are derived for imaginary B from Equations (32) through (35) with variations of sign. These equations are solved simultaneously as

$$\Phi_0^g = \frac{R_0^g (\gamma^g \sum_t^g - \sum_{s_1}^{g \rightarrow s_0}) - BR_1^g}{(\sum_t^g - \sum_{s_0}^{g \rightarrow s_0}) (\gamma^g \sum_t^g - \sum_{s_1}^{g \rightarrow s_0}) + \frac{B^2}{3}} \quad (38)$$

$$\Phi_1^g = \frac{R_1^g + \frac{B}{3}\Phi_0^g}{\gamma^g \sum_t^g - \sum_{s_1}^{g \rightarrow s_0}} \quad (39)$$

where

$$R_0^g = \sum_{g'=1, g' \neq g}^G \sum_{s_0=0}^{g' \rightarrow g} \Phi_0^{s_0} \frac{\Delta g'}{\Delta g} + \frac{\chi^g}{\Delta g} \quad \text{and} \quad R_1^g = \sum_{g'=1, g' \neq g}^G \sum_{s_1=1}^{g' \rightarrow g} \Phi_1^{s_1} \frac{\Delta g'}{\Delta g}$$

When upscattering is present, Gauss-Seidel iterative scheme is used.

2.1.3 Convergence on Gauss-Seidel Iterative Scheme

The calculation will be converged when the following equations are satisfied at all energy points.

$$\frac{|\phi_i^{(m+1)} - \phi_i^{(m)}|}{\phi_i^{(m+1)}} < \varepsilon \quad \text{and} \quad \frac{|J_i^{(m+1)} - J_i^{(m)}|}{J_i^{(m+1)}} < \varepsilon ,$$

where ε is the user input convergence criteria. The results are then normalized to have one total scalar flux.

2.2 Bondarenko Method

The multigroup approximation requires the groupwise cross sections and the energy texture is necessarily coarse with respect to the resonance structure in many materials. The resonance results in self-shielding effect. The magnitude of this self-shielding effect is in general a complicated function of the geometry and composition of the system. However, it has been found that a simple model called the Bondarenko Method⁸ or Background Cross Section Method¹⁷ does a surprisingly good job of representing the effects for many applications.⁹ This method was adopted in the NJOY's GROUPR and MATXS modules and the TRANSX code.¹⁰ COMBINE7.1 followed those steps taken in the NJOY and TRANSX codes. The flux is assumed to vary inversely as the total macroscopic cross section. In the Bondarenko model, the narrow resonance (NR) approximation and the B_N approximation for large systems are invoked.⁹ The model flux for the group averages for isotope i is written as

$$\Phi_l^i(E) = \frac{C(E)}{[\sigma_0^i + \sigma_l^i(E)]^{l+1}} \quad (40)$$

where $C(E)$ is the smooth part of the shape of the flux, $\sigma_l^i(E)$ is the microscopic total cross section for isotope i , and σ_0^i is called the background cross section (it represents the effects of all the other isotopes). The effect of the total cross section in the denominator is to put a dip in the flux for each peak in the cross section, and σ_0^i controls the relative size of the dip. A resonance material in a dilute mixture or in small pieces does not disturb a smooth flux very much by its presence—this is called the infinitely dilute case. When σ_0^i approaches a very large number, it becomes an infinitely dilute case. The l dependence shown here is appropriate for a large system with nearly isotropic scattering (the B_0 approximation), and it was used when the MATXS file was generated from NJOY.

The multigroup form of this model flux is

$$\Phi_{lg}^i = \frac{C_g}{[\sigma_{0,g}^i + \sigma_{t,g}^i]^{l+1}} \quad (41)$$

The resonance absorption changes with the temperature due to Doppler broadening of the resonances. In order to take into account the effect of Doppler broadening, the basic cross sections in the resonance region must be adjusted appropriately for the broadening before they are used in computing group constants.

The Bondarenko method is basically an “infinite medium” method that parameterizes cross sections for a nuclide as a function of temperature, T , and the “background dilution” cross section, σ_0 , of all other nuclides mixed with the nuclide. Simplistically, given the temperature and background dilution cross-section values, one determines self-shielded cross sections by interpolating in tables. Since self-shielding causes the “background dilution” values that a nuclide sets to change, an iterative procedure involving all nuclides is used. The geometric lump effect when present is accounted for by augmenting the background cross section.

For a homogeneous mixture, the appropriate background cross section is

$$\sigma_{0,g}^i = \frac{1}{N_i} \cdot \sum_{j \neq i} N_j \cdot \sigma_{t,g}^j(\sigma_{0,g}^i) \quad (42)$$

Where N is the number density for the isotope and $\sigma_{t,g}$ is the self-shielded total cross section of an energy group g . Because $\sigma_{t,g}$ depends on $\sigma_{0,g}$, finding $\sigma_{0,g}$ is an iterative process. For a mixture of resonance materials, interference between resonances in different materials is handled in an average sense only.

For a lump of resonance material embedded in a large moderating region, escapes from the lump also increase the background cross section. To account for this, the $\sigma_{0,g}$ value is augmented by an escape cross section

$$\sigma_{e,g}^i = \frac{1}{N_i \bar{l}} \quad (43)$$

where \bar{l} is the mean chord length of lump given by

$$\bar{l} = \frac{4V}{S} \quad (44)$$

and where V and S are the volume and surface area of the lump. Multizone situations, such as reactor lattices, are accounted for by the use of Dancoff factors, which, in effect, modify the escape probability and, hence, the value of σ_e . The mean chord length \bar{l} can be adjusted away from the geometric value of Equation (44) to compensate for the presence of other lumps (Dancoff correction) or for shortcoming in the escape probability model used to obtain Eq. (43). In the rational approximation, the Dancoff correction is equivalent to increasing the mean chord length, \bar{l} , by the factor $1/(1-c)$ or equivalently decreasing the surface area of lump by $1-c$ as in

$$\sigma_{e,g}^i = \frac{1}{N_i \cdot \bar{l} \cdot \frac{1}{(1-c)}} \quad (45)$$

when Bell corrections are applied

$$\sigma_{e,g}^i = \frac{1}{N_i \cdot \bar{l}} \cdot \frac{b_1 \cdot (1-c)}{1 + (b_2 - 1) \cdot c} \quad (46)$$

where b_1 and b_2 are called Bell corrections. When $b_1 = b_2$, the constant is usually called the Levine factor and Equation (46) becomes

$$\sigma_{e,g}^i = \frac{1}{N_i \cdot \bar{l}} \cdot \frac{1}{\frac{1}{b} + \frac{c}{1-c}} \quad (47)$$

where

- $b = 1.26$ for the slab geometry
- $= 1.35$ for the cylindrical geometry
- $= 1.30$ for the spherical geometry.

The so-called ‘‘Levine factors,’’ b , are approximate geometry dependent factors that are approximately correct for inaccuracies in the Rational Approximation.

When a double heterogeneity occurs due to fuel grains present within the macroscopic fuel lump, the Dancoff factor c' specifies the mutual shielding between these grains, independent of c for the lumps themselves. To better account for the double heterogeneity due to fuel grains present within the macroscopic fuel lump, a correction has been made to the escape probability and given by Stamatelatos and LaBauve¹⁸ as

$$\sigma_{e,g}^i = \frac{1}{N_i \left[\bar{l} \cdot \left(\frac{1}{b} + \frac{c}{1-c} \right) + \bar{l}_g \left(\frac{1}{a} + \frac{c'}{1-c'} \right) \right]} \quad (48)$$

where

- $\bar{l}_g =$ the average chord length of a single isolated spherical fuel grain
- $c' =$ the Dancoff factor for fuel grains
- $A = 1.77$, the Levine factor for spherical grains.

The following equation for the background cross section has been applied

$$\sigma_{0,g}^i = \sigma_{e,g}^i + \frac{\sum_{i \neq j} N_j \cdot \sigma_{t,g}^j(\sigma_{0,g}^j)}{N_i} . \quad (49)$$

2.2.1 Fine-Group Cross Section Generation in Bondarenko Format

In COMBINE7.1, a 167 fine group structure is used and the multigroup cross section constants are generated in this fine group structure to be used in the B_N solution.

The NJOY99.259 version¹⁵ was used to generate a 167 fine-group cross-section library, MATXS.LIB, in MATXS format (Bondarenko format) on sets of background cross sections and temperatures including thermal scattering cross sections. For $C(E)$ in Equation (40), an NJOY built-in spectrum, Thermal--1/E--Fast Reactor--Fission + Fusion, is used. The equations providing the fundamental definitions in NJOY for the multigroup cross sections and the group-to-group matrix are

$$\sigma_{t,l,g} = \frac{\int_g \sigma_t(E) \phi_l(E) dE}{\int_g \phi_l(E) dE} , \quad (50)$$

$$\sigma_{x,g} = \frac{\int_g \sigma_x(E) \phi_0(E) dE}{\int_g \phi_0(E) dE} , \quad (51)$$

$$\sigma_{x,l,g' \rightarrow g} = \frac{\int_g dE \int_{g'} dE' \sigma_{xl}(E' \rightarrow E) \phi_l(E)}{\int_g \phi_l(E) dE} . \quad (52)$$

The energy-dependent cross-section database is now derived entirely from ENDF/B-VII.0 nuclear data with the exception of Zr element cross-section data, which is based on ENF/B-VI.8 nuclear data. All materials have either $S(\alpha,\beta)$ or free thermal scattering matrices.

2.2.2 Bondarenko Self-Shielding Interpolation

Bondarenko self-shielding is performed in COMBINE7.1 by background cross section and temperature interpolation. The interpolation is first performed for the background cross sections at each temperature. The generated cross sections for the set of preselected temperatures are then interpolated for the problem-dependent temperature. In the background cross-section interpolation, a log-log N^{th} order for the vector cross sections, and log-linear N^{th} order Lagrangean schemes are employed with a variation to the first order for the extremely high or low problem-dependent background cross section. The temperature interpolation uses a log-log N^{th} order Lagrangean scheme. Iteration is necessary to arrive at the correct background cross sections. Three iterations are performed for all isotopes. The first iteration is based on the infinite dilution of the rest isotopes for total cross sections. The accuracy, convergence, and stability of these schemes have been sufficiently tested and are satisfactory.

2.3 Resonance Region

The material cross-section libraries supplied for each material have complete multigroup cross sections based on Bondarenko method. The weakness of the Bondarenko model occurs for thermal reactor analysis in the “epithermal” energy region from about 4 eV to around 200 or 300 eV.¹⁰ In this region, the resonances are no longer narrow, and the flux shape given by Equation (40) is no longer sufficiently accurate. For those materials where resolved resonance parameters are present via RERES.LIB, a Nordheim numerical solution¹¹ is applied as an option. Before B_1 or B_3 Equations are solved, the resonance parameters in the material libraries must be converted into average, self-shielded, temperature dependent, groupwise cross sections.

2.3.1 Resolved Resonances—Nordheim Numerical Method

The balance equation for the collision density in a homogeneous mixture of moderators and resonance absorbers in an infinite medium is¹⁹

$$F(E) = \phi(E) \Sigma_t(E) = \sum_k \int_E^{E/\alpha_k} \frac{\phi(E') \Sigma_s^k(E') dE'}{(1 - \alpha_k) E'} \quad (53)$$

where

$\phi(E)$ = scalar neutron flux

Σ_t = total macroscopic cross section

Σ_s^k = $N_k \sigma_{sk}$ = macroscopic scattering cross section for material k

N_k = atomic density of material k

σ_k = microscopic cross section of material k

$\alpha_k = \left(\frac{A_k - 1}{A_k + 1} \right)^2$, A_k = ratio of isotopic mass to mass of the neutron for material k

$F(E)$ = collision density at energy E.

The right-hand side of Equation (53) requires a different integration limit for each moderator k. The flux $\phi(E)$ at each resolved resonance undergoes a severe depression at each strongly absorbing resonance. One or many resonances may fall within any given COMBINE multigroup. The average, self-shielded, absorption integral in each multigroup g within the resonance range is then given by

$$I_{ag}^k = \int_{E_g}^{E_{g+1}} \phi(E) \sigma_c^k(E) dE \quad (54)$$

where $\phi(E)$ is the solution of Equation (53) over the energy interval for the multigroup and σ_c is the capture cross section. Equation (53) is solved in lethargy space where

$$du = -\frac{dE}{E}$$

$$dE = -E du$$

$$E = E_1 e^{-u}$$

Therefore, $dE = -E_1 e^{-u} du$.

Equation (55) is transformed to¹¹

$$\begin{aligned}
I_{cg}^k &= E_1 \int_{u_{g-1}}^{u_g} \phi[E(u)] \sigma_c^k [E(u)] e^{-u} du \\
I_{cg}^k &= E_1 \int_{u_{g-1}}^{u_g} F[u(E)] \frac{\sigma_c^k(u) e^{-u}}{\Sigma_t(u)} du
\end{aligned} \tag{55}$$

where $F[u(E)]$ is the collision density per unit energy in lethargy coordinates. The mixed lethargy-energy form of Equation (55) results from the fact that the integration is performed on a lethargy mesh, but the resonance cross sections are calculated in energy space because the cross sections are not easily transformed to lethargy coordinates. Equations similar to Equation (55) may be written for the fission and elastic scattering integrals using $\sigma_f^k(u)$ or $\sigma_s^k(u)$ in place of $\sigma_c^k(u)$.

If absorption occurs in an isolated lump surrounded by an infinite sea of moderators, the introduction of the lump escape probability²⁰ $P_0(\bar{l}, \Sigma_t)$, is given in terms of the average chord length of the lump, \bar{l} . This enables Equation (53) to be modified to closely approximate the heterogeneous absorption rate in the lump-moderator assembly. The collision density in the lump now consists of two distinct types of events:

1. Those neutrons that have had their last collision in the lump, which is given by the right-hand side of Equation (53) multiplied by the probability of colliding in the lump, $[1 - P_0(\bar{l}, \Sigma_t)]$, times V_F , the volume of the fuel lump.
2. Those neutrons that stream into the lump at lethargy $u(E)$ from outside the lump, multiplied by the moderator escape probability²⁰ $P_M(\bar{l}, \Sigma_t)$, times the volume of the external moderator, V_M , contained in a unit cell.

$$V_F F(u) = V_F \left[1 - P_0(\bar{l}, \Sigma_t) \right] \sum_k \frac{1}{1 - \alpha_k} \int_{u - \varepsilon_k}^u F(u') \frac{\Sigma_s^k(u')}{\Sigma_t(u')} du' + V_M P_M \phi_M(u) \Sigma_M(u) \tag{56}$$

where

$$\varepsilon_k = 1n \left(\frac{1}{\alpha_k} \right)$$

and $\phi_M(u)$ is the average, asymptotic, equilibrium neutron flux in the moderator residing outside the lump. The normalization of Equation (56) is arbitrary, since the point wise collision density $F(u)$ will only be used to obtain average cross sections over the multigroups in the resolved resonance range.

$\phi[u(E)]$ is set equal to $1/E$ in the region outside the lump, i.e., $\phi_{asym}[u(E)] = e^u / E_1$.

The moderator terms in Equation (56) may be removed by means of the reciprocity relation⁹

$$P_M V_M \Sigma_M = P_F V_F \Sigma_{tF} \tag{57}$$

Equation (56) then becomes

$$F(u) = (1 - P_0) \sum_{k=1}^7 \frac{1}{1 - \alpha_k} \int_{u - \varepsilon_k}^u F(u') \frac{\sigma_s^k(u')}{\sigma_t(u')} du' + P_0 \sigma_t(u) \frac{e^u}{E_1} \tag{58}$$

where σ_s^k and σ_t are given by Equations (62) and (63), expressed in terms of the scattering per absorber atom.

$$P_0 = P_0(\bar{l}, \Sigma_t) \quad (59)$$

where

$$\bar{l} = \bar{l}_0 = \frac{4V}{S}, \text{ single isolated lump}$$

$$\frac{V}{S} = \text{ratio of volume of the absorber lump to the surface area}$$

$$= 1/2 \times \text{half thickness—plate geometry}$$

$$= 1/2 \times \text{radius—cylindrical geometry}$$

$$= 1/3 \times \text{radius—spherical geometry}$$

The escape probability P_0 is tabulated¹¹ for single isolated lumps. When a Dancoff factor C is incorporated to represent the mutual shielding in a repetitive array,²¹ the escape probability P_0 is modified to be^{1,22}

$$P = \frac{GP_0(1-C)}{\left[1 - (1 - \bar{l}\Sigma_t P_0)C\right]} \quad (60)$$

where P_0 in Equation (60) is the escape probability for a single isolated lump, P represents the mutually shielded value, C is the Dancoff Ginsberg correction factor for a regular array of lumps, and G is a double heterogeneity correction for the self-shielding of fuel grains within the absorber lump²³

$$G = \left[1 + \sum_t \bar{l}_g \left(\frac{1}{a} + \frac{C'}{1-C'}\right)\right]^{-1} \quad (61)$$

where

$$\bar{l}_g = \text{average chord length within a fuel grain, independent of } \bar{l}, \text{ the average chord length in the lump}$$

$$C' = \text{Dancoff factor for the fuel grains in the lump, independent of } C$$

$$a = 1.77\text{—the Levine factor for spherical grains, A correction factor for the Wigner Rational Approximation for } P_0, \text{ which is employed in deriving Equation (62).}$$

When a double heterogeneity occurs due to fuel grains present within the macroscopic fuel lump, the Dancoff factor C' specifies the mutual shielding between these grains, independent of C for the lumps themselves.

In Equation (58), up to seven moderators are included for the down scatter source within the lump, the first always being the absorber atom itself. Three additional moderators and three additional admixed resonance absorbers with different masses can also be included.³ This limit is felt to be sufficient for almost any fuel pin one would encounter in practice.

The cross sections in Equation (58) are evaluated relative to the number of absorber atoms as in

$$\sigma_s^k = \frac{\sum_s^k}{N_a} \quad (62)$$

where

N_a = atom density of the absorber atom in the lump.

$$\sigma_t = \sigma_a + \sigma_s + \sigma_m^1 + \sigma_m^2 + \sigma_m^3 + \sigma_a^1 + \sigma_s^1 + \sigma_a^2 + \sigma_s^2 + \sigma_a^3 + \sigma_s^3 \quad (63)$$

where: σ_s is the resonance scattering of the absorber atom itself; σ_m^i represents the three moderator's scattering cross sections per absorber atom; σ_a^i represents the three admixed absorber's absorption cross sections per absorber atom; and σ_s^i represents the three admixed absorber's scattering cross sections per absorber atom. The absorption cross section of the three additional moderators is assumed to be very small compared with the principal absorber or the admixed absorbers.

Equation (58) has proven itself to be remarkably accurate in many applications. A number of unique approximations are used in deriving Equation (58), the most important of which is the "flat flux assumption."²⁴ The spatial dependence of the flux across the lump has been subsumed into the escape probability P_0 , which permits the elimination of the spatial dependence of the flux in Equation (58). P_0 is evaluated as a function of energy only. The approximation which makes this possible is that at each energy, the escape probability is evaluated as if only the average flat flux in the lump were known relative to the asymptotic flat flux existing outside the lump. The escape probability P_0 under the flat flux approximation is then given by²⁴

$$P_0 \approx \frac{\bar{\phi}_{lump}}{\bar{\phi}_{asym}} \quad (64)$$

If an average flat flux can be assumed in the lump, the escape probability absorbs the spatial dependence in Equation (58). $P_0(\bar{l}, \Sigma_t)$ is evaluated at each energy across the resonance since $\Sigma_t(E)$ is a strong function of energy at resonance. Equation (64) is a truly remarkable result that makes possible a separate two-stage solution to a difficult problem; the first stage being the calculation of the escape probability P_0 .¹¹ Equation (58) is solved numerically on a very fine energy mesh across each lethargy group where one or more resonances may reside.

2.3.2 Doppler Broadening of Resolved Resonance Parameters

Subroutines adopted from the NJOY code and incorporated in COMBINE7.1 numerically Doppler broaden the SLBW, MLBW, and R-M format resonance parameters by the kernel broadening method.²⁵ The subroutines were verified by kernel broadening the SLBW option and comparing with that using the ψ - χ function that was used in the previous COMBINE versions. At each mesh point the capture, fission, and elastic cross sections are calculated, accumulating contributions from all the resonances in the same resonance range. Figure 2 shows the Doppler broadened cross section as an example.

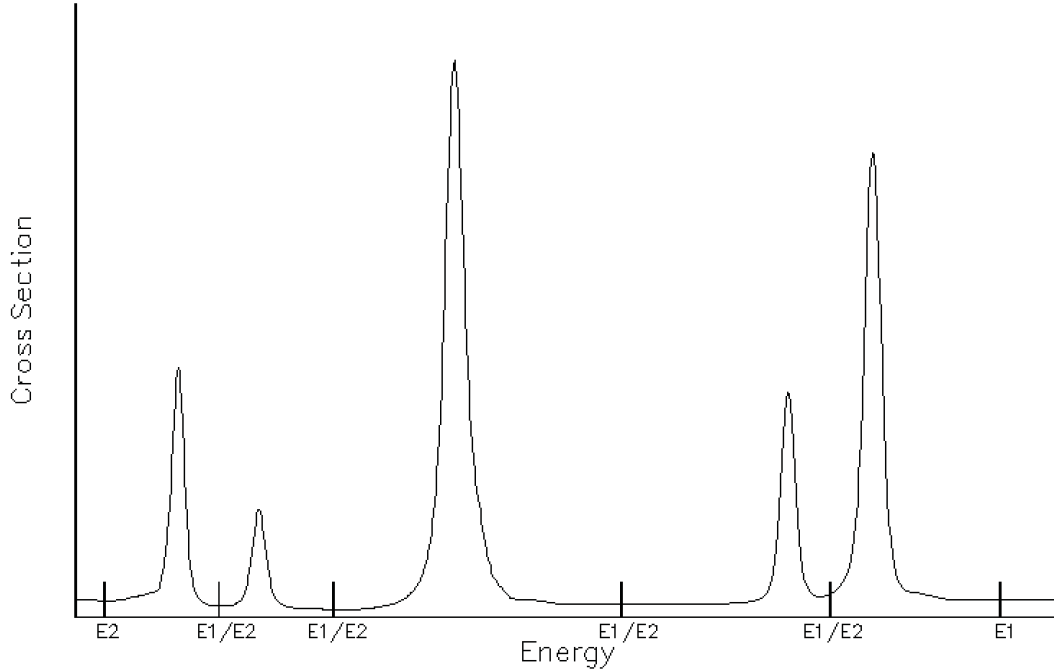


Figure 2. An example of Doppler broadened resonance cross sections.

2.3.3 Determination of E_1/E_2 and the Number of Meshes for a Resonance

The first energy, E_1 , corresponds to the first fine group energy boundary encountered just below the upper limit of the highest resolved resonance energy range. It can be the user input at any fine group energy boundary lower than that. The next E_1 (or E_2) is at the midpoint between the next two neighboring resonances, and so on. The lowest E_2 is also adjusted to correspond to the fine group energy boundary. For each resonance, a resonance integration interval is formed by E_1 and E_2 . Considering an equal lethargy interval solution, a mesh size and the number of mesh intervals within the resonance integration are calculated according to the following recipe, which was adopted from GAM-II code²² and modified.

$$r = 5.0 + 0.5 \sqrt{K * 273.0 * E_0 / AWRI} / \Gamma \quad (65)$$

$$\varepsilon = 1.0 / [AWR * \text{int}\{0.5 * r * \sqrt{1.0 / (K * 273.0 * AWRI)} * |E_0| + 1.0\} * \text{fmult}] \quad (66)$$

$$\text{mesh} = \frac{\log(E_1 / E_2)}{\varepsilon} \quad (67)$$

where: mesh is the number of mesh intervals, K is the Boltzmann constant = 8.6173×10^{-5} eV/K, the constant 273.0 defines the mesh reference temperature T_0 , $AWRI$ is the ratio of mass of a particular isotope to that of a neutron, Γ is the total resonance width, E_1 and E_2 are the high and low energy boundaries of the integration for a resonance, E_0 is the resonance energy, and fmult is the user input control parameter to make mesh coarse or finer (default= 1.0).

The number of mesh intervals is then made to be an even number so that the total number of mesh points become odd for Simpson's integration. The last mesh point of the previous resonance integration interval corresponds to the first mesh point of the present resonance integration interval, and so on. The lethargy mesh is generated independently for each resonance from midpoint to midpoint between resonances; therefore, the mesh spacing from resonance to resonance varies. The highest E_1 and lowest E_2 can be controlled by user input, other than the default values set in "reres.lib" and adjusted to the group boundaries in the code. The maximum allowable number of mesh intervals in a resonance

integration interval is coded to be 1400. When the admixed resonance absorbers are present, the Doppler broadened cross sections are generated over these mesh points.

2.3.4 Absorber Narrow Resonance- Moderator Asymptotic Flux Approximation

In the Narrow Resonance (NR) approximation, the resonances are so narrow that all moderators, including the absorber, can scatter past the resonance. The scattering cross section over most of this range is essentially just that for potential scattering σ_p . The integral term in Equation (56) becomes

$$\frac{1}{1-\alpha_k} \int_{u-\varepsilon_k}^u F(u') \frac{\sigma_s^k(u')}{\sigma_t(u')} du' = \frac{\sigma_p^k}{1-\alpha_k} \cdot \int_{u-\varepsilon_k}^u \phi(u') du' = \frac{\sigma_p^k}{1-\alpha} \cdot \int_{u-\varepsilon_k}^u \frac{e^{u'}}{E_1} du' = \sigma_p^k \frac{e^u}{E_1}, \quad (68)$$

when the asymptotic flux, $\phi_{asym}[u(E)] = e^u / E_1 = w(u)$, is applied.

The criteria to determine this approximation is when $\ln(\frac{E_i}{\alpha E_1}) / \varepsilon \leq 1001$.

In the thermal energy range, $E \leq 5kT$, the flux shape is rather Maxwellian than e^u/E_1 ,²⁶

$$\phi_{asym}[u(E)] = 5.936526 / (kT)^2 \cdot E_1 e^{-u} e^{\frac{E_1 e^{-u}}{kT}} = w(u). \quad (69)$$

2.3.5 Self-Shielding Elastic Scattering Transfer Matrix

The solution of Equation (20) or (38) and (39) requires the self-shielded resolved resonance contributions to the elastic scatter matrix for the Legendre moments through $L = 3$ or $L = 1$, respectively. Departing from the previous versions, a simple normalization scheme is employed for this, utilizing the already available transfer matrix from Bondarenko self-shielded transfer matrix,

$$\sigma_{s,g' \rightarrow g}^l = (\sigma_{s,g' \rightarrow g}^l)_{Bondarenko} \cdot \frac{(\sigma_{s,g'}^0)_{Nordheim}}{(\sigma_{s,g'}^0)_{Bondarenko}}. \quad (70)$$

2.3.6 Numerical Integration with Simpson's Rule

Combining the integral form, absorber narrow resonance-moderator asymptotic flux approximation, and the thermal upscattering term, the numerical integration is expressed as

$$F(u) = \left\{ 1 - (1-P(u)) \frac{\varepsilon}{3\sigma_t(u)} \left[(\delta(N_0) \frac{\sigma_{s0}(u)}{\alpha_0} + \sum_i^3 \delta(N_{a_i}) \frac{\sigma_{sa_i}(u)}{\alpha_{a_i}} + \sum_j^3 \delta(N_{m_j}) \frac{\sigma_{sm_j}(u)}{\alpha_{m_j}}) \right] \right\}^{-1} \cdot \left\{ (1-P(u)) \varepsilon \left[\frac{\delta(N_0)}{3\alpha_0} \frac{I}{u-n\varepsilon} F(u') \frac{\sigma_{s0}(u')}{\sigma_t(u')} + \sum_i^3 \frac{\delta(N_{a_i})}{3\alpha_{a_i}} \frac{I}{u-n\varepsilon} F(u') \frac{\sigma_{sa_i}(u')}{\sigma_t(u')} + \sum_j^3 \frac{\delta(N_{m_j})}{3\alpha_{m_j}} \frac{I}{u-n\varepsilon} F(u') \frac{\sigma_{sm_j}(u')}{\sigma_t(u')} \right] + \delta(up) \sum_{g'} F_{g'} \frac{\sigma_{sg' \rightarrow g}^{upscat}}{\sigma_{tg'}} \frac{\Delta g'}{\Delta g} \right\} + \left[(1-P(u)) (\delta(NR) \sigma_{p_0} + \sum_i^3 \delta(A_{a_i}) \sigma_{pa_i} + \sum_j^3 \delta(A_{m_j}) \sigma_{pm_j} + P(u) \sigma_t(u) \right] w(u) \quad (71)$$

where $\delta(N_x)$ means Nordheim integral treatment application for the resonance absorber, admixed resonance absorbers, admixed moderators, $\delta(NR)$, $\delta(A_a)$, $\delta(A_m)$ means application of absorber

narrow resonance-moderator asymptotic flux approximation instead of Nordheim integral treatment, δ (up) means application of upscattering when thermal upscattering is present

$$\begin{aligned} \int_{u-\varepsilon}^{u-\varepsilon} F(u') \frac{\sigma_s(u')}{\sigma_t(u')} = 2 \sum_{i=1}^2 (3-i) \sum_{j=1}^{\frac{n-i+1}{2}} F[u-(2j+i-2)\varepsilon] \frac{\sigma_s[u-(2j+i-2)\varepsilon]}{\sigma_t[u-(2j+i-2)\varepsilon]} \\ + F(u-\varepsilon n) \frac{\sigma_s(u-\varepsilon n)}{\sigma_t(u-\varepsilon n)} \end{aligned} \quad (72)$$

is the Simpson's rule integration.

When thermal upscattering is present, iteration is needed. Since the convergence is rapid when the available flux in the code is utilized, only once more iteration is performed.

2.3.7 Group Averaging

Two options are available for converting the resonance integrals in Equation (53) into average multigroup cross sections, depending on whether one desires averages over the whole cell or just over the absorber lump. The average cross section is defined by

$$\sigma_{xg} = \frac{E_1 \int_{u_{i-1}}^{u_i} F(u) \frac{\sigma_x(u)}{\sigma_t(u)} e^{-u} du}{E_1 \int_{u_{i-1}}^{u_i} \phi(u) e^{-u} du} \quad (73)$$

where σ_x is the reaction cross section being averaged, $F(u)$ is given by Equation (58), and σ_t is given by Equation (63). The reaction cross section is averaged over the absorber lump flux,

$$\phi(u) = F(u)/\sigma_t(u) = \text{lump flux}$$

After obtaining capture/fission and scattering cross sections from Nordheim treatment, these cross sections overwrite the previous cross sections.

2.3.8 Dancoff-Ginsburg Correction Factor Calculation

Computation of the Dancoff factor C for arbitrary shapes and spacing of lumps is very difficult. Most accurate determinations have been performed for regular arrays of cylindrical fuel pins. An external code like SUPERDAN can provide Dancoff factors.²⁷ One option in COMBINE is an exact calculation described below. In the event that a precise calculation is not possible due to geometric irregularity or nonavailability, Bell offers an approximate formula based on the most general assumptions, which can be used as a last resort. Bell's formula can be written as²⁸

$$C \approx \frac{\lambda_1}{\frac{4V_1}{S_a} + \lambda_1} \quad (74)$$

where

S_a = surface area of the absorbing lump

V_1 = the average external moderator volume per absorber lump

λ_1 = the external moderator mean-free-path in the same units as V_1 and S_a .

Equation (74) is deceptive in its simplicity considering the exact definition in Equation (75). It is exact in the limits of very large or very small lumps. The Rational Approximation for P_o has been used in deriving Equation (74) along with other assumptions, so it should be used only as a first order

approximation when no other method is available. Equation (74) can be used with any regular or irregular geometry and is independent of geometric details other than average values of V_1 and S_a . A precise calculation of C for cylindrical pins is included in COMBINE and is described below.

The cylindrical pin Dancoff correction is computed in COMBINE following the methods of Gelling and Sauer.²⁹ This correction may be calculated for an infinite lattice composed of cylindrical pins in either a rectangle or a hexagon. Pins are assumed to be black to resonance-energy neutrons.

The Dancoff correction is defined as:²⁴

$$C = \frac{\int dS \int \vec{n} \cdot \vec{\Omega} \exp[-\Sigma l(\vec{s}, \vec{\Omega})] d\Omega}{\int dS \int \vec{n} \cdot \vec{\Omega} d\Omega} \quad (75)$$

where $l(\vec{s}, \vec{\Omega})$ is a chord that extends from the lump surface element dS in the direction $\vec{\Omega}$ through the moderator to the point of intersection with a neighboring lump. Σ is the cross section for removal of neutrons from the energy range of the resonance and is the normal to the lump surface element.

In the case of a lattice composed of cylindrical pins, the Dancoff correction may be expressed as

$$C = \frac{4}{\pi} \int_0^{2\pi} \frac{d\rho}{2} \int_{-1}^1 \frac{d\xi}{2} K_{i3}[\Sigma R_0 \cdot S] \quad (76)$$

The parameters are defined in Figure 3, and

$$K_{i3} = \int_0^{\infty} \exp[-x \cosh(u)] \cosh^{-3} u du \quad (77)$$

is the Bickley function of the third order.

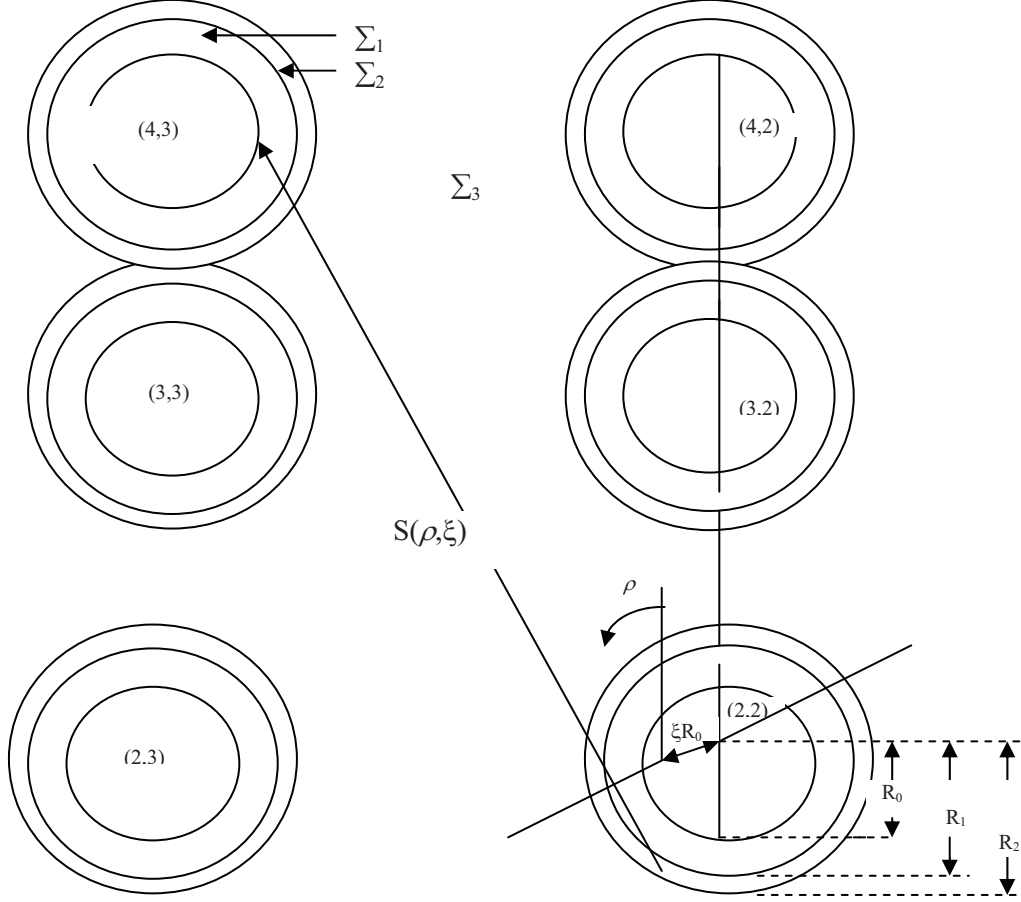


Figure 3. Parameters of the rectangular cell.

The two-dimensional lattice is represented exactly for a pin surrounded by up to four annular moderating regions and an external moderator. A library of pin configurations is contained within the code. A pin location is specified by the row n and the column m , where m and n are in units of pitch.

Heterogeneity of the moderating region is accounted for by defining the argument of the Bickley function²⁹ as

$$\sum R_0 \cdot S = R_0 \sum_{i=1}^N \Sigma_i S_i \quad (78)$$

where s_i is the length of the chord through region i , having total cross section Σ_i .

The integral in Equation (76) is evaluated using the trapezoidal approximation. Because of symmetry, the upper limit is taken as $\pi/4$ for a rectangular lattice and $\pi/6$ for a hexagonal lattice. The integral over ρ is evaluated by using 20 equal angular intervals, and for each value of ρ the integral over ξ is evaluated by using 100 increments of equal length. For each set of (ρ, ξ) values, the length of the chord S_i through each region is calculated and the Bickley function is evaluated by the approximation

$$K_{i3}(x) = \frac{e^{-x}}{(0.6366198x + 1.6211389)^{1/2}} \cdot \frac{x^2 + 6.399407x + 5.066719}{x^2 + 6.766116x + 5.066719} \quad (79)$$

This approximation yields values of $k_{i3}(x)$ to an accuracy of $\pm 0.05\%$.

2.4 Computation of Thermal Disadvantage Factors

The absorber lump appears black to neutrons at the peak resonance cross sections. For neutrons at thermal energies, the same lump is more than grey. As a consequence, corrections for thermal scattering are much more important. Amouyal and Benoist³⁰ have developed integral transport theory for the calculation of thermal disadvantage factors in grey absorber lumps. Strawbridge³¹ has modified this theory to include a third clad region. The three region cell equations for the point wise disadvantage factors W_i in a cylindrical cell are,³⁰

$$\frac{W(R_0)}{W_0} = 1 + \frac{\sum_{a0}(E)}{\sum_{t0}(E)} \left[\frac{1 - P_e}{P_e} - R_0 \sum_{t0}(E) \right] \times \left\{ 1 + \alpha \frac{\sum_{s0}(E)}{\sum_{t0}(E)} + \beta \left[\frac{\sum_{s0}(E)}{\sum_{t0}(E)} \right] \right\} \quad (80)$$

where

- W_0 = average energy dependent disadvantage factor in the cylindrical absorber rod
- $W(R_0)$ = energy dependent disadvantage factor at the surface of the absorber rod between the rod and the clad
- $\sum_{a0}(E)$ = absorption cross section in the absorber rod
- $\sum_{t0}(E)$ = total cross section in the absorber rod
- $\sum_{s0}(E)$ = scattering cross section in the absorber rod
- R_0 = radius of the absorber rod
- P_e = $P_e[\bar{l}_0, \sum_{t0}^*(E)]$ = the first flight escape probability in a cylindrical absorber rod at energy E

where

- $\bar{l}_0 = 2 R_0$
- α, β = tabulated empirical factors to correct the first flight escape probability P_e for the effects of scattering within the absorber rod.

Equation (80) resulted from considerations by A/B (Amouyal/Benoist) to adjust the first flight escape probability P_e (correct for a black pin) for the effects of scattering in a grey pin. The basis A/B thermal equation suppressing energy dependence, is

$$\frac{W(R_0)}{W_0} = \frac{1}{P_s(\bar{l}_0, \sum_{t0})} - R_0 \sum_{a0} \quad (81)$$

where P_s is the escape probability for a single grey pin corrected for multiple scattering within the pin.

$$P_s(\bar{l}_0, \sum_{t0}) = \left(1 + \frac{\sum_{a0}}{\sum_{t0}} \left\{ A \left[1 + \alpha \frac{\sum_{s0}}{\sum_{t0}} + \beta \left(\frac{\sum_{s0}}{\sum_{t0}} \right)^2 \right] + R_0 \sum_{t0} \right\} \right)^{-1} \quad (82)$$

where

$$A = \frac{1 - P_e}{P_e} - R_0 \sum_{t0}$$

$P_e[\bar{l}_0, \sum_t(E)]$ is obtained from the tabular lookup used for resolved resonances.

When Equation (82) is substituted into Equation (81) we obtain Equation (80). For a black pin, $\Sigma_s = 0$ and Equation (81) can be reduced to Wigner's Rational Approximation using the flat flux assumption.

$$\frac{W(R_0)}{W_0} = \frac{1}{P_0(\bar{l}_0, \Sigma_{a0})} - R_0 \Sigma_{a0} = \frac{W_1}{W_0} - R_0 \Sigma_{a0}$$

where $\frac{1}{P_0} \approx \frac{W_1}{W_0}$ and W_1 is the asymptotic average flux in the moderator region outside the black absorber rod. Since the flat flux assumption implies a discontinuity in the flux at the boundary

$$W(R_0) = \frac{W_1 + W_0}{2}$$

$$\frac{W_1 + W_0}{2W_0} + R_0 \Sigma_{a0} = \frac{1}{P_0}$$

$$\frac{W_1}{W_0} + 1 + 2R_0 \Sigma_{a0} = \frac{2}{P_0}$$

$$P_0 = \frac{1}{1 + \bar{l}_0 \Sigma_{a0}} \equiv \text{Rational Approximation,}$$

which is the Wigner's Rational Approximation equation when Σ_{a0} replaces Σ_{i0} . The ABH³⁰ equation for the external moderator Region 1, with absorption in the moderator included and an additional clad Region 2 separating the absorber and moderator, is

$$\frac{W_1}{W_0} = \frac{W(R_0)}{W_0} + \frac{\Delta W_2}{W_0} + \frac{3}{2} R_0^2 \Sigma_{a0} \left[1 + \frac{V_2}{V_0} \frac{\Sigma_{a2}}{\Sigma_{a0}} \frac{W_2}{W_0} \right] F \quad (83)$$

where

$$F = G \Sigma_{t1} + \frac{1}{R_2} \left(\lambda_1 - \frac{2}{3} \right)$$

$$G = \frac{R_1^2}{R_1^2 - R_2^2} \left[\frac{R_1^2}{R_1^2 - R_2^2} \ln \left(\frac{R_1}{R_2} \right) - \frac{3}{4} + \frac{R_2^2}{4R_1^2} \right]$$

$$\lambda_1 = 0.710446 \left[\frac{1 + 1.5207587 \frac{3D_1}{2R_1}}{1 + 0.8103127 \frac{3D_1}{2R_1}} \right] \text{ (the extrapolation length for the inner surface of the moderator}$$

region)³²

W_1 = disadvantage weight for the external moderator region

W_2 = disadvantage weight for the clad region

Σ_{t1} = the total cross section in the moderator region

Σ_{a2} = the absorption cross section in the clad region

R_2 = the outer radius of the clad region

R_1 = the outer radius of the moderator region

D_1 = the diffusion coefficient in the moderator region.

The equation for the clad disadvantage factor W_2 is

$$\frac{W_2}{W_0} = \frac{W(R_0)}{W_0} + \frac{\Delta W_2}{2W_0} \quad (84)$$

where

$$\frac{\Delta W_2}{2} = \text{average incremental rise in the flux across the clad region.}$$

This can be obtained from simple diffusion theory by balancing the volume absorption rate in the absorbing rod to the diffusion current entering the rod,

$$\begin{aligned} W_0 \sum_{a0} V_0 &= D_2 \left. \frac{\Delta W_2}{\Delta R} \right|_{R_0} 2\pi R_0 \\ \frac{\Delta W_2}{W_0} &= \frac{\sum_{a0} \pi R_0^2 (R_2 - R_0)}{2\pi R_0 D_2} \\ \frac{\Delta W_2}{2W_0} &= \frac{\sum_{a0} R_0 (R_2 - R_0)}{4D_2} \end{aligned} \quad (85)$$

where D_2 is the diffusion coefficient in the clad region.

The weights W_0 , W_1 , and W_2 are normalized at each energy group as

$$W_0 V F_0 + W_2 V F_2 + W_1 V F_1 = 1 \quad (86)$$

where $V F_0$, $V F_2$, and $V F_1$ are the volume fractions of the absorber, clad and moderator regions, respectively.

Dividing Equation (86) by W_0 , we have

$$\frac{1}{W_0} = V F_0 + \left[\frac{W_2}{W_0} \right] V F_2 + \left[\frac{W_1}{W_0} \right] V F_1. \quad (87)$$

When Equations (80), (84), and (85) are solved for W_2/W_0 , and Equation (83) is solved for W_1/W_0 , Equation (87) is solved for W_0 . Then

$$W_2 = \left(\frac{W_2}{W_0} \right) W_0 \quad (88)$$

$$W_1 = \left(\frac{W_1}{W_0} \right) W_0. \quad (89)$$

2.4.1 Slab Geometry Disadvantage Weights

The equations for plate type geometry are taken from They's³³ and are similar, but differ due to the difference in divergence.

$$\frac{W(X_0)}{W_0} = 1 + \frac{\sum_{a0}}{\sum_{t0}} A \left[1 + \alpha \frac{\sum_{s0}}{\sum_{t0}} + \beta \left[\frac{\sum_{s0}}{\sum_{t0}} \right]^2 \right] \quad (90)$$

where

$$A = \frac{1-P_e}{P_e} - 2X_0 \Sigma_{t0}$$

$$\frac{W_1}{W_0} = \frac{W(X_0)}{W_0} + \frac{\Delta W_2}{W_0} + \Sigma_{a0} X_0 [\Sigma_1^*(X_1 - X_2) + 3\lambda_1 - 2]$$

$$\frac{\Delta W_2}{W_0} = \frac{\Sigma_{a0} X_0 (X_2 - X_0)}{2D_2}$$

$$\frac{W_2}{W_0} = \frac{W(X_0)}{W_0} + \frac{\Delta W_2}{2W_0}$$

where $\lambda_1=0.710446$ is the extrapolation length for the inner surface of the moderator region and Σ_1^* is the moderator region transport cross section. X_0 , X_1 , and X_2 plate geometry dimensions and all other quantities are defined as in the corresponding cylindrical geometry equations. Equations (86) to (89) are then solved for the disadvantage weights.

2.4.1.1 Self-Shielding Factors

Disadvantage factor weighted self-shielding factors SSF (ISO,g) are calculated at each energy group g for every isotope ISO in the 3 region cell.

$$SSF(ISO,g) = \frac{\sum_{j=1}^3 W_j^g VF_j N_j^{ISO}}{DENS(ISO)} \quad (91)$$

where

$$DENS(ISO) = \sum_{j=1}^3 VF_j N_j^{ISO} \quad (92)$$

VF_j = volume fraction of the j region in the cell

N_j^{ISO} = the isotopic density in each region of the cell.

The self-shielding factors SSF(ISO,g) are printed to the output. Effective cell-average microscopic cross sections of reaction type x at each mesh point are obtained from

$$\langle \sigma_{x,g}^{ISO} \rangle = SSF(ISO, g) \sigma_{x,g}^{ISO} \quad (93)$$

The fine group cross sections in the thermal energy range (1.0e-5—5.0435 eV) are replaced by those self-shielded with the ABH method in the three region geometry when this option is requested.

2.5 Age Equations

An option to perform an age calculation utilizing a moments method, which was available in the GAM-1 code, has been retained in COMBINE. The derivation of this method is described in Reference 13 and has been omitted here. However, the final equations solved for the age are briefly described below. In multigroup form, the *ith* group moment equations for ϕ_{00_i} , ϕ_{11_i} , and ϕ_{20_i} are

$$\Sigma_{t_i} \phi_{00_i} = \sum_{j=1}^i (\Sigma_{s0j \rightarrow i} + \Sigma_{inj \rightarrow i} + 2 \Sigma_{n,2nj \rightarrow i}) \phi_{00_j} \Delta_j + S_i \quad (94)$$

$$\sum_{t_i} \phi_{11_i} = \sum_{j=1}^i \sum_{slj \rightarrow i} + \phi_{11_j} \Delta_j + \phi_{00_i} \quad (95)$$

$$\sum_{t_i} \phi_{20_i} = \sum_{j=1}^i (\sum_{s0j \rightarrow i} + \sum_{inj \rightarrow i} + 2 \sum_{n,2nj \rightarrow i}) \phi_{20_j} \Delta_j + \frac{\phi_{11_i}}{3} \quad (96)$$

where all cross section definitions are the same as those described previously for the B-1 solution. Solving each moment equation for the i th group we have the final solution equations:

$$\phi_{00_i} = \frac{\sum_{t_i} \phi_{00_i} = \sum_{j=1}^i (\sum_{s0j \rightarrow i} + \sum_{inj \rightarrow i} + 2 \sum_{n,2nj \rightarrow i}) \phi_{00_j} \Delta_j + S_i}{\sum_{j=i+1}^{NOG} (\sum_{s0i \rightarrow j} + \sum_{in_i \rightarrow j} + 2 \sum_{n,2n_i \rightarrow j}) \Delta_j - \sum_{n,2n_i \rightarrow i} \Delta_i} \quad (97)$$

$$\phi_{11_i} = \frac{\phi_{00_i} + \sum_{j=1}^{i+1} \sum_{slj \rightarrow i} + \sum_{in_j \rightarrow i} \phi_{11_j} \Delta_j}{\sum_{ti} - \sum_{sl_i \rightarrow i} \Delta_i} \quad (98)$$

$$\phi_{20_i} = \frac{\frac{\phi_{11_i}}{3} + \sum_{j=1}^{i-1} (\sum_{s0j \rightarrow i} + \sum_{inj \rightarrow i} + 2 \sum_{n,2nj \rightarrow i}) \phi_{20_j} \Delta_j}{\sum_{j=i+1}^{NOG} (\sum_{s0i \rightarrow j} + \sum_{in_i \rightarrow j} + 2 \sum_{n,2n_i \rightarrow j}) \Delta_j - \sum_{n,2n_i \rightarrow i} \Delta_i} \quad (99)$$

$$\tau_i = \frac{\phi_{20_i}}{\phi_{00_i}} = \text{age to group } i. \quad (100)$$

2.6 Transport Approximations

The difference between the S_N and P_N require¹⁰

$$\sigma_{lg' \rightarrow g}^{SN} = \sigma_{lg' \rightarrow g}^{PN} \quad \text{for } g' \neq g \quad (101)$$

and

$$\sigma_{lg \rightarrow g}^{SN} = \sigma_{lg \rightarrow g}^{PN} - \sigma_{ltg}^{PN} + \sigma_g^{SN} \quad (102)$$

where σ_g^{SN} is not determined. The choice of σ_g^{SN} gives rise to a “transport approximation” and various recipes are in use:

- Consistent-P approximation is

$$\sigma_{lg \rightarrow g}^{SN} = \sigma_{lg \rightarrow g}^{PN} - (\sigma_{ltg}^{PN} - \sigma_{0tg}^{PN}) \quad (103)$$

- Inconsistent-P approximation is

$$\sigma_{lg \rightarrow g}^{SN} = \sigma_{lg \rightarrow g}^{PN} - (\sigma_{ltg}^{PN} - \sigma_{N+1tg}^{PN}) \quad (104)$$

- Diagonal transport approximation

$$\sigma_{\ell g \rightarrow g}^{SN} = \sigma_{\ell g \rightarrow g}^{PN} - (\sigma_{\ell t g}^{PN} - \sigma_{N+1 t g}^{PN} + \sigma_{N+1 g \rightarrow g}^{PN}) \quad (105)$$

- Bell-Hansen Sandmeier or extended transport approximation

$$\sigma_{\ell g \rightarrow g}^{SN} = \sigma_{\ell g \rightarrow g}^{PN} - (\sigma_{\ell t g}^{PN} - \sigma_{N+1 t g}^{PN} + \sum_{g'} \sigma_{N+1 g \rightarrow g'}^{PN}) \quad (106)$$

When the P_N to S_N correction is requested in the COMBINE7.1 input, the average of the above approximations is used for B-1 calculation but only the consistent-P approximation is used for B-3 calculation.

3. ONE-DIMENSIONAL TRANSPORT CALCULATION

The ANISN/PC code for one-dimensional transport theory calculations is incorporated in the COMBINE7.1. The ANISN portion solves the multigroup finite difference discrete ordinates equations with anisotropic scattering by using the fine group cross section constants, generated for the stacked zero-dimensional or infinite media. Thus calculated fluxes are used to spatially collapse the fine group constants to better reflect the spatial self-shielding. In the discrete ordinates method, the neutron transport equation is solved in a discrete set of directions only. Angular integrals are then approximated by sums over discrete directions and angular derivatives by differences. The detail of ANISN/PC code can be found in the ANISN/PC manual¹⁴ pdf file, included as a part of COMBINE7.1 code package.

Currently, the ANISN inputs are externally provided in the COMBINE7.1 batch run stream as described in the input description. The spatial coalescing formulas are separately described in the user's guide section.

4. USER'S GUIDE

4.1 Derivation of Diffusion Coefficient and Transport Cross Section

Although it is not evident from a cursory examination of B-1 equations, the mathematical structure of the system of equations resulting in Equations (30) and (31) is predetermined by the assumptions embodied in Equation (5). The assumptions, mathematically valid for a bare critical system satisfying simple diffusion boundary conditions, are characteristic of the broad generalities leading to the so-called First Fundamental Theorem of Reactor Theory.¹⁸ The usual approach to the B-N energy-dependent equations involves taking the Fourier transform of the steady-state transport equation for a slab, with the implication that diffusion boundary conditions are somehow applicable to any order N.

The conceptual difficulty with this approach is that the resultant equations obscure any direct relationship between the spatial and energy dependence of the variables, unless the resultant equations are first subjected to Fourier inversion. Such a relationship is required to derive a rigorous definition of the energy-dependent diffusion coefficient by means of Fick's law. The procedure of deriving the B-1 equations by use of Equation (5) and diffusion theory boundary conditions for the scalar flux enables one to accomplish this end in a straightforward way.

Equation (5) establishes the desired relationship between the variables subject to the boundary conditions at the extrapolated boundary of the slab. Only the real part of e^{-iBx} satisfies the boundary conditions for the spatially dependent scalar flux. The scalar flux is obtained from Equations (5), (8), and (9) in the conventional manner.

$$\Phi(x, \mu, E) = e^{-iBx} \psi(B, \mu, E)$$

$$\Phi_0(x, E) = \int_{-1}^1 \Phi(x, \mu, E) d\mu = e^{-iBx} \int_{-1}^1 \psi(B, \mu, E) d\mu = e^{-iBx} \phi_0(B, E) \quad (107)$$

From Fick's law, we obtain the relationship between the scalar flux and current

$$\vec{J}(x, E) = -D(E) \vec{\nabla} \Phi_0(x, E) = -\vec{k} D(E) \frac{d}{dx} \Phi_0(x, E) = D(E) B \phi_0(B, E) i \vec{k} e^{-iBx} \quad (108)$$

where \vec{k} is the unit vector in the x direction.

Therefore, $\vec{J}(x, E)$ is also separable in space and energy, a result consistent with Equation (5).

$$\therefore \vec{J}(x, E) = J(B, E) i \vec{k} e^{-iBx} \quad (109)$$

$$\text{where } J(B, E) = D(E) B \phi_0(B, E) \quad (110)$$

It has been pointed out that Equation (110) does not give a clear-cut relationship between $J(E)$ and $\phi_1(E)$ in Equations (30) and (31) since Fick's law is perfectly general. An alternate method of obtaining Equation (110) will be given, which helps clear up any ambiguity that may exist. Using the same assumptions and utilizing Equations (5), (8), and (9), we have

$$\vec{J}^*(x, E) = \vec{k} \int_{-1}^1 \mu \Phi(x, \mu, E) d\mu = \vec{k} \int_{-1}^1 \mu e^{-iBx} \psi(B, \mu, E) d\mu = i \vec{k} \phi_1(B, E) e^{-iBx} \text{ when B is real,}$$

$$= \vec{k} \phi_1(B, E) e^{-iBx} \text{ when B is imaginary.}$$

Introducing Fick's law without reference to the scalar flux boundary conditions we have

$$\vec{J}^*(x, E) = -D(E)\vec{\nabla}\Phi_0(x, E) = D(E)B\phi_0(B, E)i\vec{k}e^{-iBx} \quad .$$

Now equate $\vec{J}^*(x, E)$ from the two preceding equations to obtain a result similar to Equation (110) as

$$\vec{J}^*(x, E) = \phi_1(B, E)i\vec{k}e^{-iBx} = D(E)B\phi_0(B, E)i\vec{k}e^{-iBx} \quad \text{when B is real,}$$

$$= \phi_1(B, E)\vec{k}e^{-iBx} = D(E)B\phi_0(B, E)i\vec{k}e^{-iBx} \quad \text{when B is imaginary;}$$

$$\therefore \vec{J}(B, E) = \phi_1(B, E) = D(E)B\phi_0(B, E) \quad \text{when B is real,}$$

$$= iD(E)B\phi_0(B, E) \quad \text{when B is imaginary.} \quad (111)$$

From Equation (107), $D(E)$ is defined as

$$D(E) = \frac{\phi_1(B, E)}{B\phi_0(B, E)} \quad \text{when B is real,}$$

$$= \frac{\phi_1(B, E)}{iB\phi_0(B, E)} \quad \text{when B is imaginary.} \quad (112)$$

Equation (112) gives an unambiguous definition of the diffusion coefficient within the framework of the B-1 equations for a bare slab. The definition of the B-1 transport cross section at energy E in the domain of Fick's law is

$$\Sigma_{tr}(E) = \frac{1}{3D(E)} = \frac{B\phi_0(B, E)}{3\phi_1(B, E)} \quad \text{when B is real,}$$

$$\Sigma_{tr}(E) = \frac{1}{3D(E)} = \frac{iB\phi_0(B, E)}{3\phi_1(B, E)} \quad \text{when B is imaginary.} \quad (113)$$

In order to use Equation (113), the current from the solution run needs to be nonzero. Thus, when a zero buckling is input to the code, neither the diffusion coefficient nor the transport cross section is calculated. This situation corresponds to an infinite medium problem for which there is no net neutron current flow. If a diffusion coefficient is desired for a near infinite medium situation, a small but finite buckling input to the code will produce the desired results.

4.2 Summary Edits for Broad Group Constants

The equations for calculating the average cross sections are presented in this section in as complete a manners practical. This should facilitate the proper use of the average cross sections generated by the spectrum code.^{3,4}

The COMBINE spectrum, cross-section library tape contains data tabulated for 167 fine lethargy groups. In a normal spectrum problem, the data are coalesced into a broad group structure, specified by the user, containing one or more fine groups per broad group. The coalescing is performed by utilizing 167 fine group fluxes and/or currents as the weighting functions. These energy dependent fluxes and currents may either be calculated for a particular reactor system or taken from an immediately preceding problem. The latter type of calculation is referred to as a cell calculation. The output from a spectrum problem normally includes average macroscopic cross-section data and may include average microscopic data for each material in the macroscopic calculation, if desired. As an alternative to the normal output, the user may request the calculation of macroscopic effective diffusion theory constants (blackness theory) in lieu of the normal cross section output.

Figure 4 illustrates the notation used in describing the average cross-section data and the relation of the fine-group data to the broad-group data generated in a spectrum problem. In Figure 4, broad group G contains the fine groups I through I+N and all averages for broad group G are performed over this range of fine groups.

In the notation used above, NOG refers to the number of fine groups and NOAG refers to the number of broad groups.

Fine Groups	1	2	3	...	I-1	I	I+1	...	I+N-1	I+N	I+N+1	...	K-1	K	K+1	...	K+N-1	K+N	K+N+1	...	NOG-1	NOG
Broad Groups	1	...						G								G'						NOAG

Figure 4. Spectrum group structure.

The average cross sections are determined by the familiar relation

$$\bar{\Sigma} = \frac{\int_E \Sigma(E)w(E)dE}{\int_E w(E)dE} \quad (114)$$

where $\bar{\Sigma}$ represents the energy dependent cross section $\Sigma(E)$, and $w(E)$ is the energy dependent weighting function, normally either the fluxes or the currents. In the actual calculation, the continuous functions of the cross section and weighting parameter are represented by 167 fine group average values associated with a lethargy width, Δ_i . Thus,

$$\bar{\Sigma} = \frac{\sum_i \Sigma_i w_i \Delta_i}{\sum_i w_i \Delta_i} \quad (115)$$

In all cases, the integrations are performed utilizing the trapezoidal rule.

4.2.1 Average Macroscopic Cross Sections

The macroscopic cross-section data generated by the COMBINE7.1 code is described below in considerable detail to facilitate its proper use. In all cases, the average quantity has been defined for the broad group G where

$$\Sigma_i (cm^{-1}) = \sum_{k=1}^{NOI} N_k \sigma_i^k \Rightarrow \text{macroscopic cross section for } i^{\text{th}} \text{ fine group of a system}$$

containing NOI materials

where N_k and σ_i^k are the atom density (# of atoms $\times 10^{-24}$ per cubic centimeter) and microscopic cross section (barns/atom), respectively, for the k^{th} material and

Δ_i => lethargy width of fine group i

ϕ_i => average scalar flux in fine group i

J_i => average current (P_1 flux) in fine group i

ψ_i => average P_2 flux for group i

χ_i => average P_3 flux for group i

$\bar{\Sigma}_{xG}$ => average cross section for broad group G for a particular reaction denoted by x

Φ_G => integrated scalar flux for group G

J_G => integrated current (P_1 flux) for group G

Ψ_G => integrated P_2 flux for group G

χ_G => integrated P_3 flux for group G.

The integrated fluxes for broad group G are calculated as

$$\Phi_G = \sum_{i=1}^{i+N} \phi_i \Delta_i \quad (116)$$

$$J_G = \sum_{i=1}^{i+N} J_i \Delta_i \quad (117)$$

$$\Psi_G = \sum_{i=1}^{i+N} \psi_i \Delta_i \quad (118)$$

$$\chi_G = \sum_{i=1}^{i+N} \chi_i \Delta_i \quad (119)$$

Average absorption cross section

$$\bar{\Sigma}_{aG} = \frac{\sum_{i=1}^{i+N} \Sigma_{a_i} \phi_i \Delta_i}{\Phi_G} \quad (120)$$

Average fission cross section

$$\bar{\Sigma}_f = \frac{\sum_{i=1}^{i+N} \Sigma_{f_i} \phi_i \Delta_i}{\Phi_G} \quad (121)$$

Average number of neutrons per fission times the fission cross section

$$\nu \bar{\Sigma}_f = \frac{\sum_{i=1}^{i+N} \nu_i \Sigma_{f_i} \phi_i \Delta_i}{\Phi_G} \quad (122)$$

Average number of neutrons produced per fission

$$\bar{\nu}_G = \frac{\bar{\nu} \sum f_G}{\sum f_G} \quad (123)$$

Average capture cross section

$$\bar{\Sigma}_{c_G} = \bar{\Sigma}_{a_G} - \bar{\Sigma}_{f_G} \quad (124)$$

Average elastic, inelastic, $(n,2n)$, $(n,3n)$, or $(n,4n)$ cross section for isotropic transfer from group G to G

$$\bar{\Sigma}_{x_{G \rightarrow G'}} = \frac{\sum_{i=I}^{I+N} \sum_{k=K}^{K+N} \sum_{x_{i \rightarrow k}} \phi_i \Delta_i}{\Phi_G} \quad x_{i \rightarrow k} = \begin{cases} s_0 \text{ (elastic)} \\ \text{in (inelastic)} \\ n, 2n \text{ reactions} \\ n, 3n \text{ reactions} \\ n, 4n \text{ reactions} \end{cases} \quad (125)$$

Average linearly anisotropic component of elastic or inelastic transfer cross section from group G to G'

$$\bar{\Sigma}_{x1_{G \rightarrow G'}} = \frac{\sum_{i=I}^{I+N} \sum_{k=K}^{K+N} \sum_{x_{i \rightarrow k}} J_i \Delta_i}{J_G} \quad x_{i \rightarrow k} = \begin{cases} s_i \text{ (elastic)} \\ \text{in (inelastic)} \end{cases} \quad (126)$$

Average P_2 component of the elastic transfer cross section from group G to G

$$\bar{\Sigma}_{s2_{G \rightarrow G'}} = \frac{\sum_{i=I}^{I+N} \sum_{k=K}^{K+N} \sum_{2_{i \rightarrow k}} \psi_i \Delta_i}{\Psi_G} \quad (127)$$

Average P_3 component of the elastic transfer cross section from group G to G

$$\bar{\Sigma}_{s3_{G \rightarrow G'}} = \frac{\sum_{i=I}^{I+N} \sum_{k=K}^{K+N} \sum_{3_{i \rightarrow k}} \chi_i \Delta_i}{\chi_G} \quad (128)$$

Average total transfer cross section for transfer from group G to G

$$\bar{\Sigma}_{t_{G \rightarrow G'}} = \bar{\Sigma}_{s0_{G \rightarrow G'}} + \bar{\Sigma}_{in_{G \rightarrow G'}} + 2\bar{\Sigma}_{n,2n_{G \rightarrow G'}} + 3\bar{\Sigma}_{n,3n_{G \rightarrow G'}} + 4\bar{\Sigma}_{n,4n_{G \rightarrow G'}} \quad (129)$$

Average of isotropic elastic, inelastic, $(n,2n)$, $(n,3n)$, or $(n,4n)$ total scattering cross section

$$\bar{\Sigma}_{t_{xG}} = \sum_{G'=G}^{NOAG} \bar{\Sigma}_{x_{G \rightarrow G'}} \quad \chi_{G \rightarrow G'} = \begin{cases} s_0 \text{ (elastic)} \\ \text{in (inelastic)} \\ n, 2n \text{ reactions} \\ n, 3n \text{ reactions} \\ n, 4n \text{ reactions} \end{cases} \quad (130)$$

Average linearly anisotropic component of the elastic total scattering cross section

$$\bar{\Sigma}_{t_{s1G}} = \sum_{G'=G}^{NOAG} \bar{\Sigma}_{1_{G \rightarrow G'}} \quad (131)$$

Average out-scatter cross section

$$\bar{\Sigma}_{out_G} = \sum_{G'=G+1}^{NOAG} \left[\bar{\Sigma}_{s0_{G \rightarrow G'}} + \bar{\Sigma}_{in_{G \rightarrow G'}} + \bar{\Sigma}_{n,2n_{G \rightarrow G'}} + \bar{\Sigma}_{n,3n_{G \rightarrow G'}} + \bar{\Sigma}_{n,4n_{G \rightarrow G'}} \right] + \sum_{G'=G-\max up}^{G-1} \bar{\Sigma}_{up_{G \rightarrow G'}} \quad (132)$$

Average removal cross section

$$\bar{\Sigma}_{r_G} = \bar{\Sigma}_{a_G} + \bar{\Sigma}_{out_G} + \sum_{G'=G-\max up}^{G-1} \bar{\Sigma}_{up_{G \rightarrow G'}} \quad (133)$$

Average total cross section

$$\bar{\Sigma}_{t_G} = \bar{\Sigma}_{a_G} + \bar{\Sigma}_{s0_G} + \bar{\Sigma}_{in_G} + \bar{\Sigma}_{n,2n_G} + \bar{\Sigma}_{n,3n_G} + \bar{\Sigma}_{n,4n_G} \quad (134)$$

Integrated fission source

$$S_G = \sum_{i=1}^{I+N} S_i \quad (135)$$

Average inverse velocity

$$\left(\bar{1/v} \right)_G = \frac{\sum_{i=1}^{I+N} (1/v)_i \Phi_i \Delta_i}{\Phi_G} \quad (136)$$

Average diffusion coefficient (from Fick's law)

$$\bar{D}_G = \frac{J_G}{B\Phi_G} \quad (137)$$

Average transport cross section

$$\bar{\Sigma}_{tr_G} = \frac{1}{3\bar{D}_G} = \frac{B\Phi_G}{3J_G} \quad (138)$$

If a cell calculation is performed—a spectrum obtained from a previous problem is used as a weighting function to generate average cross sections for another material—the diffusion coefficients and transport cross sections are defined in terms of cross sections of the material being averaged. An appropriate definition can be obtained from Equation (37). By first solving Equation (37) for $\frac{B}{3}\phi$, and

then dividing both sides by $J_i(\phi_1)$. We then have

$$\bar{\Sigma}_{tr_{G_{cell}}}^g = \frac{\gamma^g \Sigma_t^g \Phi_1^g - \sum_{g'=1}^G \Sigma_{s1}^{g' \rightarrow g} \Phi_1^{g'} \frac{\Delta g'}{\Delta g}}{\Phi_1^g} \quad (139)$$

and

$$\bar{D}_{G_{cell}} = \frac{1}{3 \bar{\Sigma}_{tr_{G_{cell}}}} \quad (140)$$

In addition to the usual average cross-section data described above, some other miscellaneous cross-section data are calculated and printed out for the user. These quantities include the absorption and out-scatter cross sections for each broad group corrected for the (n,2n), (n,3n), and (n,4n) reaction. In the usual few group diffusion code the out-scatter cross section is generally used both as a removal term and a source term. However, the standard out-scatter term calculated by COMBINE accounts for the loss of one neutron by an (n,2n), (n,3n), or (n,4n) reaction in a particular broad group. Therefore, when this same term is used as a source term for the next group in a few group diffusion theory calculation of reactivity, it represents only one-half, one-third, or one-fourth of the actual source into that group from the (n,2n), (n,3n), or (n,4n) transfer reaction. Thus, in the corrected cross-section data, the out-scatter cross section is defined as

$$\bar{\Sigma}_{outG}^* = \sum_{G'=G+1}^{NOAG} \left(\bar{\Sigma}_{s0_{G \rightarrow G'}} + \bar{\Sigma}_{in_{G \rightarrow G}} + 2 \bar{\Sigma}_{n,2n_{G \rightarrow G'}} + 3 \bar{\Sigma}_{n,3n_{G \rightarrow G'}} + 4 \bar{\Sigma}_{n,4n_{G \rightarrow G'}} \right) + \sum_{G'=G-\max up}^{G-1} \bar{\Sigma}_{up_{G \rightarrow G'}} \quad (141)$$

where now a corrected absorption term is defined as

$$\Sigma_{a_G}^* = \Sigma_{a_G} - \sum_{G'=G}^{NOAG} \Sigma_{n,2n_{G \rightarrow G'}} - 2 \sum_{G'=G}^{NOAG} \Sigma_{n,3n_{G \rightarrow G'}} - 3 \sum_{G'=G}^{NOAG} \Sigma_{n,4n_{G \rightarrow G'}} \quad (142)$$

to conserve neutrons. The last term on the right-hand side of Equation (141) reflects the thermal outgoing upscattering.

4.2.2 Monoenergetic Transport Cross Section

The monoenergetic transport cross section offers an alternative to the Fick's law definition given by Equation (138) or (139) and has the redeeming feature that is always positive regardless of the shape of the spectrum. It is the classical value based on its definition from the one-energy transport equation.⁹ For broad group G, the macroscopic value is

$$\bar{\Sigma}_{tr_G} = \bar{\Sigma}_{t_G} - \Sigma_{t_{s \setminus G}} \quad (143)$$

Where the cross sections on the right-hand side are given by Equations (134) and (131).

4.2.3 Average Microscopic Cross Sections

The average microscopic cross sections are defined in a manner similar to the macroscopic cross sections. The main difference is the use of the microscopic cross section, σ , in the place of the macroscopic cross section, Σ . The one exception is the definition of a microscopic transport cross section. A unique definition of a microscopic transport cross section presents a conceptual difficulty in the same way that a microscopic diffusion coefficient would. The macroscopic values are extensive quantities resulting from some form of Fick's law, and there is no corresponding, physically meaningful relationship for microscopic values. Rather, it has become traditional to define a microscopic transport cross section

only in the metaphysical sense that “the whole is the sum of its assumed parts”; then from this, the macroscopic diffusion coefficient follows:

$$\bar{D}_G = \frac{1}{3 \sum_k N_k \bar{\sigma}_{mG}^k} = \frac{1}{3 \bar{\Sigma}_{mG}} \quad (144)$$

This being the case, the only thing required to define the microscopic transport cross section $\bar{\sigma}_{mG}$ in Equation (141) is a consistency relationship that will yield the proper macroscopic transport cross section for a particular mixture of materials as calculated by Equation (138). Any number of such consistency relationships could be defined and applied, as long as the macroscopic transport cross section in the denominator of Equation (143), computed from microscopic values, gives the same result as Equation (138).

One such equation that will yield the desired results is Equation (139), where Σ^* becomes the appropriate σ^k in each term of Equation (135). The broad microscopic transport cross section for the k^{th} isotope is then given by

$$\bar{\sigma}_{mG}^k = \frac{\sum_{i=1}^{I+N} \gamma_i \sigma_i J_i \Delta_i - \sum_{G'=1}^{NOAG} \sigma_{s1_{G' \rightarrow G}} J_{G'}}{J_G} \quad (145)$$

A measure of the “arbitrariness” of this definition of the microscopic transport cross section is that it is entirely possible that the microscopic transport cross section as given by Equation (145) can be negative for one or several materials in the mixture, and yet, when multiplied by N_k and summed over all materials in the mixture, will yield the proper macroscopic transport cross section as given by Equation (138). This situation occurs when the mixture contains large amounts of a strong absorber and the resultant flux and current spectra are very hard. For moderating materials with a small absorption cross section, the second term in the numerator of Equation (145) can then be the leading term due to the high current weights given the transfer cross sections $\sigma_{s1_{G' \rightarrow G}}$ when G lies in the energy range of depressed flux and current at low energy. The resultant microscopic transport cross sections, even though negative, are consistent in the sense of Equation (143), since “consistency” is all that is required of them in the definition.

The same pathologic situation can occur for cell materials being averaged over the flux and current from another spectral problem. If the spectral problem contained a very strong absorber producing a very hard spectra and the cell material does not contain much absorption, the macroscopic transport cross section from Equation (134) can be negative in low-energy groups. In this case, the negative result could be interpreted as indicating that the homogenization for the cell material was not judiciously chosen.

4.2.4 Effective Diffusion Theory Constants (Blackness Theory)

Extensive use is made of diffusion theory in nuclear reactor design analysis; however, inherent in the diffusion theory approximation is its inadequacy in highly absorbing, low scattering regions such as control rods. Because many reactor systems include such regions, the blackness theory was developed to provide a convenient technique for handling these regions without recourse to a higher order transport solution. The approach is to treat the absorbing region as a fictitious diffusing medium of the same thickness but use blackness constants in the diffusion calculation, which yield more correct fluxes than could be obtained with the usual constants. The spectrum code incorporates an option to calculate blackness theory diffusion coefficients and absorption cross sections for use in highly absorbing regions of a system under study. The assumptions made in the development of the formulism used to calculate the

effective constants are that the absorbing region is a thin slab and the immediately surrounding regions can be adequately handled by diffusion theory methods. These effective constants incorporate factors to account for the mesh structure used to describe the region in a finite difference solution of the diffusion equation. A complete development of this theory can be found in Reference 34 and a review of its use may be found in References 35 and 36.

4.2.5 Mixed Number Density (MIND) Constants

An input option allows for the production of mixed number density (MND) constants³⁷ for one single broad group in the thermal spectrum. No multiple thermal group MND constants are defined. The constants are defined as

$$\Sigma_{MND} = \overline{\Sigma V} = \frac{\int_0^{E_1} \Sigma(E) \phi_{SP}(E) dE}{\int_0^{E_1} \frac{1}{v(E)} \phi_{SP}(E) dE} = \frac{(\overline{\Sigma})_{SP}}{\left(\frac{1}{v}\right)_{SP}} \quad (146)$$

where

- Σ = the macroscopic absorption or fission cross section
- $\phi_{SP}(E)$ = thermal flux spectrum solution
- E_1 = upper energy of the single MND group
- $v(E)$ = velocity at energy E.

$$D_{MND} = \overline{D V}_{\max} = \frac{\int_0^{E_1} D(E) M(E) dE}{\int_0^{E_1} \frac{M(E) dE}{v(E)}} = \frac{(\overline{D})_{\max}}{\left(\frac{1}{v}\right)_{\max}} \quad (147)$$

$$\Sigma_{tr}^{MND} = \frac{1}{3D_{MND}} \quad (148)$$

$$\sigma_{tr}^{MND} = \left(\frac{\overline{\sigma}_{tr}}{V_{\max}} \right) = \frac{\int_0^{E_1} \frac{M(E) dE}{V(E)}}{\int_0^{E_1} \frac{M(E) dE}{\sigma_{tr}(E)}} = \frac{\left(\frac{1}{v}\right)_{\max}}{\left(\frac{1}{\sigma_{tr}}\right)_{\max}} \quad (149)$$

where “max” indicates averaging over a Maxwellian spectrum and M(E) = Maxwellian distribution at temperature T;

$$M(E) dE = \frac{E [\exp(-E/kT)]}{(kT)^2} dE \quad (150)$$

where k is Boltzmann’s constant and the average energy = 3/2kT and T corresponds to the ambient energy of the region.³⁵

For each Σ in Equations (146) through (150) there is a corresponding microscopic σ calculated for the output files. σ_{tr} replaces D. There are also normalized MND constants defined as:

$$\begin{aligned}
D^{NORM} &= \frac{D_{MND}}{2.2 \times 10^5} \\
\Sigma_a^{NORM} &= \frac{\Sigma_a^{MND}}{2.2 \times 10^5} \\
\Sigma_F^{NORM} &= \frac{\Sigma_F^{MND}}{2.2 \times 10^5}
\end{aligned} \tag{151}$$

Normalized microscopic values are defined as:

$$\begin{aligned}
\sigma_{tr}^{NORM} &= (2.2 \times 10^5) \sigma_{tr}^{MND} \\
\sigma_a^{NORM} &= \frac{\sigma_a^{MND}}{2.2 \times 10^5} \\
\sigma_F^{NORM} &= \frac{\sigma_F^{MND}}{2.2 \times 10^5}
\end{aligned} \tag{152}$$

If the “unnormalized MND values” are used in a spatial diffusion calculation, the thermal flux will be values of neutron density. If normalized values are used, the thermal flux will be the 2200 meters/sec thermal flux. Summary data printed (and punched) will include MND values of

$\Sigma_{tr}, D, \Sigma_a, \Sigma_F, \nu \Sigma_F, \sigma_{tr}, 1/3\sigma_{tr}, \sigma_a, \sigma_F, \text{ and } \nu\sigma_F.$

4.2.6 Multiplication Factors

Multiplication factors k_{inf} and k_{eff} are calculated for a COMBINE problem and printed after the broad group edits. k_{inf} is calculated as

$$k_{inf} = \frac{\sum_{G=1}^{GG} \nu \Sigma_{f_G} \phi_G}{\sum_{G=1}^{GG} \Sigma_{a_G} \phi_G} \tag{153}$$

where the numerator is the production rate of fission neutrons over the broad group spectra, the denominator is the absorption rate, and GG is the total number of broad groups. When $B = C$ or $B = -iC$ with a real constant C , then

$$k_{eff} = \frac{\sum_{G=1}^{GG} \nu \Sigma_{f_G} \phi_G}{\sum_{G=1}^{GG} (\Sigma_{a_G} + D_G C_G^2) \phi_G} \tag{154}$$

where D_G is the broad group diffusion coefficient and C_G^2 are the buckling coefficients specified in the floating point input data.

When $B = iC$,

$$k_{eff} = \frac{\sum_{G=1}^{GG} \nu \Sigma_{fG} \phi_G}{\sum_{G=1}^{GG} (\Sigma_{aG} - D_G C_G^2) \phi_G} \quad (155)$$

since there is a negative leakage. In this case k_{eff} exceeds k_{inf} .

4.2.7 The Spatial Coalescing Formulas

The spatial coalescing is carried out by weighting the various cross sections and other neutron group constants as follows. The formulas employed in the INL's internal SCAMP code³⁸ were adopted in COMBINE7.1.

Absorption Cross section:

$$\Sigma_{R,G}^a = \left(\sum_{g \text{ in } G} \sum_{r \text{ in } R} \Sigma_{r,g}^a \int_{V_r} \Phi_g \, dv \right) / \left(\sum_{g \text{ in } G} \sum_{r \text{ in } R} \int_{V_r} \Phi_g \, dv \right).$$

The broad group fission cross section is found in the same manner as the absorption cross section.

P₀ Scattering Cross Section:

$$\Sigma_{R,G \rightarrow G'}^0 = \left(\sum_{g' \text{ in } G'} \sum_{g \text{ in } G} \sum_{r \text{ in } R} \Sigma_{r,g \rightarrow g'}^0 \int_{V_r} \Phi_g \, dv \right) / \left(\sum_{g \text{ in } G} \sum_{r \text{ in } R} \int_{V_r} \Phi_g \, dv \right).$$

P₁ Scattering Cross Section :

$$\Sigma_{R,G \rightarrow G'}^1 = \left(\sum_{g' \text{ in } G'} \sum_{g \text{ in } G} \sum_{r \text{ in } R} \Sigma_{r,g \rightarrow g'}^1 \int_{V_r} J_g \, dv \right) / \left(\sum_{g \text{ in } G} \sum_{r \text{ in } R} \int_{V_r} J_g \, dv \right).$$

The P₂ and P₃ scattering cross sections are found in the same manner as the P₁ scattering cross section but using the P₂ and P₃ flux moment, respectively. However, the scalar flux is used in the code instead of higher flux moments for the P₀, P₁, and P₂ scattering cross sections.

Diffusion Coefficient:

$$D_{R,G} = \left(\sum_{g \text{ in } G} \sum_{r \text{ in } R} D_{r,g} \int_{V_r} |\text{grad } \Phi_g| \, dv \right) / \left(\sum_{g \text{ in } G} \sum_{r \text{ in } R} \int_{V_r} |\text{grad } \Phi_g| \, dv \right),$$

where, in each space interval, $\text{grad } \Phi = (\Phi_{m+1} - \Phi_m) / (x_{m+1} - x_m)$.

Transport Cross Section:

$$\Sigma_{R,G}^{tr} = 1 / (3D_{R,G}).$$

Fission Spectrum:

$$\chi_{R,G} = \left(\sum_{g \text{ in } G} \sum_{r \text{ in } R} \chi_{r,g} \int_{V_r} S_f \, dv \right) / \left(\sum_G \sum_{g \text{ in } G} \sum_{r \text{ in } R} \chi_{r,g} \int_{V_r} S_f \, dv \right),$$

where $S_f^r = \frac{1}{\lambda} \sum_g v \Sigma_g^f \Phi_g$ and $\lambda = \text{eigenvalue}$.

Neutrons per Fission Times the Fission Cross Section:

$$v \Sigma_{R,G}^f = \frac{\left[\left(\sum_{g \text{ in } G} \sum_{r \text{ in } R} v \Sigma_{r,g}^f \int_{V_r} \Phi_g \, dv \right) \left(\sum_G \sum_{g \text{ in } G} \sum_{r \text{ in } R} \chi_{r,g} \int_{V_r} S_f \, dv \right) \right]}{\left[\left(\sum_{g \text{ in } G} \sum_{r \text{ in } R} \int_{V_r} \Phi_g \, dv \right) \left(\sum_{r \text{ in } R} \int_{V_r} S_f \, dv \right) \right]}.$$

Parallel Buckling:

$$B_{R,G}^{2_{\square}} = \left[\sum_{g \text{ in } G} C_{\rho} (x_u^{\rho} J_{u,g} - x_l^{\rho} J_{l,g}) \right] / \left(D_{R,G} \sum_{g \text{ in } G} \sum_{r \text{ in } R} \int_{V_r} \Phi_g \, dv \right),$$

where $\rho=0, 1, \text{ and } 2$ for slab, cylindrical, and spherical geometry, respectively, and $C_0=1, C_1=2\pi, C_2=4\pi$.

Perpendicular Buckling:

$$B_{R,G}^{2_{\perp}} = \left(\sum_{g \text{ in } G} \sum_{r \text{ in } R} D_{r,g} B_{r,g}^{2_{\perp}} \int_{V_r} \Phi_g \, dv \right) / \left(D_{R,G} \sum_{g \text{ in } G} \sum_{r \text{ in } R} \int_{V_r} \Phi_g \, dv \right).$$

Total Cross Section:

$$\Sigma_{R,G}^T = \Sigma_{R,G}^a + D_{R,G} B_{R,G}^{2_{\perp}} + \sum_{G'} \Sigma_{R,G \rightarrow G'}^0.$$

The following formulas were used to calculate the neutron group constants from the transport current and the flux gradient.

Diffusion Coefficient:

$$D'_{R,G} = \left(\sum_{g \text{ in } G} \sum_{r \text{ in } R} \int_{V_r} |J_g| \, dv \right) / \left(\sum_{g \text{ in } G} \sum_{r \text{ in } R} \int_{V_r} |\text{grad } \Phi_g| \, dv \right).$$

Transport Cross Section:

$$\Sigma_{R,G}^{tr'} = 1 / (3D'_{R,G}).$$

Parallel Buckling:

$$B_{R,G}^{2_{\square}} = D_{R,G} B_{R,G}^{2'_{\square}} / D'_{R,G}.$$

Perpendicular Buckling:

$$B_{R,G}^{2_{\perp}} = D_{R,G} B_{R,G}^{2'_{\perp}} / D'_{R,G}.$$

Flux Volume Integrals:

$$\Phi_{R,G} V_R = \sum_{g \text{ in } G} \sum_{r \text{ in } R} \int_{V_r} \Phi_g \, dv.$$

Average Fluxes:

$$\Phi_{R,G} = \frac{\sum_{g \text{ in } G} \sum_{r \text{ in } R} \int_{V_r} \Phi_g \, dv}{\sum_{r \text{ in } R} \int_{V_r} \Phi_g \, dv}.$$

Average Currents:

$$J_{R,G} = \frac{\sum_{g \text{ in } G} \sum_{r \text{ in } R} \int_{V_r} J_g \, dv}{\sum_{r \text{ in } R} \int_{V_r} \Phi_g \, dv}.$$

The disadvantage factor for region r and neutron group g is computed in terms of scalar flux, volume weighted average by the formula

$$d_{r,g} = \left[\int_{V_r} \Phi_g \, dv / v_r \right] / \left[\sum_r \int_{V_r} \Phi_g \, dv / \sum_r v_r \right].$$

The following glossary of terms are used in the above formulas:

- a - superscript denoting absorption cross section
- f - superscript denoting fission cross section
- g - subscript denoting the g^{th} fine group of neutrons
- G - subscript denoting the G^{th} broad group of neutrons
- r - subscript denoting the r^{th} fine region
- R - subscript denoting the R^{th} broad region
- Φ - scalar flux
- J - net current
- v - volume
- ν - neutron per fission
- m - subscript denoting space point index
- l - subscript denoting space point number of lower boundary of broad region R
- u - subscript denoting space point number of upper boundary of broad region R
- x - space variable.

5. COMBINE7.1 FILES DESCRIPTION

Logical Unit	Name/status	Format	Usage
401	matxs.lib	unformatted	Boondarenko based cross section library
402	rerex.lib	formatted	Resolved resonance parameters library
403	combine.inp	formatted	COMBINE input
404	combine.out	formatted	COMBINE output
405	anisn.inp	formatted	ANISN input
406	anisn.out	formatted	ANISN output
430	combine.sig/ anisnc4.lib	formatted	Formerly nt4=4 in ANISN
437	combine.flx	formatted	Flux output
435	anisnc4.flux	formatted	Formerly 10 in ANISN
445	anisnc4.pun	formatted	Formerly 7 in ANISN
439	scratch	unformatted	temporary self shielded static cross sections, adum, generated in s.r spectrum
411–429	scratch	unformatted	temporary cross section files for cases to be 1-D transport (ANISN) corrected when ioned = 1, to be used in s.r. xscoal with ioned = 2.
431	scratch	direct access	total cross sections for Bondarenko self shielding
432	scratch	unformatted	static (adum) cross section file for region 1 in ABH
433	scratch	unformatted	static (adum) cross section file for region 2 in ABH
434	scratch	unformatted	static (adum) cross section file for region 3 in ABH
436	scratch	unformatted	temporary flux and higher moments
438	scratch	unformatted	shielded bondarenko cross section file, adum, generated in s.r. bondar
440	scratch	unformatted	(sigaz(i),sigfz(i),sigsz(i),amu1(i),i=1,np) for the pricipal resonance absorber after doppler broadening
441	scratch	unformatted	temporary (sigaz(i),sigfz(i),sigsz(i),amu1(i),i=1,np) for the pricipal and admixed resonance absorbers before doppler broadening
442	scratch	unformatted	sa0,ss0,etc., and collision probability file for ABH
446	scratch	unformatted	(sigaz(i),sigfz(i),sigsz(i),amu1(i),i=1,np) for the first admixed resonance absorber after doppler broadening
447	scratch	unformatted	(sigaz(i),sigfz(i),sigsz(i),amu1(i),i=1,np) for the second admixed resonance absorber after broadening
448	scratch	unformatted	(sigaz(i),sigfz(i),sigsz(i),amu1(i),i=1,np) for the third resonance absorber after doppler broadening
443	scratch	formatted	formats and writes broad group output data in s.r. xscoal for post processing
444	scratch	unformatted	
450–499	scratch	unformatted	thermal matrix cross sections for isotopes used in both sr. bonche and bondar, is+449
407	scratch	unformatted	Formerly nt8=8 in ANISN
408	scratch	unformatted	Formerly nt9=9 in ANISN
409	scratch	unformatted	Formerly nt1=1 in ANISN
410	scratch	unformatted	Formerly ntt=2 in ANISN
449	scratch	unformatted	Formerly 3 in ANISN

6. COMBINE7.1 INPUT DATA FILE ORGANIZATION

A problem consists of a title record, comment records (optional), data records, and a terminator record. A listing of the records is printed at the beginning of each problem. The order of the title, data, and comment records is unimportant except that only the last title record, or the last data record having a particular data record number, will be used.

When a format error is detected, a line containing a dollar sign (\$) located under the character causing the error and a comment giving the column of the error is printed. An error flag is set such that input processing continues, but the problem will be aborted at the end of input processing.

1. **Title Record.** *A title record must be entered for each problem.* A title record is identified by an equal sign (=) as the first nonblank character. The title record is normally placed first in the problem.
2. **Comment Records.** An asterisk (*) or a dollar sign (\$) appearing as the first nonblank character identifies the record as a comment record. Blank records are treated as comment records. The only processing of comment records is printing of contents. Comment records may be placed anywhere in the input file.
3. **Data Records.** The data records contain a varying number of fields, which may be integer, floating point, or alphanumeric. Blanks preceding and following fields are ignored.

The first field on a data record is a record number that must be an unsigned integer. If the first field has an error or is not an integer, an error flag is set. Consequently, data on the record are not used and the record will be identified by the record number in the list of unused data records. After each record number and the accompanying data are read, the record number is compared to previously entered record numbers. If a matching record number is found, the data entered on the previous record are replaced by the data on the current record. If the record being processed contains only a record number, the record number and the data entered on the previous record are deleted. If a record causes replacement or deletion of data, a statement is printed indicating that the record is a replacement.

A number field on a data record is started by either a digit (0 through 9), a sign (+ or -), or a decimal point (.). A comma or a blank (with one exception noted below) terminates a particular number field. The number field has a number part, and optionally, an exponent part. A number field without a decimal point or an exponent is an integer field; a number field with either a decimal point, an exponent, or both is a floating-point field. A floating-point field without a decimal point is assumed to have a decimal point immediately in front of the first digit. The exponent denotes the power of 10 to be applied to the number part of the field. The exponent part has an E and a sign (+ or -) followed by a number giving the power of 10. These rules for floating point numbers are identical to those for entering data in FORTRAN e or f format fields except that no blanks (one exception) are allowed between characters. Floating point data punched by FORTRAN programs can be read. To permit reading of floating point data, a blank following an E denoting an exponent is treated as a plus sign. Acceptable ways of entering floating-point numbers, all containing the quantity 12.45, are illustrated by six fields: 12.45, +12.45, 1245+2, 1.245+1, 1.245e1, and 1.245e+1.

4. **Terminator Records.** A record having a period as the first nonblank character is used as a terminator. Most previous input records are erased before the input to the next problem is processed. Therefore, each problem must contain a complete input data file sufficient for that type of problem. Also, the final problem is terminated by a period record.
5. **Data Record Summary.** A data record contains: the record number and a descriptive title of the data contained on the record; an explanation of any variable data input on this record; and the order of the data on the record, the variable name, and the input data requirements, where applicable. Any variable names beginning with the letters I, J, K, L, M, or N are of type INTEGER. Any variable names starting with another letter are of type REAL. After N words on a record, default values will be used for the rest. However, data items should not be skipped up to N words.

6.1 Problem/1-D Data Records

First card:

Position	Name	Description of Data
Word 1	NPROB	Number of Problems
Word 2	N1DC	Number of spatial coalescing
Word 2	NPROBID	Problem ID, equivalent to MTLNO as in the 1030101 card

This is the first card in combine.inp, which is always required. All words are required.

Second Card:

Position	Name	Description of Data
Word 1	IONED	Type of problem to be performed 0 Standard zero-dimensional COMBINE problem. 1 COMBINE/ANISN/COMBINE sequence. 2 COMBINE/ANISN/spatial weighting/COMBINE/ANISN/COMBINE sequence. -1 ANISN only.
Word 2	NSTACK	Total number of stacked cases in a problem.
Word 3	NSTACKID	NSTACK ID, equivalent to MTLNO as in the 1030101 card

This is the second card in combine.inp, which is always required. All words are required.

When IONED = 0, a standard COMBINE only is performed for the zero-dimensional cell calculation and the COMBINE input data as described in the next section follows. PROBID, N1DP and NSTACKID should be set to zero in this case.

When IONED = 1, a standard COMBINE calculation in the full 167 fine-group structure is performed, generating anisnc4.lib. An ANISN input file, 'anisn.inp1' with the igm=167, is required. An ANISN calculation is performed to provide flux and moments back to COMBINE portion. The broad group (as specified in the input) cross section coalescing is performed in COMBINE portion, generating 'combine.sig'. PROBID, N1DP, NSTACKID can be set to zero in this case.

When IONED = 2, N1DC > 0, and NPROBID > 0, a standard COMBINE calculation in the full 167 fine-group structure is performed, generating anisnc4.lib. An ANISN input file, 'anisn.inp1' is required. An ANISN calculation is performed to provide flux and moments back to COMBINE portion. A spatial coalescing is performed for the NSTACK cases in the 167 fine-group structure. Additional COMBINE problems are performed and the spatial and energy coalescing are performed over NPROB problems. Additional ANISN inputs are anisn.inp2, anisn.inp3, etc.

When IONED = -1, a standard ANISN calculation is performed, no more COMBINE input data is required. The files 'anisn.inp1' and 'anisnc4.lib' are required.

6.2 Title Record and Integer Data Records

6.2.1 Title Record

A title record must be present for each problem and is identified by an equal sign (=) as the first character on the record.

6.2.2 Problem Basic Control Information Record 1010101

This record is required for each problem. The first four words are always required. (N words, $4 \leq N \leq 9$)

Position	Name	Description of Data
Word 1	NTYPE	Type of calculation to be performed. 1— Standard B-1 flux approximation if LEG = 1, or Standard B-3 flux approximation if LEG = 3. 2— Standard P-1 flux approximation if LEG = 1. $\gamma(E) = 1.0$ in Equation (16). 4— Cell calculation; fluxes, from the preceding problem will be used for averaging cross sections. Currents will be recalculated from Equations (32) and (162) using the P-1 approximation with $\gamma(E) = 1.0$. 6— Blackness calculation; fluxes from the preceding problem will be used to obtain effective diffusion theory cross sections.
Word 2	LEG	1— B-1 or P-1 calculation. 3— B-3 calculation.
Word 3	NOI	Number of materials in the spectrum, cell or blackness calculation ($1 < NOI < 50$).
Word 4	NOUG	Total number of broad groups in the spectrum, cell or blackness calculation ($1 < NOUG < 167$).
Word 5	MICR	Microscopic cross section option (must be set to 1 if microscopic cross sections are to be output to the ASCII cross section file. 0— No average microscopic data desired. (Default) 1— Calculate average microscopic cross sections.
Word 6	MSTU	Source option. 0 Unit source in fine group MGHS -1— Fission rate weighted spectrum will be used. N— Fission spectrum of the material XX in the 10420XX card (N = XX). When rabs in 1043XXY $\neq 0$, MSTU is reset to -1. When NTYPE = 4, can be set to 0 (no effect).
Word 7	MGHS	Speifies fine group number for unit source. Rewiured only if a unit source is desired, i.e., if MSTU=0. When NTYPE = 4, can be set to be 0 (no effect).
Word 8	MAXIT	Maximum number of iterations when up scattering is present. When 0, the code sets MAXIT = 500. The conversion iteration stops when satisfied either "CONV" or MAXIT criteria. When there is no up scattering, no iteration is needed.
Word 9	ICHET	0— No ABH thermal calculation is being requested. No 2XXXXXX records will be present. (Default) 1— An ABH thermal calculation will be performed for rectangular geometry. Input is on 2XXXXXX records. 2— Cylindrical ABH geometry. 3— Spherical ABH geometry.
Word 10	ISN	Transport correction

Position	Name	Description of Data
		0— P_N to S_N correction desired.(default).
		1— No transport correction.
Word 11	MAGE	Age calculation option.
		0— No age calculation desired. (Default)
		1— Age calculation desired.
Word 12	MNDFLG	0— No Mixed number density calculation. (Default)
		1— Mixed number density calculation. Requires 1490001 record.

6.2.3 Energy Group Structure Record 10102YY

This record is required for the first problem. YY specifies up to 20 continuation records. (N words, $1 \leq N \leq 167$)

Position	Name	Description of Data
Word 1 to Word NOUG	NGP (I)	Broad energy group structure starting with the <i>upper limit</i> of the first broad group. ($1 < I < 167$). See Table 1 following input description. The upper limit of broad group number 1 must be the fine group number 1 (corresponding to 20.0 MeV). $1 < \text{number of broad groups} < 167$

6.2.4 Resonance Calculation Option Record 102010Y.

This record is required only if Nordheim resonance calculations are to be performed for resonance materials. If this record is not present, NXSR = 0 for all materials. Y specifies up to nine continuation records. (N words, $1 \leq N \leq 50$)

Position	Name	Description of Data
Word 1 to NOI	NXSR (I)	Resonance calculation option ($1 < I < 50$).
		0—Bondarenko self shielding treatment.
		1—Nordheim self shielding treatment (use only for those isotopes with $iwr > 0$, see Table 2).
		2—Average of Bondarenko and Nordheim treatments. Highly recommended for the case of LEU.

6.2.5 Macroscopic Interface File Option Record 1030101

This record is only required for each problem for which macroscopic cross-section data are to be output to the interface file, combine.sig. (N words, $2 \leq N \leq 5$)

Position	Name	Description of Data
Word 1	IPUN	Macroscopic interface file data option. 0—No output macroscopic data desired 1—Output the macroscopic cross sections to the ASCII cross-section file. 2—Output the calculated energy-dependent fluxes in neutral ASCII format (COMBINE.FLX). 3—Output both the macroscopic cross sections and the fluxes.
Word 2	MTLNO	Material number used to reference interface file macroscopic cross-section data. If $MTL(I) < 900$, isotope chi values will be added in the '5d' record of the ISOTXS format, having ICHI set to 1, regardless whether they are all 0.0.
Word 3	NCOP	Format flag for ASCII cross section output file. 0—INL format. (Default) 1—ANISN format. 2 CCCC ISOTOX format 3—AMPX Working Library format suitable for KENO5A. (not working currently, to be fixed)
Word 4	IAD	Option parameter that will be placed in columns 2 and 3 of the title record accompanying the macroscopic data to indicate to the diffusion or transport theory codes how these data are to be used in updating a cross-section library file associated with these codes. (Used only with INL format). 0—Completely replace material MTLNO on the library tape. (Default) 1—Replace only those values on the library tape for material MTLNO which are entered on the interface records.
Word 5	IDIFF	Option parameter that will be placed in columns 4 and 5 of the title record accompanying the diffusion or transport theory codes indicating whether to use the values of the diffusion coefficients or transport cross sections. (Used only with INL format). 0—Use the transport cross sections (Monoenergetic definition). (Default) 1—Use the diffusion coefficients (Fick's law definition).

6.2.6 Microscopic Interface File Option Record 10302XX

These records are required only for those materials for which microscopic cross-section data are to be output to the interface file, combine.sig. The material number is indicated by XX ($1 \leq XX \leq \text{NOI}$) (N words, $2 \leq N \leq 4$). Also MICR on record 1010101 must be = 1.

Position	Name	Description of Data
Word 1	NPUN(I)	Microscopic interface file output option for material I. 0—Do not output microscopic data for this material. 1—Output self-shielded microscopic cross-section data.
Word 2	MTL(I)	Material number used to reference microscopic cross-section data for material I. This is used for INL and ISOTXS format output. For ANISN and AMPX format, the materials are output numbered in ascending order as processed. If $\text{MTL(I)} < 900$, isotope chi values will be added in the '5d' record of the ISOTXS format, having ICHI set to 1, regardless whether they are all 0.0.
Word 3	NAD(I)	Option parameter that will be placed in columns 2 and 3 of the title record accompanying the interface microscopic data for Material I to indicate to the diffusion or transport theory codes how these data are to be used in updating a cross-section library file associated with these codes. (Used only with INL format). 0—Completely replace material MTL(I) on library file. (Default) 1—Replace only those values on the library file for material MTL(I) that are entered on the records.
Word 4	NDIFF(I)	Option parameter that will be placed in columns 4 and 5 of the title record accompanying the interface microscopic data for material I to indicate to the diffusion or transport theory codes whether to use the values of either the transport cross section or the values of the quantity $1/(3\sigma_{tr})$. (Used only with INL format). 0—Use the transport cross section (monoenergetic definition). (Default) 1—Use the quantity $1/(3\sigma_{tr})$ (Fick's law definition).

6.3 Floating Point Data Records

6.3.1 General Floating Point Data Record 1041001

This record is required for each problem. (N words, $1 \leq N \leq 3$)

Position	Name	Description of Data
Word 1	BUCK	Constant buckling, cm ⁻² (B2 value must be nonzero and positive). -1.0—Read 14700YY and 14710YY records for broad group wise buckling and buck sign. Requires 14700YY and 14710YY records.
Word 2	BUCKSIGN	0.0—Exp (-iBx) spatial distribution, i.e., fundamental mode cosine shape. (Default) -1.0—Exp (-Bx) spatial distribution +1.0—Exp (+Bx) spatial distribution Applied when BUCK > 0.0.
Word 3	CONV	Convergence criteria for fluxes and currents or for renormalization factor. (If not specified or zero, the code sets CONV = 0.00001.)
Word 4	PF	Packing fraction for the pebble bed application.
Word 5	PEBRAD	Pebble radius (cm)

Note: Word 4 and Word 5 are for diffusion coefficient correction to account for the neutron streaming in pebble beds as described in Reference 39.

6.3.2 Material Specification Record 10420XX

These records are required for each problem. The material number is indicated by XX ($1 \leq XX \leq \text{NOI}$). (N words, $3 \leq N \leq 6$)

Position	Name	Description of Data
Word 1	BISO(I)	ENDF material identification number for Ith material. Optionally if negative, print out the Bondarenko self-shielded fine-group vector cross sections, including damage, heat, and kerma.
Word 2	TISO(I)	Temperature (K) for Ith material.
Word 3	DENS(I)	Homogeneous atom density $\times 10^{-24}$ of the Ith material. May not be zero. Set to a very small number to force an infinite dilution calculation.
Word 4	THERMS(I)	0.0—static thermal scattering (no upscattering). (Default) 1.0—free gas thermal scattering (will include upscattering). (see Table 3) 2.0—S(α, β) thermal scattering (will include upscattering). (see Table 3)
Word 5	EPFISS(I)	Total thermal energy yield/fission (w-sec/fiss). (Default = 0.0)
Word 6	SSFF(I)	Self-shielding factor flag for Ith material. 0.0—no input of additional self-shielding factors. (Default) 1.0—additional self-shielding factors input by broad group. The self-shielding factors are input on records 146XXYY. All cross sections already processed either by Bondarenko self-shielding treatment or by additional ABH or Nordeim treatment will be multiplied by these additional self-shielding factors. Care should be taken when this option is used.

6.3.3 Material Resonance Specification Record 1043XXY

These records are required only for those materials for which a resonance calculation is to be performed. XX indicates the material number where (1 < XX < NOI) and Y specifies up to 9 continuation records. These records are used for the Nordheim resonance treatment when NXSR = 1.0 and also for the heterogeneous effect in the Bondarenko treatment when NXSR = 0.0. (N words, 3 < N < 23)

Position	Name	Description of Data
Word 1	TEMP(I)	Temperature (K) of absorber lump.
Word 2	GEOM(I)	Geometry of absorber lump. 0.0—Homogeneous medium. DENS(I) is atom density. (see 10420XX record) 1.0—Slab Geometry heterogeneous. 2.0—Cylindrical Geometry heterogeneous. 3.0—Spherical Geometry heterogeneous.
Word 3	DZERO(I)	Heterogeneous absorber atom density in absorber lump x 10 ⁻²⁴ . May not be zero. Set to a very small number to force an infinite dilution calculation.
Word 4	ABAR(I)	Lump dimension—radius of cylinder or sphere or thickness of slab in centimeters.
Word 5	CIN(I)	Dancoff-Ginsburg fuel lump correction factor or option flag. (If no shadowing, CIN = 0.0, also CIN is not used if IGEOM(I) = 0.) 0.0 to 1.0—Value of the correction factor CIN which is to be read in. 2.0—Calculate correction factor (cylinders only). 3.0—Same as for “last material,” which required a correction factor. (Caution: The user should exercise care in using this option.) “Last Material” here means preceding MATXS ID in the order on library file.
Word 6	ELZERO(I)	Double heterogeneity fuel lump spherical grain average chord length. See Equation (61) in text. $\bar{l}_G = \frac{4V}{S} = \frac{4}{3}r \text{ cm}$
Word 7	CZERO(I)	Double heterogeneity fuel lump grain Dancoff factor C ₀ . See Equations (43) and (99) in text. This is independent of CIN(I).
Word 8	S(I)	0.0—Use ϕ_{lump} . (Default). 1.0—Calculate volume fraction weighted cross sections between those over the lump flux (ϕ_{lump}) and those over the asymptotic flux (ϕ_{asym}) outside the lump.
Word 9	AMOD(I,1)	First admixed moderator ID. The XX in 10420XX record (not BISO). (Real)
Word 10	AMOD(I,2)	Second admixed moderator ID. The XX in 10420XX record. (Real)
Word 11	AMOD(I,3)	Third admixed moderator ID. The XX in 10420XX record. (Real)
Word 12	ADENM(I,1)	Atomic density of the first admixed moderator, AMOD(I,1).
Word 13	ADENM(I,2)	Atomic density of the second admixed moderator, AMOD(I,2).
Word 15	RABS(I,1)	First admixed resonance absorber ID. The XX in 10420XX record (not BISO). (Real)
Word 16	RABS(I,2)	Second admixed resonance absorber ID. The XX in 10420XX record. (Real)
Word 17	RABS(I,3)	Third admixed resonance absorber ID. The XX in 10420XX record. (Real)
Word 18	ADENABS(I,1)	Atomic density of the first admixed resonance absorber, RABS(I,1).
Word 19	ADENABS(I,2)	Atomic density of the second admixed resonance absorber, RABS(I,2).
Word 20	ADENABS(I,3)	Atomic density of the third admixed resonance absorber, RABS(I,3).
Word 21	RTYPE1(I)	= 0.0—All waves available in RERES.LIB. (Default) > 0.0—s-wave only.

Position	Name	Description of Data
Word 22	RTYPE2(I)	= 0.0—Use E_{high} as in the RERES.LIB. (Default) > 0.0—Reset E_{high} to RTYPE2(I).
Word 23	RTYPE3(I)	= 0.0—Use E_{low} as in the RERES.LIB. (Default, currently set to 0.0125 eV) > 0.0—Reset E_{low} to RTYPE3(I).
Word 24	RTYPE4(I)	> 10.0—NINT(RTYPE4(I)) is the minimum number of mesh points per resonance (Default, set to 10). Currently, the code sets the maximum number of mesh points per resonance to 1400.

6.3.4 Material Dancoff Specification Record 1044XXY

These records are required for all materials for which a fuel lump Dancoff calculation is to be performed. XX indicates the material number where $1 \leq XX \leq \text{NOI}$, and Y specifies up to nine continuation records. (N words, $8 \leq N \leq 12$)

Position	Name	Description of Data
Word 1	REG(I)	Number of nonabsorber regions in unit cell ($\text{REG}(I) < 5$).
Word 2	XK(I)	Lattice arrangement of cylindrical pins. 1.0—Rectangular. 2.0—Hexagonal.
Word 3	RADX(I,1)	Outer radius, in centimeters, of first nonabsorber region in unit cell, i.e., region immediately adjacent to absorber lump. ABAR(I) on record 10430IY is the radius of the absorber R_0 in Equations (77) and (79).
Word 4	RADX(I,2)	Outer radius of second nonabsorber region in unit cell.
Word 5	RADX(I,3)	Outer radius of third nonabsorber region in unit cell.
Word 6	RADX(I,4)	Outer radius of fourth nonabsorber region in unit cell.
Word 7	RADX(I,5)	Outer radius of fifth nonabsorber region in unit cell.
Word 8	SIG(1,1)	Macroscopic total cross section of first nonabsorber region in unit cell.
Word 9	SIG(I,2)	Macroscopic total cross section of second nonabsorber region in unit cell.
Word 10	SIG(I,3)	Macroscopic total cross section of third nonabsorber region in unit cell.
Word 11	SIG(I,4)	Macroscopic total cross section of fourth nonabsorber region in unit cell.
Word 12	SIG(I,5)	Macroscopic total cross section of fifth nonabsorber region in unit cell.

NOTE: The macroscopic total cross section in each nonabsorber region is the average macroscopic scattering plus absorption cross section in the resolved resonance range Σ_r in Equation (78). The radius of the last nonabsorber region is the average radius of the unit cell based on the last moderator volume in the hexagonal or square lattice pitch.

6.3.5 Material General Resonance Data Record 10450XX

These records are required only for those materials for which the user desires to modify the standard resonance calculational procedure. XX indicates that material number where $1 \leq XX \leq \text{NOI}$. (N words, $1 \leq N \leq 3$).

Position	Name	Description of Data
Word 1	THERMUP(I)	0.0—No thermal upscattering in the Nordheim resonance treatment. (Default) 1.0—Thermal upscattering in the Nordheim resolved resonance treatment.

Position	Name	Description of Data
Word 2	FMULT(I)	A factor which will multiply the recommended mesh spacing to obtain a coarse or finer mesh to use in performing the resolved resonance calculation. Default value is 1.0. If less than 1.0, less meshes are used. If greater than 1.0, more meshes are used. The maximum number of mesh intervals per resonance, however, is limited to 904. The minimum is 10.
Word 3	XLMT(I)	0.0—All resonances are used in constructing cross sections. (Default) X—The number of neighboring resonances in either direction to be considered. (Not recommended)

6.3.6 Material Self-Shielding Factor Records (146XXYY)

These records are required only for those materials if self-shielding factors are to be input, i.e., if SSFF(I) = 1.0 for material XX. NOUG values must be input. XX specifies the material number, where $1 < XX < NOI$, and YY specifies up to 20 continuation records.

Position	Name	Description of Data
Word 1 to NOUG	SSFBG(J)	Self-shielding factors for material I (specified by XX) and broad group J, listed in consecutive order. ($1 < J < NOUG$) These data are necessary only for those materials that require self-shielding factors. Input self-shielding factors in the epithermal energy groups for materials with a resonance range will double self-shield resonance materials which are automatically self-shielded on records 1044XXY. Input self-shielding factors in this energy range should be 1.0 or an infinitely dilute resonance calculation should be performed to prevent double self-shielding of resonances (caveat emptor).

6.3.7 Broad Group Buckling Factor Records (14700YY)

This record is required only if broad group wise buckling is to be input, i.e., if buck ≤ 0.0 for the problem. NOUG nonzero and positive values must be input. YY specifies up to 20 continuation records. (NOUG words).

Position	Name	Description of Data
Word 1 to NOUG	BUCKBG(J)	Broad group wise buckling corresponding to 101020Y record. ($1 \leq J \leq NOUG$) (must be nonzero and positive)

6.3.8 Broad Group Buckling Sign Records (14710YY)

This record is required only if broad group wise buckling is present in 14700YY record. NOUG values must be input. YY specifies up to 20 continuation records. (NOUG words).

Position	Name	Description of Data
Word 1 to NOUG	GBSIGN(J)	Broad group wise buckling sign corresponding to 14700YY record. ($1 \leq J \leq NOUG$). 0.0— exp (-iBx) spatial distribution, i.e., fundamental mode cosine shape. -1.0— exp (-Bx) spatial distribution +1.0— exp (+Bx) spatial distribution

6.3.9 Blackness calculation option Record (1480001)

This record is required if the blackness calculation has been requested on Record 1010101 (NTYPE = 6). (N words, $2 \leq N \leq 5$)

Position	Name	Description of Data
Word 1	TH	Thickness of highly absorbing region, in centimeters, for which a "Blackness theory" calculation of effective diffusion constants is desired.
Word 2	H	Width of mesh, in centimeters, used to describe the interior of a highly absorbing region in a diffusion theory calculation.
Word 3	CB	A quantity occurring in the blackness theory equations which can be approximated by $3 \left(\frac{\sum_{tr}}{\sum_t} \right)$ where \sum_{tr} and \sum_t represent the transport and total cross sections, respectively, for the regions immediately surrounding the blackness region. (Default = 3.0, assuming $\frac{\sum_{tr}}{\sum_t}$ to be unity)
Word 4	AK1	First blackness coefficient. (usually set to 1.0). (Default = 1.0)
Word 5	AK2	Second blackness coefficient. (usually set to 1.0). (Default = 1.0)

6.3.10 MND calculation option Record (1490001)

If the MND option has been requested on Card 1010101 (MNDFLG = 1), MND constants will be printed out for D , Σ_a , Σ_f macro and σ_{tr} , σ_a , σ_f microscopic cross sections. No MND constants will be output in the ASCII file. The other cross sections that are output will not be MND constants. (N words, $2 \leq N \leq 2$)

Position	Name	Description of Data
Word 1	IENDMN (Integer)	Highest fine energy group included in MND calculation.
Word 2	TPMND	Temperature of Maxwellian spectrum for MND calculation.

NOTE: *The MND option can only be used for a single thermal group. No multithermal group MND option is defined.*

6.4 Mixed Integer and Floating Point Data Records

ABH input data on 2XXXXXX series records are only required if ICHET = 1 on the first input record.

6.4.1 ABH REGION DESCRIPTION RECORDS 2010401

This record is required for each problem if the ABH option is to be run. (4 words) See Equations (166) through (175) in the text.

Position	Name	Description of Data
Word 1	NREG	Number of regions in ABH calculation. NREG must be set to 3.)
Word 2	RAD(1)	Outer radius of region 1 (cm) (half thickness of fuel slab).
Word 3	RAD(2)	Outer radius of region 2 (cm) (cladding).
Word 4	RAD(3)	Outer radius of region 3 (cm) (moderator half thickness in slab geometry).

6.4.2 ABH Material Description for Each Region Record 2015XY

These records are required for each problem if the ABH option is to be run. X specifies the region number, where $1 \leq X \leq 3$, and Y specifies up to 19 continuation records. Up to NOI materials may be specified per region (N words, $3 \leq N \leq 101$).

Position	Name	Description of Data
Word 1	NMAT	Number of materials in region specified by X (integer).
Word 2	IJSO(1,X)	First material identification number. The XX in 10420XX record.
Word 3	ADENS(1,X)	Heterogeneous atom density $X \cdot 10^{-24}$ of the first material in region X.
Word 4	IJSO(2,X)	Second material identification number. The XX in 10420XX record.
Word 5	ADENS(2,X)	Heterogeneous atom density $X \cdot 10^{-24}$ of the second material in region X.

NOTE 1: In the event the problem requestor wishes to include materials in the ABH calculation with zero atom density to force the generation of thermal self-shielded microscopic cross sections, an arithmetic indefinite will occur. To overcome this defect, use a very small atom density, e.g., 10^{-15} for these materials.

NOTE 2: All materials included in the 10420XX cards (NOI materials) should be used in the 20105XY cards.

6.5 Fine Energy Group Structure

Group Number	Upper Energy (eV)	Group Number	Upper Energy (eV)	Group Number	Upper Energy (eV)	Group Number	Upper Energy (eV)
1	2.0000E+07	43	9.6112E+02	85	1.1300E+00	127	3.5000E-01
2	1.6905E+07	44	7.4852E+02	86	1.1250E+00	128	3.4000E-01
3	1.4918E+07	45	5.8295E+02	87	1.1100E+00	129	3.3000E-01
4	1.3499E+07	46	4.5400E+02	88	1.0900E+00	130	3.2000E-01
5	1.1912E+07	47	3.5358E+02	89	1.0800E+00	131	3.1000E-01
6	1.0000E+07	48	2.7536E+02	90	1.0700E+00	132	3.0000E-01
7	7.7880E+06	49	2.1445E+02	91	1.0600E+00	133	2.9000E-01
8	6.0653E+06	50	1.6702E+02	92	1.0500E+00	134	2.8000E-01
9	4.7237E+06	51	1.3007E+02	93	1.0250E+00	135	2.7000E-01
10	3.6788E+06	52	1.0130E+02	94	1.0000E+00	136	2.6000E-01
11	2.8650E+06	53	7.8893E+01	95	9.9000E-01	137	2.5000E-01
12	2.2313E+06	54	6.1442E+01	96	9.8000E-01	138	2.4000E-01
13	1.7377E+06	55	4.7851E+01	97	9.7000E-01	139	2.3000E-01
14	1.3534E+06	56	3.7267E+01	98	9.5000E-01	140	2.2000E-01
15	1.0540E+06	57	2.9023E+01	99	9.3000E-01	141	2.0000E-01
16	8.2085E+05	58	2.2603E+01	100	9.1000E-01	142	1.8000E-01
17	6.3928E+05	59	1.7603E+01	101	8.9000E-01	143	1.6000E-01
18	4.9787E+05	60	1.3710E+01	102	8.7600E-01	144	1.4000E-01
19	3.8774E+05	61	1.0677E+01	103	8.5000E-01	145	1.2000E-01
20	3.0197E+05	62	8.3153E+00	104	8.0000E-01	146	1.0000E-01
21	2.3518E+05	63	6.4760E+00	105	7.5000E-01	147	9.5000E-02
22	1.8316E+05	64	5.0435E+00	106	7.0000E-01	148	9.0000E-02
23	1.4264E+05	65	3.9279E+00	107	6.8300E-01	149	8.5000E-02
24	1.1109E+05	66	3.0590E+00	108	6.5000E-01	150	8.0000E-02
25	8.6517E+04	67	2.3824E+00	109	6.2500E-01	151	7.5000E-02
26	6.7379E+04	68	2.3300E+00	110	6.0000E-01	152	7.0000E-02
27	5.2475E+04	69	2.2900E+00	111	5.9000E-01	153	6.5000E-02
28	4.0868E+04	70	2.2000E+00	112	5.7500E-01	154	6.0000E-02
29	3.1828E+04	71	2.1000E+00	113	5.5000E-01	155	5.0000E-02
30	2.4788E+04	72	2.0000E+00	114	5.3200E-01	156	4.0000E-02
31	1.9305E+04	73	1.9000E+00	115	5.0000E-01	157	3.0000E-02
32	1.5034E+04	74	1.8600E+00	116	4.9000E-01	158	2.5000E-02
33	1.1709E+04	75	1.7800E+00	117	4.8000E-01	159	2.0000E-02
34	9.1188E+03	76	1.7000E+00	118	4.7500E-01	160	1.5000E-02
35	7.1017E+03	77	1.6000E+00	119	4.7000E-01	161	1.0000E-02
36	5.5308E+03	78	1.5000E+00	120	4.6000E-01	162	8.0000E-03
37	4.3074E+03	79	1.4400E+00	121	4.5000E-01	163	7.0000E-03
38	3.3546E+03	80	1.3500E+00	122	4.3000E-01	164	5.0000E-03
39	2.6126E+03	81	1.3000E+00	123	4.2000E-01	165	4.0000E-03
40	2.0347E+03	82	1.2500E+00	124	4.1400E-01	166	2.0000E-03
41	1.5846E+03	83	1.2000E+00	125	3.8000E-01	167	1.0000E-03
42	1.2341E+03	84	1.1500E+00	126	3.6000E-01		1.0000E-05

6.6 Materials in the “MATXS” Fine Group Cross Section Library and the “RERES” Resolved Resonance Library

Element/ isotope	ENDF/B Material ID	Resolved Resonance in reres.lib*	Thermal Scattering**	Element/ Isotope	ENDF/B Material ID	Resolved Resonance in reres.lib	Thermal Scattering
H-1	125	0	H in H ₂ O, f	Ca-48	2049	2	f
H-1	126	0	H in ZrH	Sc-45	2125	2	f
H-1	127	0	H in Ch2	Ti-46	2225	2	f
H-2	128	0	D in D ₂ O, f	Ti-47	2228	2	f
H-3	131	0	f	Ti-48	2231	2	f
He-3	225	0	f	Ti-49	2234	2	f
He-4	228	0	f	Ti-50	2237	2	f
Li-6	325	0	f	V	2300	5	f
Li-7	328	0	f	Cr-50	2425	3	f
Be-9	425	0	Be-metal	Cr-52	2431	3	f
Be-9	426	0	Be in BeO	Cr-53	2434	3	f
B-10	525	0	f	Cr-54	2437	3	f
B-11	528	0	f	Mn-55	2525	2	f
C	600	0	graphite, f	Fe-54	2625	3	f
N-14	725	0	f	Fe-56	2631	3	f
N-15	728	0	f	Fe-57	2634	3	f
O-16	825	0	f	Fe-58	2637	3	f
O-16	826	0	O in BeO	Co-58	2722	2	f
O-17	828	0	f	Co-58m	2723	2	f
F-19	925	0	f	Co-59	2725	3	f
Na-22	1122	0	f	Ni-58	2825	3	f
Na-23	1125	2	f	Ni-59	2828	2	f
Mg-24	1225	0	f	Ni-60	2831	3	f
Mg-25	1228	0	f	Ni-61	2834	3	f
Mg-26	1231	0	f	Ni-62	2837	3	f
Al-27	1325	3	f	Ni-64	2843	3	f
Si-28	1425	3	f	Cu-63	2925	3	f
Si-29	1428	3	f	Cu-65	2931	3	f
Si-30	1431	3	f	Zn	3000	5	f
P-31	1525	0	f	Ga-69	3125	2	f
S-32	1625	2	f	Ga-71	3131	2	f
S-33	1628	2	f	Ge-70	3225	2	f
S-34	1631	2	f	Ge-72	3231	2	f
S-36	1637	0	f	Ge-73	3234	2	f
Cl-35	1725	0	f	Ge-74	3237	2	f
Cl-37	1731	0	f	Ge-76	3243	2	f
Ar-36	1825	2	f	As-74	3322	2	f
Ar-38	1831	2	f	As-75	3325	2	f
Ar-40	1837	3	f	Se-74	3425	2	f
K-39	1925	2	f	Se-76	3431	2	f
K-40	1928	0	f	Se-77	3434	2	f
K-41	1931	2	f	Se-78	3437	2	f
Ca-40	2025	2	f	Se-79	3440	0	f
Ca-42	2031	2	f	Se-80	3443	2	f
Ca-43	2034	2	f	Se-82	3449	2	f
Ca-44	2037	2	f	Br-79	3525	2	f
Ca-46	2043	0	f	Br-81	3531	2	f

Element/ isotope	ENDF/B Material ID	Resolved Resonance in reres.lib*	Thermal Scattering**	Element/ Isotope	ENDF/B Material ID	Resolved Resonance in reres.lib	Thermal Scattering
Kr-78	3625	2	f	Rh-105	4531	1	f
Kr-80	3631	2	f	Pd-102	4625	2	f
Kr-82	3637	0	f	Pd-104	4631	2	f
Kr-83	3640	2	f	Pd-105	4634	2	f
Kr-84	3643	2	f	Pd-106	4637	2	f
Kr-85	3646	2	f	Pd-107	4640	2	f
Kr-86	3649	2	f	Pd-108	4643	2	f
Rb-85	3725	2	f	Pd-110	4649	2	f
Rb-86	3728	2	f	Ag-107	4725	2	f
Rb-87	3731	2	f	Ag-109	4731	2	f
Sr-84	3825	2	f	Ag-110m	4735	2	f
Sr-86	3831	2	f	Ag-111	4737	2	f
Sr-87	3834	2	f	Cd-106	4825	2	f
Sr-88	3837	2	f	Cd-108	4831	2	f
Sr-89	3840	0	f	Cd-110	4837	2	f
Sr-90	3843	0	f	Cd-111	4840	2	f
Y-89	3925	2	f	Cd-112	4843	2	f
Y-90	3928	2	f	Cd-113	4846	2	f
Y-91	3931	0	f	Cd-114	4849	2	f
Zr	4000	5	Zr in ZrH	Cd-115m	4853	2	f
Zr-90	4025	2	f	Cd-116	4855	2	f
Zr-91	4028	2	f	In-113	4925	2	f
Zr-92	4031	2	f	In-115	4931	2	f
Zr-93	4034	2	f	Sn-112	5025	2	f
Zr-94	4037	2	f	Sn-113	5028	2	f
Zr-95	4040	0	f	Sn-114	5031	2	f
Zr-96	4043	2	f	Sn-115	5034	2	f
Nb-93	4125	1	f	Sn-116	5037	2	f
Nb-94	4128	2	f	Sn-117	5040	2	f
Nb-95	4131	0	f	Sn-118	5043	2	f
Mo-92	4225	2	f	Sn-119	5046	2	f
Mo-94	4231	2	f	Sn-120	5049	2	f
Mo-95	4234	2	f	Sn-122	5055	2	f
Mo-96	4237	2	f	Sn-123	5058	0	f
Mo-97	4240	2	f	Sn-124	5061	2	f
Mo-98	4243	2	f	Sn-125	5064	2	f
Mo-99	4246	0	f	Sn-126	5067	0	f
Mo-100	4249	2	f	Sb-121	5125	2	f
Tc-99	4325	2	f	Sb-123	5131	2	f
Ru-96	4425	0	f	Sb-124	5134	0	f
Ru-98	4431	0	f	Sb-125	5137	0	f
Ru-99	4434	2	f	Sb-126	5140	2	f
Ru-100	4437	2	f	Te-120	5225	0	f
Ru-101	4440	2	f	Te-122	5231	2	f
Ru-102	4443	2	f	Te-123	5234	2	f
Ru-103	4446	2	f	Te-124	5237	2	f
Ru-104	4449	2	f	Te-125	5240	2	f
Ru-105	4452	0	f	Te-126	5243	2	f
Ru-106	4455	0	f	Te-127m	5247	0	f
Rh-103	4525	2	f	Te-128	5249	2	f

Element/ isotope	ENDF/B Material ID	Resolved Resonance in reres.lib*	Thermal Scattering**	Element/ Isotope	ENDF/B Material ID	Resolved Resonance in reres.lib	Thermal Scattering
Te-129m	5253	0	f	Nd-144	6031	2	f
Te-130	5255	2	f	Nd-145	6034	2	f
Te-132	5261	2	f	Nd-146	6037	2	f
I-127	5325	2	f	Nd-147	6040	2	f
I-129	5331	2	f	Nd-148	6043	2	f
I-130	5334	2	f	Nd-150	6049	2	f
I-131	5337	0	f	Pm-147	6149	2	f
I-135	5349	0	f	Pm-148	6152	0	f
Xe-123	5422	0	f	Pm-149	6155	0	f
Xe-124	5425	2	f	Pm-151	6161	2	f
Xe-126	5431	2	f	Sm-144	6225	2	f
Xe-128	5437	2	f	Sm-147	6234	2	f
Xe-129	5440	2	f	Sm-148	6237	2	f
Xe-130	5443	2	f	Sm-149	6240	2	f
Xe-131	5446	2	f	Sm-150	6243	2	f
Xe-132	5449	2	f	Sm-151	6246	2	f
Xe-133	5452	0	f	Sm-152	6249	2	f
Xe-134	5455	2	f	Sm-153	6252	2	f
Xe-135	5458	1	f	Sm-154	6255	2	f
Xe-136	5461	2	f	Eu-151	6325	2	f
Cs-133	5525	2	f	Eu-152	6328	2	f
Cs-134	5528	2	f	Eu-153	6331	2	f
Cs-135	5531	2	f	Eu-154	6334	2	f
Cs-136	5534	0	f	Eu-155	6337	2	f
Cs-137	5537	0	f	Eu-156	6340	2	f
Ba-130	5625	2	f	Eu-157	6343	2	f
Ba-132	5631	2	f	Gd-152	6425	3	f
Ba-133	5634	2	f	Gd-153	6428	3	f
Ba-134	5637	2	f	Gd-154	6431	3	f
Ba-135	5640	2	f	Gd-155	6434	3	f
Ba-136	5643	2	f	Gd-156	6437	3	f
Ba-137	5646	2	f	Gd-157	6440	3	f
Ba-138	5649	2	f	Gd-158	6443	3	f
Ba-140	5655	2	f	Gd-160	6449	3	f
La-138	5725	2	f	Tb-159	6525	2	f
La-139	5728	2	f	Tb-160	6528	3	f
La-140	5731	2	f	Dy-156	6625	2	f
Ce-136	5825	2	f	Dy-158	6631	2	f
Ce-138	5831	2	f	Dy-160	6637	2	f
Ce-139	5834	2	f	Dy-161	6640	2	f
Ce-140	5837	2	f	Dy-162	6643	2	f
Ce-141	5840	2	f	Dy-163	6646	2	f
Ce-142	5843	2	f	Dy-164	6649	2	f
Ce-143	5846	2	f	Ho-165	6725	2	f
Ce-144	5849	0	f	Ho-166m	6729	2	f
Pr-141	5925	2	f	Er-162	6825	2	f
Pr-142	5928	2	f	Er-164	6831	2	f
Pr-143	5931	2	f	Er-166	6837	2	f
Nd-142	6025	2	f	Er-167	6840	2	f
Nd-143	6028	2	f	Er-168	6843	2	f

Element/ isotope	ENDF/B Material ID	Resolved Resonance in reres.lib*	Thermal Scattering**	Element/ Isotope	ENDF/B Material ID	Resolved Resonance in reres.lib	Thermal Scattering
Er-170	6849	2	f	U-233	9222	3	f
Lu-175	7125	2	f	U-234	9225	2	f
Lu-176	7128	2	f	U-235	9228	3	f
Hf-174	7225	2	f	U-236	9231	2	f
Hf-176	7231	2	f	U-237	9234	1	f
Hf-177	7234	2	f	U-238	9237	3	f
Hf-178	7237	2	f	U-239	9240	1	f
Hf-179	7240	2	f	U-240	9243	1	f
Hf-180	7243	2	f	U-241	9246	1	f
Ta-181	7328	2	f	Np-235	9340	0	f
Ta-182	7331	2	f	Np-236	9343	2	f
W-182	7431	2	f	Np-237	9346	2	f
W-183	7434	2	f	Np-238	9349	0	f
W-184	7437	2	f	Np-239	9352	0	f
W-186	7443	2	f	Pu-236	9428	2	f
Re-185	7525	2	f	Pu-237	9431	0	f
Re-187	7531	2	f	Pu-238	9434	1	f
Ir-191	7725	2	f	Pu-239	9437	3	f
Ir-193	7731	2	f	Pu-240	9440	2	f
Au-197	7925	2	f	Pu-241	9443	3	f
Hg-196	8025	2	f	Pu-242	9446	1	f
Hg-198	8031	2	f	Pu-243	9449	1	f
Hg-199	8034	2	f	Pu-244	9452	1	f
Hg-200	8037	2	f	Pu-246	9458	0	f
Hg-201	8040	2	f	Am-241	9543	1	f
Hg-202	8043	2	f	Am-242	9546	2	f
Hg-204	8049	0	f	Am-242m	9547	2	f
Pb-204	8225	2	f	Am-243	9549	1	f
Pb-206	8231	3	f	Am-244	9552	0	f
Pb-207	8234	3	f	Am-244m	9553	0	f
Pb-208	8237	3	f	Cm-241	9628	0	f
Bi-209	8325	2	f	Cm-242	9631	1	f
Ra-223	8825	0	f	Cm-243	9634	1	f
Ra-224	8828	0	f	Cm-244	9637	2	f
Ra-225	8831	0	f	Cm-245	9640	2	f
Ra-226	8834	2	f	Cm-246	9643	2	f
Ac-225	8925	0	f	Cm-247	9646	1	f
Ac-226	8928	0	f	Cm-248	9649	1	f
Ac-227	8931	0	f	Cm-249	9652	2	f
Th-227	9025	0	f	Cm-250	9655	2	f
Th-228	9028	2	f	Bk-249	9752	2	f
Th-229	9031	2	f	Bk-250	9755	2	f
Th-230	9034	1	f	Cf-249	9852	2	f
Th-232	9040	3	f	Cf-250	9855	1	f
Th-233	9043	0	f	Cf-251	9858	1	f
Th-234	9046	0	f	Cf-252	9861	1	f
Pa-231	9131	3	f	Cf-253	9864	1	f
Pa-232	9134	2	f	Cf-254	9867	0	f
Pa-233	9137	3	f	Es-253	9913	1	f
U-232	9219	3	f	Es-254	9914	0	f

Element/ isotope	ENDF/B Material ID	Resolved Resonance in reres.lib*	Thermal Scattering**	Element/ Isotope	ENDF/B Material ID	Resolved Resonance in reres.lib	Thermal Scattering
Es-255	9915	0	f	Fm-255	9936	0	f
<p>* Presence of resolved resonance parameters in the reres.lib. iwrr = 0: No resonance parameters, includes only awr and ap 1: Single-Level Breit-Wigner (SLBW) format 2: Multilevel Breit-Wigner (MLBW) format 3: Reich-Moore (R-M) format 4: multi-isotope SLBW format 5: multi-isotope MLBW format ** S(α,β) thermal scattering, otherwise specified as "F", which is free-gas thermal scattering. Cross sections are mostly processed at T=293, 900, 1300, and 2200 K and at $\sigma_0 = 1.0e10e4, 1.0e2, 1.0$ barns. For some important isotopes, cross sections are processed with up to 8 σ_0 values and as low as 0.01 barns. For those having the free (f)/S(α,β) thermal scattering cross sections, the temperatures are dictated by the ENF/B-VII.0. The maximum temperature for free or S(α,β) thermal scattering is 800 K for H-1 in H₂O, 1200 K for H-1 in ZrH, 350 K for H-1 in CH₂, 650 K for H-1 in D₂O, 1200 K for Be, 1220 K for Be in BeO, 2000 K for graphite, 2200 K for O-16, 1200 K for O-16 in BeO, 1200 K for Zr in ZrH.</p>							

6.7 MATXS.LIB File Description

file structure	record type	present if
=====		=====
	file identification	always
	file control	always
	set hollerith identification	always
	file data	always
***** (repeat for all particles)		
*	group structures	always

***** (repeat for all materials)		
*	material control	always

***** (repeat for all submaterials)		
* *	vector control	n1db.gt.0

***** (repeat for all vector blocks)		
* * *	vector block	n1db.gt.0

***** (repeat for all matrix blocks)		
* * *	matrix control	n2d.gt.0

***** (repeat for all sub-blocks)		
* * * *	matrix sub-block	n2d.gt.0

* * *	constant sub-block	jconst.gt.0

file identification	
hname, (huse(i), i=1,2), ivers	
1+3*mult	
format(4h 0v ,a8,1h*,2a8,1h*,i6)	
hname	hollerith file name - matxs - (a8)
huse	hollerith user identification (a8)
ivers	file version number
mult	double precision parameter
	1- a8 word is single word
	2- a8 word is double precision word

file control	
npart, ntype, nholl, nmat, maxw, length	
format(6h 1d ,6i6)	
npart	number of particles for which group structures are given
ntype	number of data types present in set
nholl	number of words in set hollerith identification record
nmat	number of materials on file

maxw maximum record size for sub-blocking
length length of file

 set hollerith identification
(hsetid(i),i=1,nholl)
format(4h 2d / (9a8))
hsetid hollerith identification of set (a8)
 (to be edited out 72 characters per line)

 file data
(hprr(j),j=1,npart), (hrr(k),k=1,nrr), (hmatn(i),i=1,nmat),
1(nrr(j),j=1,npart), (jinp(k),k=1,nrr), (joutp(k),k=1,nrr),
2(nsubm(i),i=1,nmat), (locm(i),i=1,nmat)
format(4h 3d ,4x,8a8/(9a8)) hprr,hrr,hmatn
format(12i6) nrr,jinp,joutp,nsubm,locm
hprr(j) hollerith identification for particle j
 n neutron
 g gamma
 p proton
 d deuteron
 t triton
 h he-3 nucleus
 a alpha (he-4 nucleus)
 b beta
 r residual or recoil
 (heavier than alpha)
hrr(k) hollerith identification for data type k
 nscat neutron scattering
 ng neutron induced gamma production
 gscat gamma scattering (atomic)
 gg gamma scattering (photonuclear)
 pn proton induced neutron production
 .
 .
 .
 dkn delayed neutron data
 dkhg decay heat and gamma data
 dkb decay beta data
hmatn(i) hollerith identification for material i
nrr(j) number of energy groups for particle j
jinp(k) type of incident particle associated with
 data type k. for dk data types, jinp is 0.
joutp(k) type of outgoing particle associated with
 data type k
nsubm(i) number of submaterials for material i
locm(i) location of material i

 group structure
(gpb(i),i=1,nrr),emin
nrr=nrr(j)
format(4h 4d ,8x,1p,5e12.5/(6e12.5))
gpb(i) maximum energy bound for group i for particle j
emin minimum energy bound for particle j

```

material control
hmat, amass, (temp(i), sigz(i), itype(i), nld(i), n2d(i),
llocs(i), i=1, nsubm)
format(4h 5d , a8, 1p, 2e12.5/(2e12.5, 5i6))
hmat      hollerith material identifier
amass     atomic weight ratio
temp      ambient temperature or other parameters for
          submaterial i
sigz      dilution factor or other parameters for
          submaterial i
itype     data type for submaterial i
nld       number of vectors for submaterial i
n2d       number of matrix blocks for submaterial i
llocs     location of submaterial i

```

```

vector control
(hvps(i), i=1, nld), (nfg(i), i=1, nld), (nlg(i), i=1, nld)
format(4h 6d , 4x, 8a8/(9a8))      hvps
format(12i6)                        iblk, nfg, nlg
hvps(i)  hollerith identifier of vector
          nelas  neutron elastic scattering
          n2n   (n, 2n)
          nnf   second chance fission
          gabs  gamma absorption
          p2n   protons in, 2 neutrons out
          .
          .
          .
nfg(i)   number of first group in band for vector i
nlg(i)   number of last group in band for vector i

```

```

vector block
(vps(i), i=1, kmax)
kmax=sum over group band for each vector in block j
format(4h 7d , 8x, 1p, 5e12.5/(6e12.5))
vps(i)   data for group bands for vectors in block j.
          block size is determined by taking all the group
          bands that have a total length less than or equal
          to maxw.

```

```

scattering matrix control
hmtx, lord, jconst,
1(jband(l), l=1, noutg(k)), (ijj(l), l=1, noutg(k))
mult+2+2*noutg(k)
format(4h 8d , 4x, a8/(12i6))      hmtx, lord, jconst,
                                   jband, ij
hmtx      hollerith identification of block
lord      number of orders present
jconst    number of groups with constant spectrum
jband(l)  bandwidth for group l
ijj(l)    lowest group in band for group l

```

```

      scattering sub-block
      (scat(k),k=1,kmax)
      kmax=lord times the sum over all jband in the group range of
        this sub-block
      format(4h 9d ,8x,1p,5e12.5/(6e12.5))
      scat(k)      matrix data given as bands of elements for initial
                    groups that lead to each final group.  the order
                    of the elements is as follows:  band for p0 of
                    group i, band for p1 of group i, ... , band for p0
                    of group i+1, band for p1 of group i+1, etc.  the
                    groups in each band are given in descending order.
                    the size of each sub-block is determined by the
                    total length of a group of bands that is less than
                    or equal to maxw.
                    if jconst.gt.0, the contributions from the jconst
                    low-energy groups are given separately.

```

```

      constant sub-block
      (spec(l),l=1,noutg(k)),(prod(l),l=11,ning(k))
      l1=ning(k)-jconst+1
      noutg(k)+jconst
      format(4h10d ,8x,1p,5e12.5/(6e12.5))
      spec          normalized spectrum of final particles for initial
                    particles in groups l1 to ning(k)
      prod          production cross section (e.g., nu*sigf) for
                    initial groups l1 through ning(k)
                    this option is normally used for the energy-independent
                    neutron and photon spectra from fission and radiative
                    capture usually seen at low energies.

```

6.8 Description of Resolved Resonance Library (reres.lib) Format

Card: title

For a material

Card: aid,iwr,awr,ap,elow,ehigh,nernis,mat (A10,I1,4E11.6,I11,I4)

If $1 \leq iwr \leq 3$

For $j=1, nernis$

Card: elt,eht,spi,ap,nls,naps,mat (4E11.6,2I11,I4)

For $l=1, nls$

Card: nrj,qx,lrx,mat (I11,E11.6,I11,33X,I4)

For $i=1, nrj$

Card: er,aj,gn,gg,gf,gt,mat (6E11.6,I4)

If $iwr \geq 4$

Card: elt,eht,mat (2E11.6,44X,I4)

For $j=1, nernis$

Card: awri,abn,naps,spi,ap,nls,mat (2E11.6,I11,2E11.6,I11,I4)

For $l=1, \max(nls)$

Card: nrj,qx,lrx,mat (I11,E11.6,I11,33X,I4)

For $i=1, nrj$

Card: igf,er,aj,gn,gg,gt,mat (I11,5E11.6,I4)

Repeat for materials

aid	material identification.
iwr	1 for single-level Breit-Wigner (SLBW), 2 for multilevel Breit-Wigner (MLBW), 3 for Reich-Moore, 4 for multiisotope SLBW, 5 for multiisotope MLBW.
awr	ratio of the material mass to that of a neutron.
ap	scattering radius in units of 10^{-12} cm.
elow	lower limit for the whole resolved resonance energy range (same as in ENDF/B-VII.0).
ehigh	upper limit for the whole resolved resonance energy range (same as in ENDF/B-VII.0).
nernis*	number of energy ranges for $iwr=1, 2, 3$ or number of isotopes for $iwr=4, 5$.
mat	ENDF/B-VII material identification number.
elt	lower limit for an energy range (adjusted for COMBINE7, differing from elow: see reres.lib).
eht	upper limit for an energy range.
nls	number of l -values (neutron orbital angular momentum).
naps	flag controlling the use of the two radii.
nrj	number of resolved resonances for a given l -value.
qx	Q-value to be added to the incident particle's center of-mass energy to determine the channel energy.
lrx	flag indicating whether this energy range contains a competitive width.
er	resonance energy.
aj	floating point value of J (the spin, or total angular momentum of the resonance).
gn	neutron width, Γ_n , evaluated at the resonance energy, er.
gg	radiation width, Γ_g .
gf	fission width, Γ_f (Γ_{fa} for R-M).
gt	resonance total width (Γ_{tb} for R-M).
awri	ratio of the mass of a particular isotope to that of a neutron
abn	the abundance of an isotope in the material
igf	isotope index

* All have only one energy range except Pu-239 which has three energy ranges.

6.9 Cross section and constants internal record

The data in the internal master cross section library consist of alphanumeric, integer, and floating point records. The alphanumeric records are used for identification purposes, the integer data for the most part indicate the number and types of records to be read, and the floating point records make up the actual cross-section data.

The initial data records on the tape are used for identification and to indicate the number of materials, fission spectra and energy groups in the library. Subsequent records describe the cross-section data, with similar types of data records being repeated for each material until all materials have been described. The materials are always arranged in the library so that the identification numbers are in ascending order. The cross-section data records in the library have been condensed as much as feasible to reduce the processing time. Therefore, the length and number of data records present for a particular material depend on the amount of data required to describe the pertinent cross sections. The minimum number of records in the library for any material is two and the maximum is four.

A detailed description of the arrangement of the data within the library, including the mnemonic names and meanings of the data in the order of their occurrences in the library is found below. The cross-section data records for each material are arranged as shown below and are repeated for each material.

6.9.1 First Data Record for Material k

Mnemonic Name	Description or Function of Data
BISO(IS)	Material number
LTOT	Integer indicating the total number of words of data contained in the cross-section vector ADUM
IWA	Absorption reaction flag. If IWA = 1, absorption cross sections are present.
IWF	Fission reaction flag. If IWF = 1, fission cross sections and the values of the average number of neutrons per fission are present. If IWA = 0, IWA is ignored.
IWS	=> No elastic scattering transfer matrices present 1 => Elastic scattering transfer matrices present
LOL(L)	Number of cross-section values in List L. L = 1 => inelastic transfer matrix is present if $ LOL1 = 1$. L = 2 => N,2N transfer matrix is present if $ LOL2 = 1$. L = 3 => P ₀ and P ₁ elastic transfer matrix is present if $ LOL3 = 1$. L = 4 => P ₂ and P ₃ elastic transfer matrix is present if $ LOL4 = 1$. L = 5 => P ₀ , N, 3N transfer matrix is present if $ LOL5 = 1$. L = 6 => P ₀ , N, 4N transfer matrix is present if $ LOL6 = 1$.
	NOTE: <i>LOL(1) and LOL(2) negative implies P₁ inelastic or P₁, N,2N matrices are also present in addition to P₀ matrices. In either case, P₁ matrix follows directly behind the P₀ matrix. The length of either matrix is $LOL(1)$ or $LOL(2)$. LA and LD vectors apply to both P₀ and P₁ matrices in both cases. Only P₀, N,3N and N,4N cross sections are allowed.</i>
LA(L)	Number of fine groups <i>scattered from</i> in list L, starting with the first fine group, i.e., number of the highest fine group for which scattering reaction of type I is present (threshold group).

Mnemonic Name	Description or Function of Data
LD(L)	Maximum number of fine groups scattered to in list L, i.e., the maximum number of groups downscattered (this value is constant for all groups in which a scattering reaction is tabulated for a particular material).
AW(IS)	The atomic weight ratio of this material.

6.9.2 Second Data Record for Material k

Mnemonic Name	Description or Function of Data
ADUM(I) (I = 1,LTOT)	<p>Vector containing the complete set of microscopic cross sections and values of neutrons produced per fission for material k. All scattering matrices are in this vector.</p> <p>The cross section values, if present, are contained in the vector in the following order:</p> <p>If IWA = 1, the first MAXG (the number of groups used) values are the absorption cross sections starting with group 1.</p> <p>If IWA = 1, and IWF = 1, the next MAXG values are the fission cross sections followed by MAXG values of neutrons produced per fission.</p> <p>If IWF = 1, the next MAXG values are the fluxes from MATXS.LIB followed by MAXG chi values (fission spectrum) for this material.</p> <p>If $LOL1 = 1$, the next LOL(1) values are the P0 inelastic cross sections for transfer from group I to group J. The list starts with I = 1 and contains the values for J ranging from 1 to LD(1) + 1. Then the values for I = 2 with J ranging from 2 to LD(1) + 2 are next, etc. until I = LA(1).</p> <p style="padding-left: 2em;">There are LD(1) + 1 values listed for each I, as long as LD(1) + I ≤ MAXG. When LD(1) + I > MAXG then only MAXG + 1 - I values are listed for I.</p> <p>If LOL1 = -1, the next LOL(1) values are the P1 inelastic cross sections for transfer from group I to group J. The structure of this list is identical to 4.</p> <p>If $LOL2 = 1$, next LOL(2) values are the P0 (n,2n) cross sections for transfer from group I to group J. The list is ordered as above for the inelastic data.</p> <p>If LOL2 = -1, the next LOL(2) values are the P1 (n,2n) cross sections for transfer from group I to group J. The structure of this list is identical to 6.</p> <p>If LOL3 = 1, the next LOL(3) values are the isotropic elastic scattering cross sections for transfer from group I to group J followed by the same number of values for the linearly anisotropic component of the elastic scattering cross sections from group I to group J.</p> <p>If LOL4 = 1, the next LOL(4) values are the P2 components of the elastic scattering cross sections for transfer from group I to J followed by the P3 components from group I to group J.</p> <p>If LOL5 = 1, the next LOL(5) values are the P0 (n,3n) cross sections for transfer from group I to group J. The list is ordered as above for the inelastic data. There is no P1 (n,3n) matrix.</p> <p>If LOL6 = 1, the next LOL(6) values are the P0 (n,4n) cross sections for transfer from group I to group J. The list is ordered as above for the inelastic data. There is no P1 (n,4n) matrix.</p>

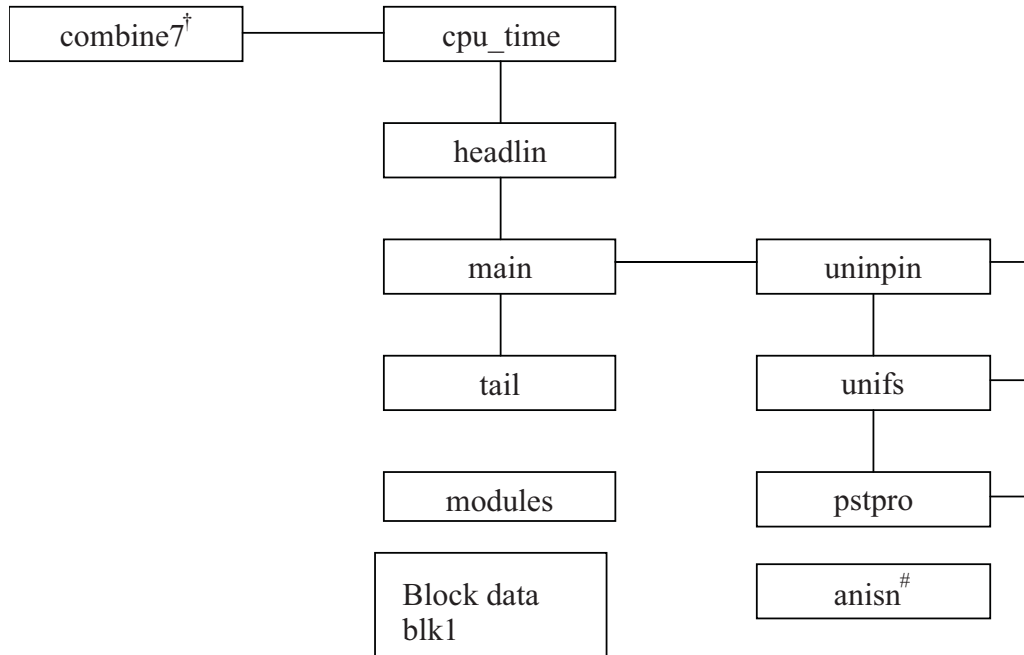
6.10 Thermal $S(\alpha, \beta)$ and Free Scattering Cross Section Internal Record

```
itfile = 449 + is
l = group scattered from
jj = group scattered to
ljj = (l-1)*maxg+jj
write (itfile) l,jj,therm0(ljj),therm1(ljj),therm2(ljj),therm3(ljj)
where
  1 ≤ is ≤ noi (noi = number of materials in the problem),
  65 ≤ l ≤ 167 (fine groups in the thermal energy range),
  65 ≤ jj ≤ 167 (fine groups in the thermal energy range),
```

7. PROGRAMMER'S GUIDE

COMBINE7.1 is written in FORTRAN 90 and is currently compiled using the Intel Visual Fortran compiler or the Lahey/Fujitsu (LF95) Fortran compiler on the Windows 32 platform. The Intel Visual Fortran compiler provides the faster run time. The source code is heavily commented to explain subroutine functions, data structures, etc. This section provides a short description of each subroutine and shows the overlay structure.

7.1 Flow Diagram



```

-- uninpin - inp - inppck
                  - inpw
                  - inpcvi - inpalf
                  - inpalf
- unindat - uninin
                  - inp2 - iinkw
                  - inpmod - inpupk
                  - endck
                  - iinkw
                  - jinkw
                  - jnp2 - jinkw
                  - jnpmod - jnpupk
                  - err
                  - unchet - jinkw
                              - jnp2 - jinkw
                                  - jnpmod - jnpupk
  
```



```

-- unifs - spectrum- mascot - output
- bondar - lethrg
- ginsburg- dancof
- skipr
- totes - skipr
- bonsig0
- lethrg
- nordheim- reslib
- grid
- cross1 - facts
- facphi
- cross2 - facts
- facphi
- cross3 - facts
- facphi
- frobns - thrinv
- abcmat
- tbroad - movpanl
- broadn - bsigma - hunky - funky
- hnabb*
- funky
- admabs - reslib
- cross1 - facts
- facphi
- cross2 - facts
- facphi
- cross3 - facts
- facphi
- frobns - thrinv
- abcmat
- tbroad - movpanl
- broadn - bsigma - hunky - funky
- hnabb*
- funky
- resol - newbv - interp
- escape - newcyl
- newslb
- trapz
- samps*
- semps*
- somps*
- sumps*
- svmps*
- swmps*
- sxmps*
- prnres
- chetxs
- chetah - getche - bonche - lethrg
- skipr
- totes - skipr
- bonsig0
- unpakk
- eprob - escap - newcy
- newsl
- benwa1 - intrp
- benwa2 - intrp

```

```

- flux - bone
- bthree - eval
- solv
- age
- blknes
- xscoal - coalesc
- mnd - maxwel
- punch
- prtscat
- unpakk
-- pstpro - stran - contrl - updn
- writhd
- writhk
- mapss
- amatin
- mapsa - writfl
- mapsi
- mapdr
- mapsk

```

Note 1: † indicates “program”,
 * “function”,
 otherwise, “subroutine”.
 # see ANISN manual.

Note 2: SR.QUIT is used at several places to close temporary files and terminate execution.
 An intrinsic subroutine, “exit” is used to terminate execution, close all files, and return control to the operating system.

7.2 Summary of Contents of Subroutines

7.2.1 Program COMBINE7.1 and Supporting Subroutines

Overall control of COMBINE7.1 is maintained in PROGRAM COMBINE7.1. It controls the flow of the overall program. COMBINE7.1 calls SR.MAIN to read and digest all of the input data, perform spectrum calculation, and process the cross-section output data into the user-specified final format. It also calls the date and time subroutines to produce the banner information printed at the beginning and end of the printed output.

SR. ABCMAT

Routine to do a matrix multiplication. Called from sr.frobns.

SR. ADMABS

Generates cross sections from the admixed absorber resonances.

SR.AGE

AGE calculates moments and Fermi age from the second moment when an age calculation is requested. These are Equations (137) through (143) in the text.

SR.AMATIN

Processes the neutral internal cross-section file prior to reformatting.

SR.BENWA1

BENWA1 calculates thermal disadvantage factors at each energy point for slab geometry. The slab geometry equations are Equations (172) to (176) in the text. The weights are then used in SR.CHETXS to calculate self-shielding factors for each material in the three region slab geometry cell described in the input data. BENWA1 is called from SR.CHETAH.

SR.BENWA2

BENWA2 calculates thermal disadvantage factors at each energy point for cylindrical geometry. The cylindrical geometry equations are Equations (166) to (175) in the text. The weights are then used in SR.CHETXS to calculate self-shielding factors for each material in the three region, cylindrical geometry cell described in the input data. BENWA2 is called from SR.CHETAH.

BLOCK DATA BLK1

Collision Probabilities from case and Placzek pin locations for dancoff calculation.

SR.BLKNES

BLKNES calculates thermal blackness coefficients for diffusion theory codes. BLKNES is called from SR.FLUX.

SR.BONCHE

Returns Bondarenko shielded cross sections. This routine is used when ABH calculation is requested.

SR.BONDAR

Bondarenko self-shields and transfers all requested library material cross sections to the file unit 419. The file unit 419 is then library file with no additional material to be processed in SR. SPECTRUM.

SR.BONE

BONE solves the B-1 or P-1 groupwise fast spectrum equations by substitution. The solution proceeds from group 1 through group 167 with the thermal upscattering iterations. These are Equations (33) and (34) in the text. The 167 group isotropic neutron flux and current are returned. BONE is called from SR.FLUX.

SR.BONSIG0

Calculates the groupwise Bondarenko background cross sections for the Bondarenko self shielding. Includes the heterogeneous component.

SR. BROADN

Doppler broaden the resolved resonance cross sections.

SR.BSIGMA

A part of Doppler broadening algorithm. Called from SR.BROADN.

SR.BTHREE

BTHREE solves the B-3 groupwise fast spectrum equations by the Gauss-Seidel iteration. These are Equations

(26) through (30) in the text. The groupwise solution proceeds from group 1 through group 167 with the thermal upscattering iteration. Four Legendre moments for the B-3 fluxes are returned for each microgroup. BTHREE is called from SR.FLUX.

SR.CHETAH

Controls the calculation of thermal disadvantage factors when ABH calculation is requested. The actual disadvantage factors are calculated in SR.BENWA1 for the slab geometry and SR.BENWA2 for the cylindrical geometry. CHETAH is called from SR.SPECTRUM.

SR.CHETAH

CHETAH controls the calculation of the thermal disadvantage factors when an ABH calculation is requested in the input. The actual disadvantage factors are calculated in SR.BENWA1 for slab geometry and SR.BENWA2 for cylindrical geometry.

SR.CHETXS

Corrects cross section in the thermal energy range by ABH's thermal disadvantage factors and substitute microscopic cross sections. Apply only to absorption, fission, and elastic cross section since inelastic, (n,xn) occur at epithermal energy range.

SR.COALSEC

COALSEC calculates the broad group fluxes, currents, and cross sections from the fast spectrum flux/current weighted values. It is called to calculate both macroscopic and microscopic values based on Equations (236) through (266) in the text. COALSEC is called from SR.XSCOAL.

SR.CONTRL

Controller for final formatting of the ASCII cross-section output file.

SR.CROSS1

CROSS1 calculates the single level Breit-Wigner resolved resonance cross sections on energy mesh generated in SR.GRID. Doppler-broadening occurs in SR.TBORAD.

SR.CROSS2

CROSS2 calculates the multi level Breit-Wigner resolved resonance cross sections on energy mesh generated in SR.GRID. Doppler-broadening occurs in SR.TBORAD.

SR.CROSS3

CROSS3 calculates the Reich-Moore resolved resonance cross sections on energy mesh generated in SR.GRID. Doppler-broadening occurs in SR.TBORAD.

SR.DANCOF

DANCOF calculates the Dancoff-Ginsburg factor C for a set of square lattice or hexagonal lattice pins in regular arrays depending upon the type of lattice requested in the input. The factor C(I) for the I resonance material is returned for each calculation. The calculation is for Equations (86) through (88) in the text. DANCOFF is called from SR.GINSBURG.

SR.ENDCK

ENDCK prints an error message when errors are detected on an input card.

SR.EPROB

Calls SR.ESCAP to calculate the escape probability, P_0 , for the cell thermal disadvantage factor calculation. The same capture probability tables are used that were constructed for the resolved resonance calculation in the fast spectrum code. EPROB is called from SR.CHETAH.

SR.ERR

ERR prints an error message indicating which items on a given input card are in error.

SR.ESCAP

Copy of SR.ESCAPE. Computes the escape probability, P_0 , to be used in the ABH solution. Used for overlay efficiency. Called from SR.EPROB.

SR.ESCAPE

ESCAPE calculates the heterogeneous lump escape probability, P_0 , used in Equation (40) for the solution of the resolved resonance collision density. ESCAPE calls SR.NEWCYL or SR.NEWSLB for table lookup values of cylindrical or slab geometries respectively. ESCAPE returns P_0 the escape probability and is called from SR.RESOL.

SR.EVAL

EVAL evaluates the B-3 coefficients A_{ij} in Equations (24). EVAL is called from SR.BTHREE.

SR.FACPHI

Calculate phase shift for the resonance calculation. Called from SR.CROSS1, CROSS2, and CROSS3.

SR.FACTS

Calculates penetration and shift factors for the resonance calculation. Called from SR.CROSS1, CROSS2, and CROSS3.

SR.FLUX

Calls SR.BONE, BTHREE, AGE, and BLKNES for the B-1 spectrum, B-3 spectrum, age, and blackness calculation, respectively.

SR.FROBNS

Inverts a complex matrix. Called from SR.CROSS3.

SR.FUNKY

Designed to define functions that appear in Doppler broadening calculations.

SR.GETCHE

GETCHE reads thermal cross-section data for each material in the three regions, cell disadvantage factor calculation. It is called by CHETAH once for each region in the cell. Macroscopic cross sections are accumulated in each region for use in the disadvantage factor calculation.

SR.GINSBURG

A drive subroutine for Dancoff-Ginsburg factor calculator.

SR.GRID

GRID calculates a discrete lethargy mesh in energy space which is used in SR.CROSS1, CROSS2, and CROSS3 to calculate the resonance cross sections used in solving Equation (40) for the collision density and Equation (56) for the resonance integrals in the resolved resonance range. The lethargy mesh is generated independently for each resonance from midpoint to midpoint between resonances. The mesh interval is directly proportional to the resonance width and inversely proportional to the resonance energy. A maximum of 900 uniform mesh intervals are permitted for each resolved resonance. However, the mesh spacing from resonance to adjacent resonance varies with gamma, the width of each resonance. The mesh spacing may be controlled by the input parameters FMULT and XLMT defined in the input instructions. The default values, however, produce optimum results. The mesh is therefore non-uniform across the series of resonance levels upstream from any given mesh point in order to calculate scatter-in sources when solving Equation (40). GRID is called from SR.NORDHEIM.

SR.HEADLIN

Prints banner page. Calls date and time.

FUNCTION.HNABB

Calculates $hn(a,b)$ for $b \geq a$ by a direct Taylor series expansion of the defining integral. Used in Doppler broadening calculation.

SR.HUNKY

This routine is designed to define functions that appear in Doppler broadening calculations.

SR.INP

Driver for the free format input package. Sets up an array of input data and a table of pointers to the data to allow free field input processing. Supervises subroutines INPALF, INPCVI, INPPCK, INPW. See the extensive comments in these subroutines for details.

SR.INP2

Routine to transfer data from input card buffer to designated storage area in core. Supervises subroutines IINKW, INPMOD/INPUPK. See the extensive comments in these subroutines for details.

SR.INTERP

INTERP is called from SR.NEWBV which is called by SR.RESOL for the resolved resonance numerical solution. NEWBV is called by RESOL to set new back values for the scatter-in source on the right-hand side of Equation (40). INTERP is called by NEWBV to interpolate from old back values to the new back value mesh.

SR.INTRP

INTRP linearly interpolates the dependent variable XY from the input table X,Y, from the argument XX. INTRP is called from SR.BENWA1 and SR.BENWA2.

SR.JNP2

Copy of SR.INP2. Supervises subroutines JINKW, JNPMOD/JNPUPK. Used for overlay efficiency.

SR.LETHRG

LETHRG calculates broad group energy boundaries and lethargy widths from the input cut point. LETHRG is called from SR.BONDAR.

SR.MAIN

Calls SR.UNINPIN for input data processing.

Calls SR.UNIFS for spectrum calculation.

Calls SR.PSTPRO for cross section post processing.

SR.MAPDR

Generate directory record for AMPX material.

SR.MAPSA

Maps cross sections into ANISN 14** format.

SR.MAPSI

Maps cross sections into CCCC ISOTXS format.

SR.MAPSK

Maps INL format data into KENO5A working library format and write.

SR.MAPSS

Maps cross sections into INL format.

SR.MAXWEL

MAXWEL generates a 101 point Maxwellian thermal flux spectrum at the input temperature requested to be used in the MND calculation of MND thermal constants. These are Equations (226) to (232) in the text. MAXWEL is called from SR.MND.

SR.MND

MND calculates Mixed Number Density constants when requested in the input. These are given in Equations (226) to (232) in the text. MND constants may only be calculated for a single thermal energy group. The MND constants are then printed for scrutiny by the user. MND is called from SR.'s MICRO and INMN3.

SR.MOV PANL

Move panel for Doppler broadening. Called from SR.TBROAD.

SR.NEWBV

NEWBV is called by SR.RESOL to calculate a set of new back values for the scatter-in source on the right-hand side of Equation (40). New back values are required because a new uniform mesh is required for Simpson's rule integration of the right-hand side of Equation (40) for the scatter-in source. SR.INTERP is called by NEWBV to interpolate to the new uniform mesh from old back values on the old non-uniform mesh generated for the cross-section calculation in SR.CROSS.

SR.NEWCY

Copy of SR.NEWCYL. Used for overlay efficiency.

SR.NEWCYL

NEWCYL is called by SR.ESCAPE to do the tabular interpolation for the capture probability P_c for cylindrical pins. The escape probability $P_0=1-P_c$.

SR.NEWSL

Copy of SR.NEWSLB. Used for overlay efficiency.

SR.NEWSLB

NEWSLB is called by SR.ESCAPE to do the tabular interpolation for the capture probability P_c for slab geometry. The escape probability $P_0=1-P_c$.

SR.NORDHEIM

Drive routine for Nordeim integral treatment for resonance integrals.

SR.OUTPUT

Writes out most of the data input.

SR.PRNRES

PRNRES prints the results of the resolved resonance calculations by fine group. PRNRES is called from SR.NORDHEIM.

SR.PRTSCAT

PRTSCAT prints out the broad group scattering matrices for both macroscopic and microscopic cross-section data. PRTSCAT is called from SR.XSCOAL.

SR.PSTPRO

Controlled for ASCII flux and cross-section output file post processing.

SR.PUNCH

PUNCH formats and writes the device-specified broad group output data. PUNCH is called from SR.XSCOAL.

SR.QUIT

Exit subroutine. Closes files and terminates program.

SR.MASCOT

Initializes macroscopic scattering cross sections and calls SR.OUTPUT. Called from SR.SPECTRUM.

SR.RESLIB

Read resolve resonance parameters from the "reres.lib" file. Reverse the order from high to low energy.

SR.RESOL

RESOL performs the calculation of the resolved resonance integrals by means of the Nordheim numerical solution. It calls SR.CROSS to generate the Doppler-broadened cross sections from the resolved resonance parameters. It solves Equation (4) at each fine lethargy mesh point for the collision density. It constructs resonance integrals from Equation (56). Shielding of the elastic scattering matrices is performed using Equations (76) through (86) in the text. SR.PRNRES is then called to print the results of the resonance calculations at the completion of the unresolved resonance calculation. RESOL is called from SR.NORDHEIM.

FUNCTION SAMPS

SAMPS integrates the scatter-in source term on the right-hand side of Equation (40) for the principal resonance absorber by means of Simpson's rule. The integration is over the back-value mesh generated in SR.NEWBV. SAMPS is called from SR.RESOL.

FUNCTIONIOM SEMPS

SEMPs integrates the scatter-in source term on the right-hand side of Equation (40) for the first input moderator by means of Simpson's rule. The integration is over the back-value mesh generated in SR.NEWBV. SEMPS is called from SR.RESOL.

SR.SKIPR

Skip forward or backward on a coded or blocked binary tape. Works on the binary "matxs.lib."

SR.SOLV

SOLV solves the B-3 Equation (26) by means of block Gauss elimination one group a time from high to low in energy. SOLV is called from SR.BTHREE.

FUNCTIONIOM SOMPS

SEMPs integrates the scatter-in source term on the right-hand side of Equation (40) for the second input moderator by means of Simpson's rule. The integration is over the back-value mesh generated in SR.NEWBV. SEMPS is called from SR.RESOL.

SR.SPECTRUM

Drives spectrum calculation by first generating the required fine group cross sections and then calculating spectrum.

SR.STRAN

Driver for reformatting the ASCII cross-section output file from internal format to the user-requested final format. Sets up storage, etc.

FUNCTIONIOM SUMPS

SEMPs integrates the scatter-in source term on the right-hand side of Equation (40) for the third input moderator by means of Simpson's rule. The integration is over the back-value mesh generated in SR.NEWBV. SEMPS is called from SR.RESOL.

FUNCTIONIOM SVMPS

SEMPs integrates the scatter-in source term on the right-hand side of Equation (40) for the first input admixed

resonance absorber by means of Simpson's rule. The integration is over the back-value mesh generated in SR.NEWBV. SEMPS is called from SR.RESOL.

FUNCTIONIOM SWMPS

SEMPS integrates the scatter-in source term on the right-hand side of Equation (40) for the second input admixed resonance absorber by means of Simpson's rule. The integration is over the back-value mesh generated in SR.NEWBV. SEMPS is called from SR.RESOL.

FUNCTIONIOM SXMPS

SEMPS integrates the scatter-in source term on the right-hand side of Equation (40) for the third input admixed resonance absorber by means of Simpson's rule. The integration is over the back-value mesh generated in SR.NEWBV. SEMPS is called from SR.RESOL.

SR.TAIL

Prints final banner. Print date, time, and elapsed run time.

SR.TBROAD

Manages the paging of cross section data for Doppler broadening.

SR.THRINV

Inverts symmetric matrix. Called from SR.FROBNS.

SR.TOTCS

Read total cross section from vector blocks in "matxs.lib" for all sibmaterials and save on direct access file, 'is' unit.

SR.TRAPZ

TRAPZ performs a trapezoidal integration of seven dependent variables from SR.RESOL over uniform mesh for one energy group in the resolved resonance range. The seven integrals are returned. TRAPZ is called from SR.RESOL.

SR.UNCHET

UNCHET reads and prints the three region ABH disadvantage factor input data on the 2000000 series cards in the input description. UNCHET is called from SR.UNINDAT only when an ABH disadvantage factor calculation is requested.

SR.UNIFS

Calls SR.SPECTRUM, which drives the spectrum calculation. Also calls SR.XSCOAL, which drives the cross section coalescing.

SR.UNINDAT

UNINDAT reads the input integer data cards in the 1000000 series and maps the input data onto modules. The data are then checked for range errors and any errors are printed. UNINDAT is called from SR.UNINPIN.

SR.UNININ

UNININ initializes the input integer data arrays before the entry of change case data. This preserves unchanged values from the previous problem. UNININ is called from SR.UNINDAT.

SR.UNINPIN

UNINPIN controls the reading of all input data on 1000000 series cards using INP subroutines. SR.UNINDAT is called to map input data which is read onto modules. UNINPIN is called from PROGRAM COMBINE7.

SR.UNPAKK

Takes the cross section data present in the ADUM array read from unit 404(???) and packs them into the local variables. UNPAKK is called from SR.GETCHE and SR.XSCOAL.

SR.UPDN

Find the largest upscatter distance, largest downscatter distance, count total number of materials in the file, and manufacture an ISOTXS 6-character name for each material.

SR.WRITFL

Utility for writing ANISN, free form, ASCII input using repeats and fills as appropriate.

SR.WRITHD

Writes header information if ISOTXS cross-section output is specified.

SR.WRITHK

Writes header for KENO5 fromat.

SR.XSCOAL

Drives the coalescing option.

8. REFERENCES

1. National Nuclear Data Center, *Evaluated Nuclear Data File (ENDF/B-VII.0)*, Brookhaven National Laboratory, December 15, 2006.
2. R. A. Grimesey, David W. Nigg, Richard L. Curtis, *COMBINE/PC-A Portable ENDF/B Version 5 Neutron Spectrum and Cross-Section Generation Program*, EGG-2589 Rev.1, February 1991.
3. R. L. Curtis et al., *PHROG -A FORTRAN-IV Program to Generate Fast Neutron Spectra and Average Multigroup Constants*, Idaho Nuclear Corp., IN-1435, April 1971.
4. R. L. Curtis and R. A. Grimesey, *INCITE: A FORTRAN-IV Program to Generate Thermal Neutron Spectra and Multigroup Constants Using Arbitrary Scattering Kernels*, Idaho Nuclear Corp., IN-1062, 1967.
5. National Nuclear Data Center, *Evaluated Nuclear Data File (ENDF/B-V)*, Brookhaven National Laboratory, 1979. R. Kinsey, *Data Formats and Procedures for the Evaluated Nuclear Data File ENDF*, BNL-NCS-50496, 1979.
6. National Nuclear Data Center, *Evaluated Nuclear Data File (ENDF/B-VI)*, Brookhaven National Laboratory, 1990. V. McLane, Editor, *ENDF-102 DATA FORMATS AND PROCEDURES FOR THE EVALUATED NUCLEAR DATA FILE ENDF-6*, BNL-NCS-44954-01/04-REV, July 1990.
7. R. E. MacFarlane and D. W. Muir, *The NJOY Nuclear Data Processing System Version 91*, Los Alamos National Laboratory, LA-12740-M, October, 1994.
8. I. I. Bondarenko, Ed., *Group Constants for Nuclear Reactor Calculations*, Consultants Bureau, New York, 1964.
9. G. I. Bell and S. Glasstone, *Nuclear Reactor Theory*, Van Nostrand Reinhold, New York, 1970.
10. R. E. MacFarlane, *TRANSX 2: A code for Interfacing MATXS Cross-Section Libraries to Nuclear Transport Codes*, LA-12312-MS, RSICC PSR-317, Los Alamos National Laboratory, July 1992.
11. L. W. Nordheim, *A Program of Research and Calculation of Resonance Absorption*, GA-2527, 1961.
12. Internal Technical Report, *ENDF/B Version 6 Nuclear Data Processing at INEL*, W. Y. Yoon, R. A. Grimesey, and C. A. Wemple, NRRT-N-91-034, 1991. Internal Letter Report, W. Y. Yoon to D. W. Nigg, *COMBINE-6 Cycle*, WYY-01-94, E&G Idaho, 1994.
13. G. D. Joanou and J. D. Dudek, *GAM-I: A Consistent P-1 Multigroup code for the Calculation of Fast Neutron Spectra and Multigroup Constants*, GA-1850, June 1961.
14. ANISN/PC Manual, D. Kent Parsons, EGG-2500, Idaho National Engineering Laboratory, December, 1988.
15. *NJOY99.0 Code System for Producing Pointwise and Multigroup Neutron and Photon Cross Sections from ENDF/B data*, RSICC PSR-480, March 2000. *Processing ENDF/VII.0 with NJOY99.161* (the latest being *NJOY99.259*), National Nuclear Data Center, December 15, 2006.
16. D. Selengut, *Critical Mass Calculations for Bare Hydrogen Moderated Reactors by Means of Transport Theory*, APEX-121, September 1952.
17. R. E. MacFarlane, R. B. Kidman and R. J. LaBauve, "The Background Cross Section Method as A General Tool for Reactor Analysis," CONF-78040, Proc. ANS Topical Meeting, Gatlinburg, Tennessee, April 1978, E. G. Silver, Ed. 1978.
18. M. G. Stamtelatos, R. J. LaBauve (LASL), "Space Shielding Cross Sections for Pebble-Bed High-Temperature Reactors," *American Nuclear Society Transactions*, 1972, pp. 600-601.

19. M. Weinberg and E. P. Wigner, *The Physical Theory of Neutron chain Reactors*, Chicago: The University of Chicago Press, 1958.
20. K. M. Case, F. de Hoffman, and G. Placzek, *Introduction to the theory of Neutron Diffusion*, Los Alamos, NM: Los Alamos Scientific Laboratory, 1953.
21. Sauer, "Thermal Utilization in the Square Cell," *Journal of Nuclear Energy*, 18, 1964, p. 425.
22. G. D. Joanou and J. S. Dudek, *GAM-II A B3 Code for the Calculation of Fast Neutron Spectra and Associated Multigroup Constants*, GA-4265, September 1963. L. Dresner, *Resonance Absorption in Nuclear Reactors*, New York: Pergamon Press, 1960.
23. M. G. Stamatelatos, "Rational Approximations for Cross-Section Space-Shielding in Doubly Heterogeneous Systems," *Nuclear Science and Engineering*, 61, 4, 1976, pp. 543-549.
24. L. Dresner, *Resonance Absorption in Nuclear Reactors*, New York; Pergamon Press, 1960.
25. D. E. Cullen, "Program SIGMA1 (version 77-1): Doppler Broadened Evaluated Cross Sections in the Evaluated Nuclear Data File/Version B (ENDF/B) Format," Lawrence Livermore National Laboratory report UCRL-50400, Vol. 17, Part B, 1977
26. N. M. Greene, L. M. Petrie, and R. M. Westfall, *NITAWL-III: SCALE System Module for Performing Resonance Shielding and Working Library Production*, pp. F2.3.2, NUREG/CR-0200, Rev 7, Volume II, Section F2, 2004.
27. K. R. Knight, SUPERDAN: Computer Programs for Calculating the Dancoff Factor of Spheres, Cylinders, and Slabs, ORNL/NUREG/CSO/Tm-2, March, 1978.
28. G. I. Bell, "A simple Treatment for Effective Resonance Absorption Cross Sections in Dense Lattices," *Nuclear Science and Engineering*, 5, 2, 1959, pp.138, 139.
29. H. Gelling and A. Sauer, *Programmbechreibung zu Dancoff Jr.*, IBM-7040, KEA-114, April 1964.
30. Amouyal, P. Benoist and J. Horowitz, "New Method for Determining the Thermal Utilization Factor in a Unit Cell," *Journal of Nuclear Energy*, 6, 1957.
31. L. E. Strawbridge, *Calculation of Lattice parameters and Criticality for Uniform Water Moderated Lattices*, WCAP-3269-25, September 1963.
32. G. E. Putnam, *MONA A Multigroup One-Dimensional Neutronics Analysis Code*, Aerojet Nuclear Company, ANCR-1051, 1972.
33. Michel H. Theys, "Integral Transport theory of Thermal Utilization Factor in Infinite Slab Geometry," *Nuclear Science and Engineering*, 7, 1, 1960, pp. 58-63.
34. W. Maynard, *Blackness Theory and Coefficients for Slab Geometry*, WAPD-TN-168, May 1959.
35. F. Henry, *A theoretical Method for Determining the Worth of Control Rods*, WAPD-218, August 1959.
36. D. Voorhis et al., *Experimental and Theoretical Study of Critical Slabs: Effect of Absorbing Membranes of Cadmium, Gold, and Boron*, WAPD-170, April 1957.
37. Radkowsky (ed.), *Naval Reactors Handbook, Volume I, Selected Basic Techniques*, TID-7050, 1964.
38. J. B. Fussell ltr to H. L. McMurry, JBF-8-70, SCAMP S_n Code Consolidation and Modification, EG&G Idaho, August 7, 1970,
39. J. Lieberoth and A. Stojadinovic, "Neutron Streaming in Pebble Beds," *Nuclear Science and Engineering*, 76, 1980, pp336-344.

APPENDIX A

INL CROSS-SECTION FORMAT DESCRIPTION

Appendix A

INL Cross-Section Format Description

The internal INEL format is based on a word-addressable card image file structure. The following tables describe this structure. A nonzero value in column 1 of a data record for a material signifies the end of data for that material. The scatter matrices do not have the $2L + 1$ term multiplied into them.

Table A-1. The library material title record summary.

Information or Mnemonic Name of Data	Record Columns	Description or Function
IAD	2-3	A nonzero value means update rather than replace or add this material to the library file.
IDIFF	4-5	A nonzero value means the SIGMU(J,IM) values are computed from the input D(J,IM) values instead of read directly.
MTLNO (or LM)	6-8	Library material identifying number.
IENPF	9-10	Controls how the energy per fission values are input: $0, \mathcal{E}_j^m = \text{EPFISS},$ $1, \mathcal{E}_j^m = \mathcal{E}_1^m,$ $2, \mathcal{E}_j^m \text{ as input, where } m = \text{MTLNO}.$
	11-12	Must be blank.
Any Hollerith characters	13-72	Library material title information.

Card 2 for kinf and keff for the macroscopic data requested,
 Energy per fission for the microscopic data requested.

Table A-2. The library material floating point data summary.

Index 1 Card Cols. 2-3	Index 2 Card Cols. 4-5	Index 3 Card Cols. 6-8	Index 4 Card Cols. 9-10	Mnemonic Name of Data	Description or Function of Data (index which increases as more data words are added across a card is enclosed in parenthesis)
1	LM	J	1	DC(J,LM)	Diffusion coefficient for group J of library material LM (when IDIFF = 1 on the title card). (J)
1	LM	J	2	SIGA(J,LM)	Absorption cross section for group J of library material LM. (J)
1	LM	J	3	SIGNU(J,LM)	Neutron per fission times fission cross section for group J of library material LM ($\nu \sum_f$).
1	LM	J	4	SIGFIS(J,LM)	Fission cross section for group J of library material LM. (J)
1	LM	J	5	C4CHI(J;LM)	Fission source for group J of library material LM. (J)
3	LM	J	K	TRMAT(J,K)	General scattering transfer cross sections \sum_{s0} , from group J to group K for library material m \equiv LM (K may be less than, equal to, or greater than J). (K)
4	LM	J	0	SIGMU(J,LM)	Transport cross section σ_{uj}^m for group j = J of library material m \equiv LM (used in group j = J for mixing the macroscopic cross section, \sum_{ij}^m , from which the macroscopic diffusion coefficient, D_j^m , for macroscopic material m is computed). This input data is used only if IDIFF = 0 or blank on the title card.(J)
6	LM	J	K	TRMAT1(J,K)	Same as INDEX1 = 3 for values of \sum_{s1}^m (K)
7	LM	J	K	TRMAT2(J,K)	Same as INDEX1 = 3 for values of \sum_{s2}^m (K)
8	LM	J	K	TRMAT3(J,K)	Same as INDEX1 = 3 for values of \sum_{s3}^m (K)

APPENDIX B

ANISN CROSS-SECTION FORMAT DESCRIPTION

Appendix B

ANISN Cross-Section Format Description

If the ANISN output format is selected, all cross sections are output in the standard ANISN card image 14** format (see Reference B-1 for details). The absorption, nu-sigma-fission, and total cross sections are always present regardless of the scattering order of the material or the current group number. For scattering orders beyond

$e = 0$, the absorption, nu-sigma-fission, and total cross sections are 0.0.

The upscatter cross sections are present only when (HIS-IHT) is greater than 1. If they are present, there are $NUS = (HIS - IHT - 1)$ locations present for every group and for every scattering order (material). This includes the physically nonexistent quantities such as σ upscattering from group (IGM + NUS) to the lowest energy group IGM. In this way, the number of upscatter cross sections for each group in the cross-section table remains constant. The cross-section arrangement is summarized in Table B-1.

Table B-1. Cross-section arrangement.

Cross Section	Group	Position Description
σ absorption	g	
$\nu\sigma$ fission	g	
σ total or σ transport	g	IHT
σ upscatter	$(g + NUS) \rightarrow g$	
•	•	
•	•	
•	•	
σ upscatter	$(g + 1) \rightarrow g$	IHS
σ self-scatter	$g \rightarrow g$	
σ downscatter	$(g - 1) \rightarrow g$	
•	•	
•	•	
•	•	
σ downscatter	$(g - NDS) \rightarrow g$	IHM
σ upscatter (code calculated)	From g	IHP = IHM + 1

Finally, it should be noted that the higher-order scattering materials are output by COMBINE/PC without the $(2\ell + 1)$ term pre-multiplied into them.

B. REFERENCE

1. D. K. Parsons, *ANISN/PC Manual*, EGG-2500, December 1988.

APPENDIX C

**CCCC INTERFACE FILE FORMATS AND
CONVENTIONS**

Appendix C

CCCC Interface File Formats and Conventions^a

ISOTXS—Nuclide (Isotope) Ordered, Multigroup Neutron Cross-Sections

The changes in ISOTXS-IV relative to ISOTXS-III are in the main part, clarifications of ambiguities present in the latter. The changes reflected in Version IV are:

- If scattering bandwidth, JBAND(J,N), is zero, no scatter data are present in block N. (see 4D record.)
- The position of self-(or within-group-) scatter must lie within the scattering bandwidth unless the bandwidth is zero, i.e.,

$$I < IJJ(J,N) < JBAND(J,N) \text{ if } JBAND(J,N) \neq 0.$$

- (See 4D record.)
- The Legendre expansion coefficient factor $(2\rho + 1)$ is not included in the P_ρ weighted transport and total cross sections. (See 5D record.)
- The $n,2n$ principal cross section (see 5D record) is clarified as the $n,2n$ reaction cross section while the $n,2n$ scatter matrix terms are clarified (see 4D record NOTE) as emission (productin) based, i.e.,

$$\sigma_{n,2n(g)} = 0.5 \sum_{g'} \sigma_{n,2n}(g \rightarrow g') \quad (\text{C-1})$$

In addition, the following is included to clarify the meaning of the vectors IDSCT(N) and LORD(N) contained in the ISOTOPE CONTROL AND GROUP-INDEPENDENT DATA (4D) record and to remove an ambiguity in the subblocking of scattering data.

IDSCT(N) specifies the identity and ordering of scattering data blocks, and LORD(N) specifies the number of Legendre orders contained in each block. Each block of scattering may be subblocked into NSBLOCK records (subblocks) where NSBLOCK is found on the FILE CONTROL (ID) record. With the single exception below, sub-blocking shall not be used (NSBLOCK > 1) if the individual blocks defined by IDSCT and LORD contain more than one Legendre order of scattering. The single exception is that subblocking may be used with more than one Legendre order per record (subblock) only if each record (subblock) contains data for a single “scattered-into” group.

Finally, the following information is reproduced from the Version III specifications for the sake of completeness.

The P_ρ weighted transport and total cross sections can be defined^b as

$$\sigma_{n,22,(g)} = 0.5 \sum_{g'} \sigma_{n,2n}(g \rightarrow g') \quad \rho = 1, \dots, \text{LTRN}, \quad (\text{C-2})$$

and

a. Extracted from LA-6941-MS, Standard Interface Files and Procedures for Reactor Physics Codes Version IV by R. Douglas O'Dell.

b. Other definitions of the P_ρ weighted transport cross section are also possible.

The P ρ weighted scattering cross sections given in the scattering blocks are defined as

$$\sigma_{i\rho}^g \equiv \frac{\int_g \sigma_\rho(E) dE}{\int_g \sigma_\rho(E) dE} \quad \rho = 0, 1, \dots, \text{LTOT}-1 \quad . \quad (\text{C-3})$$

$$\sigma_{s\rho}(g \rightarrow g') \equiv \frac{\int_g \int_{g'} \sigma_{s\rho}(E \rightarrow E') \sigma_\rho(E) dE' dE}{\int_g \sigma_\rho(E) dE} \quad (\text{C-4})$$

```

C*****
C  REVISED 11/30/76      -
C                        -
CF  ISOTXS-IV           -
CE  MICROSCOPIC GROUP NEUTRON CROSS SECTIONS      -
C                        -
CN THIS FILE PROVIDES A BASIC BROAD GROUP          -
CN LIBRARY, ORDERED BY ISOTOPE                     -
CN FORMATS GIVEN ARE FOR FILE EXCHANGE PURPOSES    -
CN ONLY                                             -
C                        -
C*****
C-----
CS  FILE STRUCTURE      -
CS                        -
CS  RECORD TYPE  PRESENT IF      -
CS  =====
CS  FILE IDENTIFICATION  ALWAYS      -
CS  FILE CONTROL  ALWAYS      -
CS  FILE DATA  ALWAYS      -
CS  FILE-WIDE CHI DATA  ICHIST .GT. 1      -
CS                        -
CS ***** (REPEAT FOR ALL ISOTOPES)      -
CS * ISOTOPE CONTROL AND GROUP      -
CS * INDEPENDENT DATA  ALWAYS      -
CS * PRINCIPAL CROSS SECTIONS  ALWAYS      -
CS * ISOTOPE CHI DATA  ICHI .GT. 1      -
CS *      -
CS * ***** (REPEAT TO NSCMAX CATTERING BLOCKS)      -
CS * * ***** (REPEAT FROM 1 TO NSBLOK)      -
CS * * * SCATTERING SUB-BLOCK  LORD (N) .GT. 0      -
CS *****      -
C                        -
C-----

```



```

C-----
CR   FILE IDENTIFICATION           -
C   -
CL  HNAME, (HUSE (I), I=1,2), IVERS   -
C   -
CW  1+3*MULT=NUMBER OF WORDS       -
C   -
CB  FORMAT (11H  OV  ISOTXS ,  1H*,   -
CB  12A6, 1H*, I6)                 -
C   -
CD  HNAME    HOLLERITH FILE NAME - ISOTXS - (A6)           -
CD  HUSE (I)  HOLLERITH USER IDENTIFICATION (A6)           -
CD  IVERS    FILE VERSION NUMBER                           -
CD  MULT     DOUBLE PRECISION PARAMETER                    -
CD   1 - A6 WORD IS SINGLE WORD                             -
CD   2 - A6 WORD IS DOUBLE PRECISION WORD                   -
C   -
C-----
C-----
CR   FILE CONTROL   (1D RECORD)       -
C   -
CL  NGROUP, NISO, MAXUP, MAXDN, MAXORD, ICHIST, NSCMAX, NSBLOK   -
C   -
CW  8 = NUMBER OF WORDS               -
C   -
CB  FORMAT (4H  1D  ,8I6)              -
C   -
CD  NGROUP    NUMBER OF ENERGY GROUPS IN FILE             -
CD  NISO     NUMBER OF ISOTOPES IN FILE                     -
CD  MAXUP    MAXIMUM NUMBER OF UPSCATTER GROUPS            -
CD  MAXDN    MAXIMUM NUMBER OF DOWNSCATTER GROUPS          -
CD  MAXORD   MAXIMUM SCATTERING ORDER (MAXIMUM VALUE OF    -
CD  LEGENDRE EXPANSION INDEX USED IN FILE).                 -
CD  ICHIST   FILE-WIDE FISSION SPECTRUM FLAG               -
CD  ICHIST .EQ. 0,    NO FILE-WIDE SPECTRUM                 -
CD  ICHIST .EQ. 1,    FILE-WIDE CHI VECTOR                  -
CD  ICHIST .GT. 1,    FILE-WIDE CHI MATRIX                  -
CD  NSCMAX   MAXIMUM NUMBER OF BLOCKS OF SCATTERING DATA  -
CD  NSBLOK   SUBBLOCKING CONTROL FOR SCATTER MATRICES. THE -
CD           SCATTERING DATA ARE SUBBLOCKED INTO NSBLOK   -
CD           RECORDS (SUBBLOCKS) PER SCATTERING BLOCK.     -
C   -
C-----

```

```

C-----
CR FILE DATA (2D RECORD) -
C -
CL (HSETID (I) , I=1 , 12) , (HISONM (I) , I=1 , NISO) , -
CL 1(CHI(J) , J=1 , , NGROUP) , (VEL (J) , J=1 , NGROUP) -
CL 2(EMAX(J) , J=1 , NGROUP) , EMIN, (LOCA(I) , I=1 , NISO) -
C -
CW (NISO+12)*MULT+1+NISO -
CW +GROUP*(2+ICHIST*(2/(ICHIST+1)))=NUMBER OF WORDS -
C -
CB FORMAT (4H 2D , 1H* , 11A6, 1H*/ HSETID,HISONM -
CB 11H* ,A6, 1H* ,9(1X,A6)/(10(10(1X,A6))) -
CB FORMAT ( 6E12.5) CHI (PRESENT IF ICHIST .EQ .1) -
CB FORMAT ( 6E12.5) VEL, EMAX, EMIN -
CB FORMAT (12I6) LOCA -
C -
CD HSETID (I) HOLLERITH IDENTIFICATION OF FILE (A6) -
CD HISONM (I) HOLLERITH ISOTOPE LABEL FOR ISOTOPE I (A6) -
CD CHI (J) FILE-WIDE FISSION SPECTRUM (PRESENT IF ICHIST. EQ .1) -
CD VEL (J) MEAN NEUTRON VELOCITY IN GROUP J (CM/SEC) -
CD EMAX (J) MAXIMUM ENERGY BOUND OF GROUP J (EV) -
CD EMIN MINIMUM ENERGY BOUND OF SET (EV) -
CD LOCA (I) NUMBER OF RECORDS TO BE SKIPPED TO READ DATA FOR -
CD ISOTOPE I. LOCA (I) = 0 -
C -
C-----
C-----
CR FILE-WIDE CHI DATA (3D RECORD) -
C -
CC PRESENT IF ICHIST .GT .1 -
C -
CL ((CHI(K,J) , K=1 , ICHIST) , J=1 , NGROUP) , (ISSPEC (I=1 , NGROUP) -
C -
CW NGROUP*( ICHIST+1)=NUMBER OF WORDS -
C -
CB FORMAT ( 4H 3D , 5E12.5/ (6E12.5)) CHI -
CB FORMAT ( 12I6) ISSPEC -
C -
CD CHI (K , J) FRACTION OF NEUTRONS EMITTED INTO ROUP J AS A -
CD RESULT OF FISSION IN ANY GROUP, USING SPECTRUM K -
CD ISSPEC ( I) ISSPEC ( I) =K IMPLIES THAT SPECTRUM K IS USED -
CD TO CALCULATE EMISSION SPECTRUMF ROM FISSION -
CD IN GROUP I -
C -
C-----

```

```

C-----
CR   ISOTOPE CONOTROL AND GROUP INDEPENDENT DATA (4D RECORD)      -
C
CL   HABSID, HIDENT, HMAT, AMASS, EFFISS, ECAPT, TEMP, SIGPOT, ADENS, KBR, ICHI,      -
CL 1IFIS, IALF, INP, IN2N, IND, INT, LTOT, LTRN, ISTRPD,              -
CL 2(IDSCT (N), N=1, NSCMAS), (LORD (N), N=1, NSCMAX),              -
CL 3((JBAND (J,N), J=1, NGROUP), N=1, NSCMAX),                      -
CL 4((IJJ(J,N), J=1, NGROUP), N=1, NSCMAX)                          -
C
CW 3*MULT+17+NSCMAX*(2*NGROUP+2) = NUMBER OF WORDS                -
C
CB   FORMAT (4H 4D ,3 (1X,A6)/ 6E12.5/                               -
CB 1(12I6))                                                         -
C
CD HABSID          HOLLERITH ABSOLUTE ISOTOPE LABEL - SAME FOR ALL      -
CD VERSIONS OF THE SAME ISOTOPE IN FILE (A6)                        -
CD HIDENT          IDENTIFIER OF LIBRARY FROM WHICH BASIC DATA        -
CD CAME (E.G. ENDF/B) (A6)                                          -
CD HMAT ISOTOPE IDENTIFICATION (E.G. ENDF/B MAT NO.)(A6)           -
CD AMASS GRAM ATOMIC WEIGHT                                          -
CD EFISS TOTAL THERMAL ENERGY YIELD/FISSION (W.SEC/FISS)          -
CD ECAPT TOTAL THERMAL ENERGY YIELD/CAPTURE (W.SEC/CAPT)          -
CD TEMP ISOTOPE TEMPERATURE (DEGREES KELVIN)                       -
CD SIGPOT AVERAGE EFFECTIVE POTENTIAL SCATTERING IN                -
CD RESONANCE RANGE (BARNS/ATOM)                                     -
CD ADENS DENSITY OF ISOTOPE IN MIXTURE IN WHICH ISOTOPE            -
CD CROSS SECTIONS WERE GENERATED (A/BARN-CM)                      -
CD KBR ISOTOPE CLASSIFICATION                                       -
CD 0=UNDEFINED -
CB 1=FISSILE -
CB 2=FERTILE -
CD 3=OTHER ACTINIDE -
CD 4=FISSION PRODUCT -
CD 5=STRUCTURE -
CD 6=COOLANT -
CD 7=CONTROL -
CD ICHI ISOTOPE FISSION SPECTRUM FLAG -
CD ICHI.EQ.1, USE FILE-WIDE CHI -
CD ICHI.EQ.1, ISOTOPE CHI VECTOR -
CD ICHI.GT.1, ISOTOPE CHI MATRIX -
CD IFIS(N,F) CROSS SECTION FLAG -
CD IFIS =0, NO FISSION DATA IN PRINCIPAL CROSS SECTION RECORD    -
CD =1, FISSION DATA PRESENT IN PRINCIPAL CROSS SECTION RECORD     -
CD IALF (N, ALPHA) CROSS SECTION FLAG -
CB SAME OPTIONS AS IFIS -
CB INP (N, P) CROSS SECTION FLAG -
CD SAME OPTIONS AS IFIS -
CD IN2N (N, 2N) CROSS SECTION FLAG -
CD SAME OPTIONS AS IFIS -
CD IND(N,D) CROSS SECTION FLAG -
CD SAME OPTIONS AS IFIS -
CD INT (N, T) CROSS SECTION FLAG -
CD SAME OPTIONS AS IFIS -

```

CD LTOT NUMBER OF MOMENTS OF TOTAL CROSS SECTION PROVIDED -
 CD IN PRINCIPAL CROSS SECTIONS RECORD -
 CD LTRN NUMBER OF MOMENTS OF TRANSPORT CROSS SECTION -
 CD PROVIDED IN PRINCIPAL CROSS SECTIONS RECORD -
 CD ISTRPD NUMBER OF COORDINATE DIRECTIONS FOR WHICH -
 CD COORDINATE DEPENDENT TRANSPORT CROSS SECTIONS -
 CD ARE GIVEN. IF ISTRPD = 0, NO COORDINATE DEPENDNET -
 CD TRANSPORT CROSS SECTIONS ARE GIVEN. -
 CB IDSCT(N) SCATTERING MATRIX TYPE IDENTIFICATION FOR -
 CB SCATTERING BLOCK N. SIGNIFICANT ONLY IF -
 CD LORD (N). GT.0 -
 CD IDSCT (N) =000 + NN, TOTAL SCATTERING, (SUM OF -
 CD ELASTIC, INELASTIC, AND N, 2N SCATTERING -
 CD MATRIX TERMS). -
 CD =100 + NN, ELASTIC SCATTERING -
 CD =200 + NN, INELASTIC SCATTERING -
 CD =300 + NN, (N, 2N) SCATTERING,-----SEE -
 CD NOTE BELOW -
 CD WHERE NN IS THE LEGENDRE EXPANSION INDEX OF THE -
 CD FIRST MATRIX IN BLOCK N -
 CD LORD (N) NUMBER OF SCATTERING ORDERS IN BLOCK N. IF -
 CD LORD (N) = 0, THIS BLOCK IS NOT PRESENT FOR THIS -
 CD ISOTOPE. IF NN IS HE VALUE TKEN FROM -
 CD IDSCT (N), THEN THE MATRICES IN THIS BLOCK -
 CD HAVE LEGENDRE EXPANSION INDICES OF NN, NN+1, -
 CB NN+2,..., NN+LORD (N) - 1 -
 CB JBAND(J,N) NUMBER OF GROUPS THAT SCATTER INTO GROUP J, -
 CD INCLUDING SELF-SCATTER, IN SCATERING BLOCK N. -
 CD IF JBAND (J,N) = 0, NO SCATTER DATA IS PRESENT IN -
 CD BLOCK N -
 CD IJJ(J,N) POSITION OF IN-GROUP SCATTERING CROSS SECTION IN -
 CD SCATTERING DATA FOR GROUP J, SCATTERING BLOCK -
 CD N, COUNTED FROM THE FIRST WORD OF GROUP J DATA. -
 CD IF JBAND (J,N). NE. 0 THEN IJJ(,N) MUST SATISFY -
 CD THE RELATION 1.LE.IJJ (J,N).LE.JBAND (J,N) -
 C -
 CN NOTE- FOR N,2N, SCATTER, THE MATRIX CONTAINS TERMS, -
 CN SCAT (J TO G), WHICH ARE EMISSION (PRODUCTION) -
 CN BASED, I.E., ARE DEFINED SUCH THAT MACROSCOPIC -
 CN SCAT (J TO G) TIMES THE FLUX IN GROUP J GIVES -
 CN THE RATE OF EMISSION (PRODUCTION) OF NEUTRONS -
 CN INTO GROUP G. -
 C -
 C-----

```

C-----
CR PRINCIPAL CROSS SECTIONS      (5D RECORD)          -
C  ((STRPL (J,L), J=1, NGROUP), L=1, LTRN),          -
CL 1((STOTPL (J,L), J=1, NGROUP), L=1, LTOT), (SNGAM(J), J=1, NGROUP), -
CL 2(SFIS (J), J=1, NGROUP), (SNUTOT (J), J=1, NGROUP), -
CL 3(CHISO (J), J=1, NGROUP), (SANLF (J), J=1, NGROUP), -
CL 4(SNP (J), J=1, NGROUP), (SN2N (J), J=1, NGROUP), -
CL 5(SND (J), J=1, NGROUP), (SNT (J), J=1, NGROUP)    -
CL 6((STRPD (J,I), J=1, NGROUP), I=1, ISTRPD)        -
C -
CW (1+LTRN+LTOT+IALF+INP+IN2N+IND+INT+ISTRPD+2*IFIS+  -
CW ICHI* (2/(ICHI+1)))*NGROUP=NUMBER OF WORDS      -
C -
CB FORMAT (4H 5D ,      5E12.5/(6E12.5)) LENGTH OF LIST AS ABOVE -
C -
CD STRPL (J,L)          PL WEIGHTED TRANSPORT CROSS SECTION      -
CD THE FIRST ELEMENT OF ARRAY STRPL IS THE                -
CD CURRENT (P1) WEIGHTED TRANSPORT CROSS SECTION          -
CD THE LEGENDRE EXPANSION COEFFICIENT FACTOR (2L+1)      -
CD IS NOT INCLUDED IN STRPL (J,L).                        -
CD SNGAM (J)          (N,GAMMA)                               -
CD SFIS (J)          (N,F) (PRESENT IF IFIS.GT.0)          -
CD SNUTOT (J)        TOTAL NEUTRON YIELD/FISSION(PRESENT IF IFIS.GT.0) -
CD CHISO (J)        ISOTOPE CHI (PRESENT IF ICHI.EQ.1)      -
CD SANLF (J)        (N, ALPHA) (PRESENT IF IALF.GT.0)      -
CD SNP (J)          (N,P) (PRESENT IF INP.GT.0)            -
CD SN2N (J)        (N, 2N) (PRESENT IF IN2N.GT.0)  ----SEE -
CD          NOTE BELOW----                                  -
CD SND (J)          (N,D) (PRESENT IF IND.GT.0)            -
CD SNT (J)          (N,T) (PRESENT IF IND.GT.0)            -
CB STRPD (J,I)      COORDINATE DIRECTION I TRANSPORT CROSS SECTION -
CB (PRESENT IF ISTRPD.GT.0)                                -
C -
CN          NOTE - THE PRINCIPAL N,2N CROSS SECTION SN2N(J) -
CN IS DEFINED AS THE N,2N CROSS SECTION SN2N(J)          -
CN I.E., SUCH THAT MACROSCOPIC SN2N(J) TIMES THE        -
CN FLUX IN GROUP J GIVES THE RATE AT WHICH N, 2N        -
CN REACTIONS OCCUR IN GROUP J.  THUS, FOR N, 2N        -
CN SCATTERING, SN2N (J) = 0.5*(SUM OF SCAT (J TO G)      -
CN SUMMED OVER ALL G).                                    -
C -
C-----

```

```

C-----
CR ISOTOPE CHI DATA (6D RECORD) -
C -
CC PRESENT IF ICHI.GT.1 -
C -
CL ((CHIISO(K,J),K=1,ICHI),J=1, NGROUP), (ISOPEC(I), I=1, NGROUP) -
C -
CW NGROUP*(ICHI+1) = NUMBER OF WORDS -
C -
CB FORMAT (4H 6D , 5E12.5)) CHIISO -
CB FORMAT (12I6) ISOPEC -
C -
CD CHIISO (K, J) FRACTION OF NEUTRONS EMITTED INTO GROUP J AS A -
CD RESULT OF FISSION IN ANY GROUP, USING SPECTRUM K -
CD ISOPEC (I) ISOPEC (I) = K IMPLIES THAT SPECTRUM K IS USED -
CD TO CALCULATE EMISSION SPECTRUM FROM FISSION -
CD IN GROUP I -
C -
C -
C-----
C-----
CR SCATTERING SUB-BLOCK (7D RECORD) -
C -
CC PRESENT IF LORD (N) .GT.0 -
C -
CL ((SCAT (K, L), K=1, KMAX), L=1, LORDN) -
C -
CC KMAX=SUM OVER J OF JBAND (J,N) WITHIN THE J-GROUP RANGE OF THIS -
CC SUB-BLOCK. IF M IS THE INDEX OF THE SUB-BLOCK, THE J-GROUP -
CC RANGE CONTAINED WITHIN THIS SUB-BLOCK IS -
CC  $JL = (M-1)*((NGROUP-1)/NSBLOK + 1)+1$  TO  $JU=MINO (NGROUP, JUP)$ , -
CC WHERE  $JUP = M* ((NGROUP-1)/NSBLOK + 1)$ . -
C -
CC LORDN = LORD (N) -
CC N IS THE INDEX FOR THE LOOP OVER NSCMAX (SEE FILE STRUCTURE) -
C -
CW KMAX*LORDN = NUMBER OF WORDS -
C -
CB FORMAT (4H 7D , 5E12.5)) -
C -
CD SCAT (K,L) SCATTERING MATRIX OF SCATTERING ORDER L, FOR -
CD REACTION TYPE IDENTIFIED BY IDSCT (N) FOR THIS -
CD BLOCK. JBAND (J, N) VALUES FOR SCATTERING INTO -
CD GROUP J ARE STORED AT LOCATIONS K=SUM FROM 1 -
CD TO (J-1) OF JBAND (J,N) PLUS 1 TO K-1+JBAND (J,N). -
CD THE SUM IS ZERO WHEN J=1. J-TO-J SCATTER IS -
CD THE IJJ (J, N) -TH ENTRY IN THE RANGE JBAND (J, N). -
CD VALUES ARE STORED IN THE ORDER (J+JUP), -
CD (J + JUP - 1),..., (J + 1), J, (J - 1),..., (J - JDN), -
CD WHERE  $JUP = IJJ (J, N) - 1$  AND  $JDN = JBAND (J, N) - IJJ (J, N)$  -
C -
C-----
CEOF

```

APPENDIX D

**VALIDATION OF COMBINE7.1 CRITICALITY
SEQUENCES**

Appendix D

Validation of COMBINE7.1 Criticality Sequences

Criticality validation calculations were performed as part of verification and validation of the code. The COMBINE7.1 criticality validation suite is a collection of 29 benchmarks taken from the *International Handbook of Evaluated Criticality Benchmark Experiments* (IHECB) [1] and/or *Cross Section Evaluation Working Group Benchmark Specifications* (CSEWG) [2]. The cases in the suite were selected to compass a variety of fissile materials in configurations that produce fast, intermediate, and thermal spectra, but were limited to those configurations which COMBINE7.1 calculation sequence, i.e., COMBINE7.1/ANISN, can afford. Some independent MCNP [3] calculations were also performed, all based on ENDF/B-VII.0 nuclear data. The distribution of cases by fuel material and spectrum is shown in Table D.1, and a brief summary of each case is followed. The results are listed in Table D.2, D.3, D.4, and D.5 for the combination of B1 or B3 and Sn correction or no Sn correction. The experiment k_{eff} values have some uncertainties involved and estimated to be mostly within 1.0000 ± 0.0050 [1]. The k_{eff} values from MCNP calculations are also included. The results show the sensitivity to the deterministic nature of the method and to the B_L approximation limited to $L=1$ or $L=3$. The results are very robust despite these limitations and are very comparable to the experiments or the MCNP results. A limited number of cases included the one-dimensional transport correction, showing a small improvement. Some sensitivity can be digested from these calculations. All the relevant input files are included in the code package.

Table D.1: Criticality Validation Suite

Spectrum		Fast		Intermediate		Thermal	
Geometry	Bare	Heavy Reflector	Light Reflector	Any	Lattice of Fuel Pins in Water	Soution	
						Bare	Reflector
HEU	GODIVA	FLATTOP-25		HCI-004		ORNL-1, ORNL-2, ORNL-10, L-8, L-9	L-7, L-10
IEU	IEU-MF-03						
LEU					TRX1, TRX2, BAPL1, BAPL2, BAPL3		
²³³ U	JEZEBEL-23	UMF002-1, UMF002-2	UMF005-1, UMF005-2				
Pu	JEZEBEL, JEZEBEL-Pu	FLATTOP- PU		PCI-001		PNL-1, PNL- 2, PNL-3, PNL-4	

GODIVA

This is a bare sphere of enriched uranium metal modeled as a homogeneous sphere of radius 8.741 cm with the composition shown in the following table (number densities are given in nuclides per barn-cm).

Isotope	Density
²³⁵ U	0.045000
²³⁸ U	0.002498
²³⁴ U	0.000492

FLATTOP-25

This is a spherical system consisting of a highly enriched uranium core in a thick natural uranium reflector. The core radius is 6.116 cm and the outer radius of the reflector is 24.13 cm. The compositions for the two regions (nuclides per bar-cm) are given in the following table.

Isotope	Core	Reflector
^{235}U	0.04449	0.00034
^{238}U	0.00270	0.04774
^{234}U	0.00049	

FLATTOP-PU

This is a spherical system consisting of a plutonium core in a thick natural uranium reflector. The radius of the core is 4.533 cm and the outer radius of the reflector is 24.13 cm. The compositions of the two regions are given in the following table.

Isotope	Core	Reflector
^{239}Pu	0.03674	
^{240}Pu	0.00186	
^{241}Pu	0.00012	
Ga	0.00138	
^{235}U		0.00034
^{238}U		0.04774

JEZEBEL

This is a bare sphere of plutonium modeled as a homogeneous sphere of radius 6.385 cm with the composition shown in the following table (all number of densities are given as nuclides per barn-cm).

Isotope	Density
^{239}Pu	0.037050
^{240}Pu	0.001751
^{241}Pu	0.000117
Ga	0.001375

JEZEBEL-23

This is a bare sphere of enriched ^{233}U metal (98.13%) with radius 5.983 cm and the composition shown in the following table (all number of densities are given as nuclides per barn-cm).

Isotope	Density
^{233}U	0.04671
^{234}U	0.00059
^{235}U	0.00001
^{238}U	0.00029

JEZEBEL-Pu

This is a bare sphere of enriched plutonium meta, containing 20.1% ^{240}Pu . It is modeled as a homogeneous sphere of radius 6.65985 cm with the composition shown in the following table (all number of densities are given as nuclides per barn-cm).

Isotope	Density
^{239}Pu	0.029946
^{240}Pu	0.007887
^{241}Pu	0.001203
^{242}Pu	0.000145
Ga	0.001372

U233-met-fast-002 (umf-002)

This is a spherical system consisting of a highly enriched ^{233}U surrounded by highly enriched ^{235}U .

- Case (1) The core radius is 5.0444 cm and the outer radius of the surrounding highly enriched ^{235}U is 6.2661 cm.
- Case (2) The core radius is 4.5999 cm and the outer radius of the surrounding highly enriched ^{235}U is 6.5887 cm.

Both critical experiments were performed at Los Alamos Scientific Laboratory.

The compositions for the two regions (nuclides per bar-cm) of these cases are given in the following table. Temperature is at 293 $^{\circ}\text{K}$.

Isotope	Case 1	Case 2
^{233}U core		
^{233}U	4.7253×10^{-2}	4.7312×10^{-2}
^{234}U	5.2705×10^{-4}	5.2770×10^{-4}
^{238}U	3.2975×10^{-4}	3.3015×10^{-4}
^{235}U Surroundings		
^{235}U	4.4892×10^{-1}	4.4892×10^{-1}
^{238}U	3.2340×10^{-3}	3.2340×10^{-3}

U233-met-fast-005 (umf-005)

This is a spherical system consisting of a highly enriched ^{233}U , reflected by beryllium.

- Case (1) The core radius is 5.0444 cm and the outer radius of the reflector is 7.0891 cm.
- Case (2) The core radius is 4.5999 cm and the outer radius of the reflector is 8.7960 cm.

Both critical experiments were performed at Los Alamos Scientific Laboratory.

The compositions for the two regions (nuclides per bar-cm) of these cases are given in the following table. Temperature is at 293 ⁰K.

Isotope	Case 1	Case 2
²³³ U core		
²³³ U	4.7253x10 ⁻²	4.7312x10 ⁻²
²³⁴ U	5.2705x10 ⁻⁴	5.2770x10 ⁻⁴
²³⁸ U	3.2975x10 ⁻⁴	3.3015x10 ⁻⁴
Beryllium Reflector		
Be	1.1984x10 ⁻¹	1.1984x10 ⁻¹
O	1.3776x10 ⁻³	1.3776x10 ⁻³

Pu-Comp-Inter-001 (PCI-001)

This is a k_{∞} experiment at the HECTOR reactor (Winfrith, UK, 1960s): a graphite moderated plutonium oxide core (5% ²⁴⁰Pu). The benchmark model is an infinite medium with a material composition appropriate to the interpolated boron/²³⁹Pu ratio. It is modeled as a homogeneous infinite medium with the composition shown in the following table (all number of densities are given as nuclides per barn-cm).

Isotope	Density
²³⁹ Pu	2.7350x10 ⁻⁴
²⁴⁰ Pu	1.5490x10 ⁻⁵
²⁴¹ Pu	1.0720x10 ⁻⁶
²⁴² Pu	5.8000x10 ⁻⁸
¹ H	1.0770x10 ⁻⁴
¹⁰ B	1.0151x10 ⁻⁴
¹¹ B	4.0859x10 ⁻⁴
C	7.0900x10 ⁻²
¹⁶ O	2.7070x10 ⁻³
⁴⁰ Ca	8.0267x10 ⁻⁴
⁴² Ca	5.3572x10 ⁻⁶
⁴³ Ca	1.1178x10 ⁻⁶
⁴⁴ Ca	1.7272x10 ⁻⁵
⁴⁶ Ca	3.3120x10 ⁻⁸
⁴⁸ Ca	1.5484x10 ⁻⁶

HEU-Comp-Inter-004 (HCI-004)

This is a k_{∞} experiment at the HECTOR reactor (Winfrith, UK, 1960s): a graphite moderated uranium oxide core. The benchmark model is an infinite medium with a material composition appropriate to the interpolated boron/ ^{235}U ratio. It is modeled as a homogeneous infinite medium with the composition shown in the following table (all number of densities are given as nuclides per barn-cm).

Isotope	Density
^{234}U	3.1200×10^{-6}
^{235}U	2.5020×10^{-4}
^{236}U	4.2670×10^{-7}
^{238}U	1.7190×10^{-5}
^1H	1.1260×10^{-4}
^{10}B	5.7849×10^{-5}
^{11}B	2.3285×10^{-4}
C	7.5650×10^{-2}
^{16}O	1.6500×10^{-2}
^{40}Ca	5.5227×10^{-4}
^{42}Ca	3.6860×10^{-6}
^{43}Ca	7.6909×10^{-7}
^{44}Ca	1.1884×10^{-5}
^{46}Ca	2.2788×10^{-8}
^{48}Ca	1.0653×10^{-6}

AQUEOUS THERML CRITICALS

Three unreflected spheres from the ORNL series were computed. These benchmarks contain ^{235}U in the form of uranyl nitrate dissolved in water. One of the devices was poisoned with boron. The CSEWG treatment for these criticals models them as bare spheres of the core solution corrected for the thin aluminum shells, nonspherical shape, fill tubes, and room return. Benchmarks ORNL-1 and ORNL-2 are of radius 34.595 cm, and ORNL-10 has a radius of 61.011 cm. The compositions specified for the CSEWG models are as follows.

Material	ORNL-1	ORNL-2	ORNL-10
^{10}B	0.0	1.0286×10^{-6}	0.0
H	0.066228	0.066148	0.066394
O	0.033736	0.033800	0.033592
N	1.869×10^{-4}	2.129×10^{-4}	1.116×10^{-4}
^{234}U	5.38×10^{-7}	6.31×10^{-7}	4.09×10^{-7}
^{235}U	4.8066×10^{-5}	5.6206×10^{-5}	3.6185×10^{-5}
^{236}U	1.38×10^{-7}	1.63×10^{-7}	2.20×10^{-7}
^{238}U	2.807×10^{-6}	3.281×10^{-6}	1.985×10^{-6}

In order to get a case with higher leakage, one additional sphere from the L series of uranyl fluoride assemblies was calculated. The L-7 assembly is modeled as an aluminum-clad sphere with radius of 11.5176 cm, respectively. The aluminum container has a thickness of 0.16, and the aluminum number density is taken to be 0.06025 per barn-cm. The number densities for the solution are given in the following table.

Material	L-7	L-8	L-9	L-10	L-11
H	0.0633680	0.0666144	0.066634	0.0647289	0.066722
O	0.0334713	0.0334357	0.0334344	0.034627	0.033473
F	0.0017873	0.00012855	0.0001027	0.0010983	0.00011249
²³⁴ U	8.7577x10 ⁻⁶	7.327x10 ⁻⁷	5.854x10 ⁻⁷	5.3816x10 ⁻⁶	5.5393x10 ⁻⁷
²³⁵ U	8.32694x10 ⁻⁴	5.99051x10 ⁻⁵	4.7856x10 ⁻⁵	5.11691x10 ⁻⁴	5.2444x10 ⁻⁵
²³⁶ U	4.2895x10 ⁻⁶	0.0	0.0	2.6359x10 ⁻⁶	2.8022x10 ⁻⁷
²³⁸ U	4.78991x10 ⁻⁵	3.638x10 ⁻⁶	2.9063x10 ⁻⁶	2.9340x10 ⁻⁵	2.9675x10 ⁻⁶

The L-7, L-10, and L-11 assembly has an additional 20.0 cm of water outside the aluminum shell (the number densities for the hydrogen and oxygen are .0666883 and .0333442 per bar-cm, respectively).

Four unreflected spheres of plutonium nitrate solution were also computed. The PNL-1 and PNL-2 benchmarks both have an effective radius of 19.509 cm. The isotopic compositions of the solutions are given in the following table.

Material	PNL-1	PNL-2
H	0.06563	0.05416
O	0.03456	0.03977
N	6.216x10 ⁻⁴	4.720x10 ⁻³
²³⁹ Pu	9.373x10 ⁻⁵	4.141x10 ⁻⁴
²⁴⁰ Pu	4.501x10 ⁻⁶	1.988x10 ⁻⁵

Similarly, the PNL-3 and PNL-4 benchmarks have an effective radius of 22.70 cm. The isotopic compositions of the solutions are given in the following table.

Material	PNL-1	PNL-2
H	0.06495	0.06041
O	0.03441	0.03712
N	7.394x10 ⁻⁴	2.775x10 ⁻³
Fe	1.294x10 ⁻⁶	1.520x10 ⁻⁶
²³⁹ Pu	5.395x10 ⁻⁵	6.633x10 ⁻⁵
²⁴⁰ Pu	2.355x10 ⁻⁶	2.895x10 ⁻⁶

LATTICE THERMAL CRITICALS

TRX LATTICES

The TRX lattices were a series using a triangular pattern of slightly-enriched metallic uranium rods in a water moderator. The CSEWG benchmarks model the unit cell with cylindrical geometry as given in the following table.

Region	Radius	Isotope	Density
Fuel	0.4915	²³⁵ U	6.253x10 ⁻⁴
		²³⁸ U	4.7205x10 ⁻²
Void	0.5042		
Clad	0.5753	Al	6.025x10 ⁻²
Moderator	*	¹ H	6.676x10 ⁻²
		¹⁶ O	3.338x10 ⁻²

The * in the table represents the outer radius of the moderator region, which varies between the two lattices analyzed here. The lattice spacings for TRX-1 and TRX-2 are 1.8060 cm and 2.1740 cm, respectively, which translate into radii of 0.9482 cm and 1.1414 cm, respectively.

The specifications in ENDF-202 suggest that these assemblies can be computed as infinite cylinders, and then a leakage correction can be applied using an homogenized B_l calculation with a total buckling of $B^2 = 0.0057 \text{ cm}^{-2}$ for TRX-1 or $B^2 = 0.005469 \text{ cm}^{-2}$ for TRX-2. The physical height is approximately 136.98 cm with vacuum boundary conditions. TRX-1 contained 764 fuel rods. When circularized, this corresponds to an effective radius of 26.209 cm. TRX-2 contained 578 fuel rods. The corresponding radius for TRX-2 is 27.441 cm. The water reflector was taken to have a thickness of about 30 cm with a vacuum boundary condition on its outer surface.

BAPL LATTICES

The BAPL lattices were a series using a triangular pattern of slightly-enriched uranium oxide rods in a water moderator. The CSEWG benchmarks model the unit cell with cylindrical geometry as given in the following table.

Region	Radius	Isotope	Density
Fuel	0.4864	²³⁵ U	3.112x10 ⁻⁴
		²³⁸ U	2.3127x10 ⁻²
		¹⁶ O	4.6946x10 ⁻²
Void	0.5042		
Clad	0.5753	Al	6.025x10 ⁻²
Moderator	*	¹ H	6.676x10 ⁻²
		¹⁶ O	3.338x10 ⁻²

The * in the table represents the outer radius of the moderator region, which varies between the three lattices analyzed here. The lattice spacings for BAPL-1, BAPL-2, and BAPL-3 are 1.5578, 1.6523, and 1.8057 cm, respectively, which translate into radii of 0.8178, 0.8675, and 0.9480 cm, respectively.

These three lattices can be calculated using the methods discussed above for the TRX lattices. The axial buckling is taken to be the same as for the TRX lattices; namely, 0.000526, giving a buckling height of 136.98 cm. The core radii can be calculated from the cell radii and the critical number of rods: 38.122 cm for BAPL-1 (2173 rods), 36.342 cm for BAPL-2 (1755-rods), and 37.623 cm for BAPL-3 (1575 rods).

Table D.2: Calculated keff eigenvalues against the measured keff =1.000 B1 and No Sn Transport Correction

IHECB/CSEWG Benchmarks	k_{eff}		
	COMBINE7.1		
	mcnp	Bondarenko Self shielding	Bondarenko + Nordheim self shielding
GODIVA (hmf-001)	1.00014(22)	0.99797	0.99797
FLATTOP-25 (hmf-028)	1.00275(24)	0.99900	0.99900
FLATTOP-Pu (pmf-006)	1.00067(25)	0.99325	0.99326
JEZEBEL (pmf-001 bare)	1.0001(20)	0.99612	0.99612
JEZEBEL-23 (umf-001)	1.00032(21)	0.99647	0.99647
JEZEBEL-Pu (pmf-002)	1.00025(20)	0.99665	0.99665
umf002-1	0.99891 (21)	0.99458/0.99408	0.99458/0.99408
umf002-2	1.00002 (21)	0.99542/0.99477	0.99542/0.99477
umf005-1	0.99396 (21)	0.98844/0.98801	0.98769/0.98801
umf005-2	0.99201 (23)	0.98201/0.98519	0.98201/0.98519
pci-001	1.01150(28)	1.00991	1.00497
hci-004	0.98781(24)	0.99223	0.98942
ORNL-1 (hst-013 Case 1)		0.99806	0.99794
ORNL-2 (hst-013 Case 2)		0.99717	0.99704
ORNL-10 (hst-032)		0.99133	0.99903
L-7 (hst009-3)		0.99835	0.99745
L-8		1.00495	1.00488
L-9		1.00292	1.00288
L-10		0.99573	0.99521
L-11 (hst012)		1.00021	1.00016
PNL-1		1.00765	1.00723
PNL-2		1.00446	1.00391
PNL-3		0.99398	0.99371
PNL-4		0.99976	0.99945
TRX1-r*	0.99908(29)	1.00196	0.99839
TRX2-r**	0.99908(28)	1.00044	1.00257
BAPL1-r**		1.00436	1.00367
BAPL2-r**		1.00136	1.00134
BAPL3-r**		1.00258	1.00271

Note: /1-D transport correction

Table D.3: Calculated keff eigenvalues against the measured keff =1.000 B1 and Sn Transport Correction

IHECB/CSEWG Benchmarks	k_{eff}		
	COMBINE7.1		
	mcnp	Bondarenko Self shielding	Bondarenko + Nordheim self shielding
GODIVA (hmf-001)	1.00014(22)	1.000190	1.000190
FLATTOP-25 (hmf-028)	1.00275(24)	0.999517	0.999518
FLATTOP-Pu (pmf-006)	1.00067(25)	0.994095	0.994097
JEZEBEL (pmf-001 bare)	1.0001(20)	0.999222	0.999223
JEZEBEL-23 (umf-001)	1.00032(21)	0.999314	0.999314
JEZEBEL-Pu (pmf-002)	1.00025(20)	0.999826	0.999828
umf002-1	0.99891 (21)	0.99865/0.99815	0.998647/0.99815
umf002-2	1.00002 (21)	0.99999/0.99935	0.999991/0.99935
umf005-1	0.99396 (21)	0.99114/0.99113	0.990633/0.99113
umf005-2	0.99201 (23)	0.98479/0.98884	0.984780/0.98879
pci-001	1.01150(28)	1.00991	1.00497
hci-004	0.98781(24)	0.99223	0.98936
ORNL-1 (hst-013 Case 1)		0.99699	0.99685
ORNL-2 (hst-013 Case 2)		0.99610	0.99594
ORNL-10 (hst-032)		0.99848	0.99849
L-7 (hst009-3)		0.99712	0.99638
L-8		1.00374	1.00364
L-9		1.00190	1.00182
L-10		0.99446	0.99400
L-11 (hst012)		0.99914	0.99906
PNL-1		1.00610	1.00570
PNL-2		1.00218	1.00173
PNL-3		0.99247	0.99218
PNL-4		0.99795	0.99763
TRX1-r*	0.99908(29)	1.00035	0.99698
TRX2-r**	0.99908(28)	1.00307	1.00132
BAPL1-r**		1.00262	1.00207
BAPL2-r**		0.99974	0.99988
BAPL3-r**		1.00115	1.00142

Note: /1-D transport correction

Table D.4: Calculated keff eigenvalues against the measured keff =1.000 B3 and No Sn Transport Correction

IHECB/CSEWG Benchmarks	k_{eff}		
	COMBINE7.1		
	mcnp	Bondarenko Self shielding	Bondarenko + Nordheim self shielding
GODIVA (hmf-001)	1.00014(22)	1.00273	1.00273
FLATTOP-25 (hmf-028)	1.00275(24)	1.00654	1.00633
FLATTOP-Pu (pmf-006)	1.00067(25)	1.00492	1.00486
JEZEBEL (pmf-001 bare)	1.0001(20)	1.00274	1.00274
JEZEBEL-23 (umf-001)	1.00032(21)	1.00278	1.00278
JEZEBEL-Pu (pmf-002)	1.00025(20)	1.00336	1.00336
umf002-1	0.99891 (21)	1.00337/1.00294	1.00337/1.00294
umf002-2	1.00002 (21)	1.00527/1.00469	1.00527/1.00419
umf005-1	0.99396 (21)	1.00136/0.99749	1.00089/0.99748
umf005-2	0.99201 (23)	1.00089/0.99686	1.00089/0.99686
pci-001	1.01150(28)	1.00991	1.00497
hci-004	0.98781(24)	0.99223	0.98942
ORNL-1 (hst-013 Case 1)		0.99890	0.99881
ORNL-2 (hst-013 Case 2)		0.99802	0.99787
ORNL-10 (hst-032)		0.99925	0.99926
L-7 (hst009-3)		1.00577	1.00485
L-8		1.00639	1.00632
L-9		1.00380	1.00367
L-10		1.00298	1.00247
L-11 (hst012)		1.00183	1.00175
PNL-1		1.01074	1.01031
PNL-2		1.00741	1.00687
PNL-3		0.99623	0.99596
PNL-4		1.00202	1.00169
TRX1-r*	0.99908(29)	1.00254	0.99890
TRX2-r**	0.99908(28)	1.00501	1.00316
BAPL1-r**		1.00465	1.00395
BAPL2-r**		1.00167	1.00169
BAPL3-r**		1.00286	1.00301

Note: /1-D transport correction

Table D.5: Calculated keff eigenvalues against the measured keff =1.000 B3 and Sn Transport Correction

k_{eff}			
COMBINE7.1			
IHECB/CSEWG		Bondarenko	Bondarenko +
Benchmarks	mcnp	Self shielding	Nordheim
			self shielding
GODIVA (hmf-001)	1.00014(22)	1.00268	1.00266
FLATTOP-25 (hmf-028)	1.00275(24)	1.00653	1.00632
FLATTOP-Pu (pmf-006)	1.00067(25)	1.00491	1.00484
JEZEBEL (pmf-001 bare)	1.0001(20)	1.00268	1.00267
JEZEBEL-23 (umf-001)	1.00032(21)	1.00261	1.00259
JEZEBEL-Pu (pmf-002)	1.00025(20)	1.00334	1.00333
ORNL-1 (hst-013 Case 1)	0.99891 (21)	0.99768	0.99758
umf002-1	1.00002 (21)	1.00325/1.00282	1.00323/1.00288
umf002-2	0.99396 (21)	1.00517/1.00459	1.00514/1.00456
umf005-1	0.99201 (23)	0.99999/0.99574	0.99954/0.99572
umf005-2	1.01150(28)	0.99655/0.99469	0.99654/0.99469
pci-001	0.98781(24)	1.00991	1.00497
hci-004		0.99223	0.98936
ORNL-2 (hst-013 Case 2)		0.99679	0.99666
ORNL-10 (hst-032)		0.99867	0.99868
L-7 (hst009-3)		1.00446	1.00355
L-8		1.00487	1.00480
L-9		1.00260	1.00250
L-10		1.00167	1.00116
L-11 (hst012)		1.00073	1.00064
PNL-1		1.00848	1.00806
PNL-2		1.00428	1.00373
PNL-3		0.99429	0.99401
PNL-4		0.99975	0.99943
TRX1-r*	0.99908(29)	1.00162	0.99807
TRX2-r**	0.99908(28)	1.00432	1.00245
BAPL1-r**		1.00387	1.00318
BAPL2-r**		1.00095	1.00096
BAPL3-r**		1.00227	1.00243

Note: /1-D transport correction

COMBINE7 EVALUATION OF THE BENCHMARK FOR THE DOPPLER REACTIVITY DEFECT

A set of computational benchmarks for the Doppler reactivity defect has been specified for fuel pin cells containing normal or enriched UO_2 fuel, reactor-recycle mixed-oxide (MOX) fuel, or weapons-grad MOX fuel. This Doppler benchmark has been approved by the Joint Benchmark Committee of the Mathematics and Computations, Reactor Physics, and Radiation Protection and Shielding Division of the American Nuclear Society. Reference (4) describes the benchmark specifications and provides a summary of the results submitted for it from many nuclear organizations. These benchmarks simulate the Doppler defect between hot zero power (HZP) at hot full power (HFP) for 16 different types of fuels in a PWR lattice. The temperature of the fuel is assumed to rise from 600 K to 900 K. It is supposed that radius fuel pin depends on fuel temperature. The moderator is borated water and contains 1400 PPM of boron. The clad is supposed to be pure natural zirconium.

The reference pin cell is that described in Fig D.1 where, from the center to the exterior, the regions are: the fuel (with external radius of 0.39398 cm and 0.39433 cm respectively for HZP and HFP), the gap (with external radius of 0.40226 cm), the clad (with external radius of 0.45972 cm) and finally the coolant. The total width of the cell is 1.26678 cm. The geometry for the benchmark is an infinite array of identical, infinitely long fuel pin cells with no axial variation. The isotopic concentrations for the benchmarks are provided in Tables D-6 through D-11. All these atomic numbers are from Reference 5.

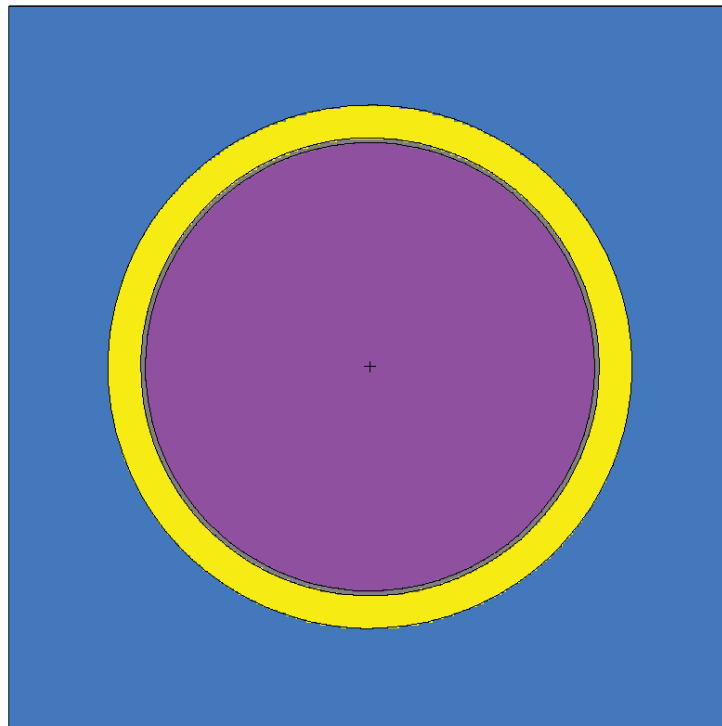


Figure D.1 Schematic of the Geometry for the Benchmarks

Table D-6, UO_2 Fuel Composition at 600 K (atoms/b-cm)

Enrichment (wt.%)	^{16}O	^{234}U	^{235}U	^{238}U
----------------------	-----------------	------------------	------------------	------------------

0.711	4.61171×10^{-2}	0	1.66029×10^{-4}	2.28925×10^{-2}
1.6	4.61218×10^{-2}	3.00175×10^{-6}	3.73618×10^{-4}	2.26843×10^{-2}
2.4	4.61260×10^{-2}	4.50257×10^{-6}	5.60420×10^{-4}	2.24981×10^{-2}
3.1	4.61297×10^{-2}	5.81576×10^{-6}	7.23867×10^{-4}	2.23352×10^{-2}
3.9	4.61339×10^{-2}	7.31651×10^{-6}	9.10661×10^{-4}	2.21490×10^{-2}
4.5	4.61371×10^{-2}	8.44205×10^{-6}	1.05075×10^{-4}	2.20093×10^{-2}
5.0	4.61397×10^{-2}	9.37998×10^{-6}	1.16749×10^{-4}	2.18930×10^{-2}

Table D-7, UO₂ Fuel Composition at 900 K (atoms/b-cm)

Enrichment (wt.%)	¹⁶ O	²³⁴ U	²³⁵ U	²³⁸ U
0.711	4.59967×10^{-2}	0	1.65595×10^{-4}	2.28328×10^{-2}
1.6	4.60014×10^{-2}	2.99391×10^{-6}	3.72462×10^{-4}	2.26251×10^{-2}
2.4	4.60056×10^{-2}	4.40981×10^{-6}	5.58956×10^{-4}	2.24393×10^{-2}
3.1	4.60093×10^{-2}	5.80057×10^{-6}	7.21977×10^{-4}	2.22768×10^{-2}
3.9	4.60134×10^{-2}	7.29740×10^{-6}	9.08283×10^{-4}	2.20911×10^{-2}
4.5	4.60166×10^{-2}	8.42000×10^{-6}	1.04801×10^{-4}	2.19519×10^{-2}
5.0	4.60192×10^{-2}	9.35548×10^{-6}	1.16445×10^{-4}	2.18358×10^{-2}

Table D-8, Reactor-Recycle MOX Fuel Composition at 600 K (atoms/b-cm)

MOX Composition (PuO ₂ wt. %)	¹⁶ O	²³⁵ U	²³⁸ U
1.0	4.61140×10^{-2}	1.64368×10^{-4}	2.26636×10^{-2}
2.0	4.61108×10^{-2}	1.62708×10^{-4}	2.24347×10^{-2}
4.0	4.61042×10^{-2}	1.59387×10^{-4}	2.19768×10^{-2}
6.0	4.60977×10^{-2}	1.56067×10^{-4}	2.15190×10^{-2}
8.0	4.60912×10^{-2}	1.52746×10^{-4}	2.10611×10^{-2}

MOX Composition (PuO ₂ wt. %)	²³⁹ Pu	²⁴⁰ Pu	²⁴¹ Pu	²⁴² Pu
1.0	1.03031×10^{-4}	6.86872×10^{-5}	3.43436×10^{-5}	2.28957×10^{-5}
2.0	2.06062×10^{-4}	1.37374×10^{-4}	6.86872×10^{-5}	4.57915×10^{-5}
4.0	4.12123×10^{-4}	2.72749×10^{-4}	1.37374×10^{-4}	9.15830×10^{-5}
6.0	6.18185×10^{-4}	4.12123×10^{-4}	2.06062×10^{-4}	1.37374×10^{-4}
8.0	8.24247×10^{-4}	5.49498×10^{-4}	2.74749×10^{-4}	1.83166×10^{-4}

Table D-9, Reactor-Recycle MOX Fuel Composition at 900 K (atoms/b-cm)

MOX Composition (PuO ₂ wt. %)	¹⁶ O	²³⁵ U	²³⁸ U
1.0	4.59936×10^{-2}	1.63939×10^{-4}	2.26044×10^{-2}
2.0	4.59904×10^{-2}	1.62283×10^{-4}	2.23761×10^{-2}
4.0	4.59838×10^{-2}	1.58971×10^{-4}	2.19194×10^{-2}
6.0	4.59773×10^{-2}	1.55659×10^{-4}	2.14628×10^{-2}
8.0	4.59708×10^{-2}	1.52347×10^{-4}	2.10061×10^{-2}

MOX Composition (PuO ₂ wt. %)	²³⁹ Pu	²⁴⁰ Pu	²⁴¹ Pu	²⁴² Pu
1.0	1.02762×10^{-4}	6.85079×10^{-5}	3.42539×10^{-5}	2.28360×10^{-5}
2.0	2.05524×10^{-4}	1.37016×10^{-4}	6.85079×10^{-5}	4.56719×10^{-5}
4.0	4.11047×10^{-4}	2.74031×10^{-4}	1.37016×10^{-4}	9.13438×10^{-5}
6.0	6.16751×10^{-4}	4.11047×10^{-4}	2.05524×10^{-4}	1.37016×10^{-4}

8.0	8.22094×10^{-4}	5.48063×10^{-4}	2.74031×10^{-4}	1.82688×10^{-4}
-----	--------------------------	--------------------------	--------------------------	--------------------------

Table D-10, Weapons-Grade MOX Fuel Composition at 600 K (atoms/b-cm)

MOX Composition (PuO ₂ wt. %)	¹⁶ O	²³⁵ U	²³⁸ U
1.0	4.61154×10^{-2}	1.64368×10^{-4}	2.26636×10^{-2}
2.0	4.61136×10^{-2}	1.62708×10^{-4}	2.24347×10^{-2}
4.0	4.61099×10^{-2}	1.59387×10^{-4}	2.19768×10^{-2}
6.0	4.61061×10^{-2}	1.56067×10^{-4}	2.15190×10^{-2}

MOX Composition (PuO ₂ wt. %)	²³⁹ Pu	²⁴⁰ Pu	²⁴¹ Pu	²⁴² Pu
1.0	2.14958×10^{-4}	1.35947×10^{-5}	9.18623×10^{-5}	2.29656×10^{-7}
2.0	4.29916×10^{-4}	2.70994×10^{-5}	1.83725×10^{-6}	4.59312×10^{-7}
4.0	8.59831×10^{-4}	5.41988×10^{-5}	3.67449×10^{-6}	9.18623×10^{-7}
6.0	1.28975×10^{-3}	8.12982×10^{-5}	5.51174×10^{-6}	1.37794×10^{-6}

Table D-11, Weapons-Grade MOX Fuel Composition at 900 K (atoms/b-cm)

MOX Composition (PuO ₂ wt. %)	¹⁶ O	²³⁵ U	²³⁸ U
1.0	4.59950×10^{-2}	1.63939×10^{-4}	2.26044×10^{-2}
2.0	4.59932×10^{-2}	1.62283×10^{-4}	2.23761×10^{-2}
4.0	4.59895×10^{-2}	1.58971×10^{-4}	2.19194×10^{-2}
6.0	4.59857×10^{-2}	1.55659×10^{-4}	2.14628×10^{-2}

MOX Composition (PuO ₂ wt. %)	²³⁹ Pu	²⁴⁰ Pu	²⁴¹ Pu	²⁴² Pu
1.0	2.14397×10^{-4}	1.35143×10^{-5}	9.16224×10^{-7}	2.29056×10^{-7}
2.0	4.28793×10^{-4}	2.70286×10^{-5}	1.83245×10^{-6}	4.58112×10^{-7}
4.0	8.57586×10^{-4}	5.40572×10^{-5}	3.66490×10^{-6}	9.16224×10^{-7}
6.0	1.28638×10^{-3}	8.10859×10^{-5}	5.49735×10^{-6}	1.37434×10^{-6}

To evaluate the COMBINE7.1 capabilities and limitations as a part of V&V, a series of calculations were performed, simulating these benchmarks. The results are compared to the in-house calculated MCNP³ results and the reported results in Reference 5.

The first series of calculations were for the HZP condition but having a uniform temperature at 300 K. The ENDF/B-VII.0 derived cross sections⁴ were also used in MCNP runs. In the COMBINE/A runs, 18-group macroscopic cell cross sections were first generated and using these cross sections, a one-zone transport calculation was made. In the COMBINE/B runs, 18 macroscopic cross sections were first generated for the three zones (fuel, cladding, and moderator, respectively). Using these cross sections, a three-zone transport calculation was made. In the COMBINE/C runs, 167 macroscopic fine-group cross sections were first generated for the three zones. Using

these cross sections, a three-zone transport calculation was made. These cross sections were spatially coalesced and then collapsed into 18 broad group cross sections. Using these cross sections, a one-zone transport calculation was made. In all transport calculations, a white outer boundary condition with equivalent the cylindrical geometry (O.D. 1.4294 cm) was used. The COMBINE results with the Bondareno self-shielding treatment are compared in Table D.12 through D-14 to those from the in-house MCNP calculations with the identical geometry, composition, and temperatures. The results with the additional Nordheim self-shielding treatment were almost identical to those from the Bodnrenko results. All the COMBINE eigenvalues are favorably comparable with those from the MCNP's. Still, the results indicate some instability in the cross section coalescing.

Table D.12 Results for UO₂ Pin cells

Enrichment (wt. %)	k_{eff}			
	MCNP	COMBINE/A	COMBINE/B	COMBINE/C
0.711	0.68227	0.68014	0.68232	0.68221
1.6	0.97813	0.97705	0.97953	0.97918
2.4	1.11498	1.11413	1.11713	1.11670
3.1	1.19236	1.19097	1.19448	1.19397
3.9	1.25440	1.25246	1.25649	1.25594
4.5	1.28880	1.28706	1.29147	1.29096
5.0	1.31347	1.31077	1.31551	1.31498

Note: all the MCNP results are with ± 0.00030

Table D.13 Results for Reactor-Recycle MOX Pin Cells

MOX Composition (PuO ₂ wt. %)	k_{eff}			
	MCNP	COMBINE/A	COMBINE/B	COMBINE/C
1.0	0.93459	0.93360	0.93464	0.93548
2.0	1.02048	1.02052	1.02108	1.02300
4.0	1.08587	1.08718	1.08720	1.09023
6.0	1.11844	1.12031	1.11980	1.12336
8.0	1.14315	1.14589	1.14503	1.14865

Table D.14 Results for Weapons-Grade MOX Pin Cells (w/ free)

MOX Composition (PuO ₂ wt. %)	k_{eff}			
	MCNP	COMBINE/A	COMBINE/B	COMBINE/C
1.0	1.08538	1.08361	1.08587	1.08553
2.0	1.19110	1.19078	1.19192	1.19142
4.0	1.26885	1.27059	1.27002	1.26963
6.0	1.30832	1.31005	1.30852	1.30840

The rest of calculations were devoted to the HZP and HFP conditions, simulating the benchmarks with the COMBINE/A option and COMBINE/B option as previously described. Tables D.15 through D.20 list the COMBINE results. The Doppler coefficient (pcm/K) of reactivity as listed is determined as

$$DC = \frac{\Delta\rho_{Dop}}{\Delta T_{fuel}}$$

Where DC is the Doppler coefficient of reactivity, ΔT_{fuel} is 300 K, and the Doppler defect is

$$\Delta\rho_{DOP} = \frac{k_{HFP} - k_{HZP}}{k_{HFP} * k_{HZP}} * 10,000$$

Table D.15 Results for UO₂ Pin cells (w/o free), COMBINE/A

Enrichment (wt. %)	k_{eff}		Doppler Coefficient (pcm/K)
	HZP	HFP	
0.711	0.66255	0.65644	-4.69
1.6	0.95841	0.94958	-3.24
2.4	1.09627	1.08633	-2.78
3.1	1.17375	1.16323	-2.57
3.9	1.23576	1.22473	-2.43
4.5	1.27065	1.25943	-2.34
5.0	1.29449	1.28310	-2.29

Table D.16 Results for Reactor-Recycle MOX Pin Cells, COMBINE/A

Enrichment (wt. %)	k_{eff}		Doppler Coefficient (pcm/K)
	HZP	HFP	
1.0	0.94161	0.93092	-4.06
2.0	1.01817	1.00616	-3.91
4.0	1.07408	1.06141	-3.70
6.0	1.10321	1.09050	-3.52
8.0	1.12708	1.11430	-3.39

Table D.17 Results for Weapons-Grade MOX Pin Cells, COMBINE/A

Enrichment (wt. %)	k_{eff}		Doppler Coefficient (pcm/K)
	HZP	HFP	
1.0	1.08620	1.07584	-2.96
2.0	1.17792	1.16560	-2.99
4.0	1.24799	1.23442	-2.94
6.0	1.28541	1.27229	-2.67

Table D.18 Results for UO₂ Pin cells , COMBINE/B

Enrichment (wt. %)	k_{eff}		Doppler Coefficient (pcm/K)
	HZP	HFP	
0.711	0.66461	0.65785	-5.15
1.6	0.96072	0.95131	-3.43
2.4	1.09916	1.08870	-2.91
3.1	1.17711	1.16617	-2.66
3.9	1.23976	1.22837	-2.49
4.5	1.27512	1.26352	-2.40
5.0	1.29935	1.28763	-2.34

Table D.19 Results for Reactor-Recycle MOX Pin Cells, COMBINE/B

Enrichment (wt. %)	k_{eff}		Doppler Coefficient (pcm/K)
	HZP	HFP	
1.0	0.94202	0.93070	-4.31
2.0	1.01806	1.00531	-4.15
4.0	1.07364	1.06037	-3.89
6.0	1.10253	1.08932	-3.67
8.0	1.12624	1.11318	-3.47

Table D.20 Results for Weapons-Grade MOX Pin Cells, COMBINE/B

Enrichment (wt. %)	k_{eff}		Doppler Coefficient (pcm/K)
	HZP	HFP	
1.0	1.08826	1.07750	-3.06
2.0	1.17883	1.16602	-3.11
4.0	1.24724	1.23322	-3.04
6.0	1.28384	1.26966	-2.90

All the eigenvalues are favorable to the reported results. All the Doppler coefficients are within 1σ of the reported average values in Reference 5 but mostly in the lower side, i.e., more negative. It is also observed that the Doppler coefficients obtained with a three-zone model are more negative than those obtained with the 0-D cell/one-zone transport calculations.

D. REFERENCE

1. *International Handbook of Evaluated Criticality Safety Benchmark Experiments*, OECD Nuclear Energy Agency report NEA/NSC/DOC(95)03, September 2005 Edition.
2. *Cross Section Evaluation Working Group Benchmark Specifications*, ENDF-202, BNL-19302, November, 1974 and September 1991 Update.
3. MCNP2.6.0 Extensions, LA-UR-08-2216, April, 2008.
4. *The ENDF/B-V.II.0-ACE Library*, D0022MNYCP00, RSICC, Oak Ridge National, Laboratory, 2008.
5. Russell D Mosteller, The Doppler-defect benchmark: overview and summary of results, Joint International Topical Meeting on Mathematics & Computation and Supercomputing in Nuclear Applications (M&C + SNA 2007), Monterey, California, April,2007.